GALACTIC COSMIC RAY COMPOSITION

Jean-Paul Meyer
Service d'Astrophysique
Centre d'Etudes Nucléaires de Saclay
France

The plan of this report on our knowledge of galactic cosmic-ray composition as it stands after the La Jolla Conference (August 1985) may seem somewhat odd to the reader. This is why I felt it prudent to give an explicit table of contents, which might help him to find his way in this maze.

In Part I, I just highlight various key new observations brought up at the conference. In Part II, I specify what I think we know on the cosmic-ray elemental composition at the sources, and on its correlation with first ionization potential (FIP). In Part III, the most important in my view, I discuss the various areas where the correlation with FIP is, really or apparently, insufficient to explain the data as they stand. The isotopic anomalies will be discussed in this context. It might also sound a bit bizarre to the reader to find the entire problem of cosmic ray propagation (compositional aspects) treated as kind of a long parenthesis in the discussion of the source abundance of Nitrogen ! In Part IV, I summarize the situation and make recommendations on key points for future work.

CONTENTS

PART III THE PROBLEMS WITH THE GALACTIC COSMIC RAY SOURCE COMPOSITION AND PROPAGATION - BEYOND THE CORRELATION WITH FIRST IONIZATION POTENTIAL

III-1. The Hydrogen and Helium deficiency problem
- III-1.1. H and He source spectra, and behaviour in SEP's
- III-1.2. Deficiency of H and He : direct injection out of the hot interstellar medium (HIM) ?

III-2. The Nitrogen deficiency problem - Cosmic ray propagation - The B-^{15}N contradiction - Distributed reacceleration ? Truncation of the PLD ?
- III-2.1. Low energy cosmic-ray propagation - The B-^{15}N contradiction - Distributed reacceleration ?
- III-2.2. The ^{14}N source abundance from low and high energy data
- III-2.3. Truncation of the exponential Path Length Distribution (PLD) ?
  - III-2.3.1. Truncation of the PLD in the GeV/n range - Data for $Z \leq 30$ - The role of interstellar He
  - III-2.3.2. Truncation of the PLD in the GeV/n range - UH nuclei data
  - III-2.3.3. Truncation of the PLD in the few 100 MeV/n range
  - III-2.3.4. Summary on the truncation of the PLD

III-3. The Germanium-Lead deficiency problem
- III-3.1. Defining the Ge and Pb/Pt anomalies
- III-3.2. The low Pb/Pt ratio : probably not explainable in terms of a truncation of the PLD
- III-3.3. The low Pb/Pt ratio - Interpretations in terms of nucleosynthesis
- III-3.4. Ge and Pb as volatility indicators
- III-3.5. Questioning the LG reference abundances for Ge and Pb
- III-3.6. Summary on the Ge-Pb deficiency problem

III-4. The C, O, ^{22}Ne, ^{25,26}Mg, ^{29,30}Si excesses
- III-4.1. Estimating the ^{22}Ne, ^{25,26}Mg, ^{29,30}Si excesses in GCR sources
- III-4.2. The common and new wisdom on He-burning and weak s-process in Wolf-Rayet stars
- III-4.3. Relating the excesses in GCRS to those in the (WR) processed component material - FIP effects in the dilution
- III-4.4. Discussion : types of dilution, observed and predicted ^{22}Ne excesses
- III-4.5. Excess ^{22}Ne : preferential injection at the decay of ^{22}Na ?

III-5. The excess of elements with $Z \geq 40$
- III-5.1. Estimating the excesses in the processed component material - FIP effects in the dilution
  - III-5.1.1. The dilution problem
  - III-5.1.2. Consequences of differential dilution
- III-5.2. Evidences for s and/or r-process excesses
  - III-5.2.1. What happens at $Z = 40$?
  - III-5.2.2. The $_{52}$Te, $_{54}$Xe, $_{56}$Ba, $_{58}$Ce quartet
- III-5.3. UH element excesses - Summary and overview

PART IV SUMMARY AND RECOMMENDATIONS

IV-1. Summary

IV-2. Recommendations for future work.

APPENDIX : Formalism for the dilution of the ^{22}Ne-rich or other processed components.

PART I

HIGHLIGHT OF KEY NEW OBSERVATIONS

I-1. ABUNDANCE OF SUB-IRON NUCLEI UP TO 200 GeV/n

It has been known since Juliusson's (1974) first study that the abundance ratios of secondary to primary nuclei decrease with energy between $\sim$ 2 and at least $\sim$ 30 GeV/n. But there was as yet no unambiguous evidence that this trend was continued beyond $\sim$ 30 GeV/n (e.g. Webber 1983a; Garcia-Munoz et al., 1984; Juliusson et al., 1983). Taking advantage of the relativistic rise of ionization chambers to resolve high energies, the HEAO 3 Heavy Nuclei Experiment (HEAO-C3) team has shown that the purely secondary/primary ratios in the Fe region definitely continue to decrease, at roughly the same rate, up to at least 200 GeV/n (Jones et al. 2, 28; fig. 1) [1].

The approximate constancy of the primary/primary Ni/Fe ratio in fig. 1 shows that the data are not affected by any large systematic bias. As regards Ar and Ca, both the secondary and the primary component are significant. Accordingly, the Ar/Fe and Ca/Fe ratios decrease with energy, but less steeply than the purely secondary/primary ratios. Beyond $\sim$ 200 GeV/n the observed ratios are however strange, with an apparent trend to rise again. The authors are very prudent as regards these highest energy points, which just represent the present state of their data analysis. It must however be noted that a preliminary analysis of balloon gas Cerenkov data by the Goddard group also suggests an increase of sub-Fe/Fe ratios somewhere beyond $\sim$ 100 GeV/n (Balasubrahmanyan et al. 2, 44). But here also the authors are prudent (and their Cr does not fit well into the picture)!

In principle, composition observations reaching energies where the secondary component is much reduced can yield most accurate values for the source abundances. Based on the data up to $\sim$ 200 GeV/n, Jones et al. (2, 28) have indeed derived estimates of the primary Ar/Fe and Ca/Fe ratios, corresponding to source ratios Ar/Fe $\approx 0.023 \pm 0.003$ and Ca/Fe $\approx 0.085 \pm 0.004$ (fig. 1) (these source ratios are $\sim$ 12 and 10% lower than the surviving primary ratios given by the authors). I feel however that these estimates cannot be considered really solid as long as the highest energy points puzzle is not solved, one way or another.

[1] Throughout this report, the papers presented at the La Jolla Conference will be quoted directly by their volume and page number in the proceedings. They are not listed at the end of the paper.

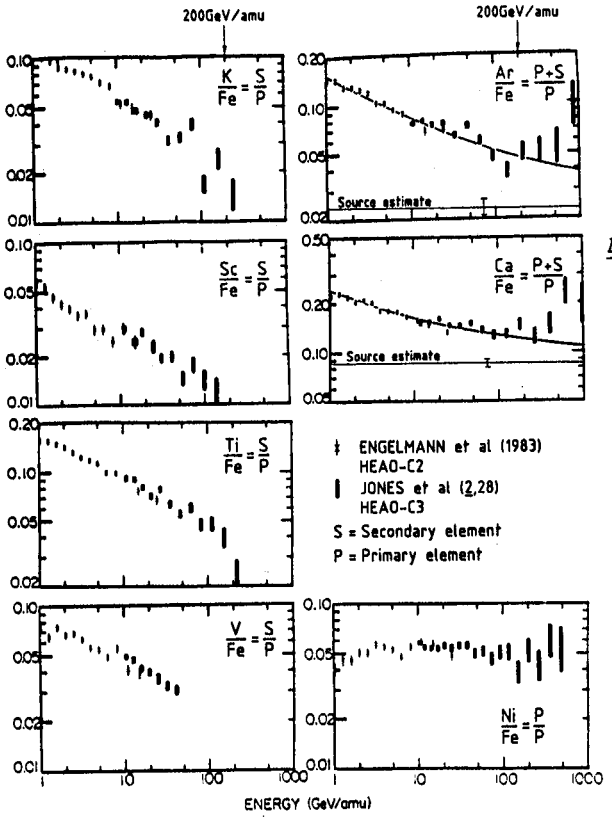

Fig. 1 Sub-Fe/Fe ratios at very high energy, as measured by the HEAO-C3 team, together with the lower energy ratios from the HEAO-C2 team (from Jones et al. 2, 28 ; fig. slightly adapted). Left column : purely secondary/primary ratios. Right column : Ni/Fe = primary/primary ratio ; Ar,Ca/Fe = mixed ratios. Also plotted are the author's fit to the data on Ar,Ca/Fe below 200 GeV/n, and the derived source ratios.

I-2. ISOTOPIC COMPOSITION OF HEAVY NUCLEI

The mass resolution now achieved by Webber et al. (2, 88) in the 400 to 700 MeV/n range for elements between N and Ca is very impressive (fig. 2). Of particular significance are the well resolved N, Mg and Ca isotopes, and especially the low ^{29,30}Si fluxes (§ II-1.2.2., III-2. and 4.).

Wiedenbeck (2, 84) and Krombel and Wiedenbeck (2, 92) also obtained quite good mass resolution on Cl, Sc and Ca around 250 MeV/n (fig. 3). They found radioactive ^{36}Cl depleted, as expected, and contributed to tightening up the source Ca abundance, based on the primary ^{40}Ca isotope, which is well resolved from the heavier, secondary isotopes (fig. 3). Webber et al. (2, 88)'s data can be used for the same purpose (§ II-1.2.2.; fig. 14).

At high energy, the HEAO 3 French-Danish experiment (HEAO-C2) team has provided new geomagnetic mean mass estimates at 3 GeV/n for elements between N and Fe (Ferrando et al. 2, 96, and priv. comm. of ^{15}N/N = 0.49 ± 0.06), whose significance, combined with the earlier HEAO-C2 data, will be discussed later (§ III-2. and 4.). Herrström and Lund (2, 100) have also shown that the ^{22}Ne enhancement at source does not vary with energy between 0.1 and 6 GeV/n.

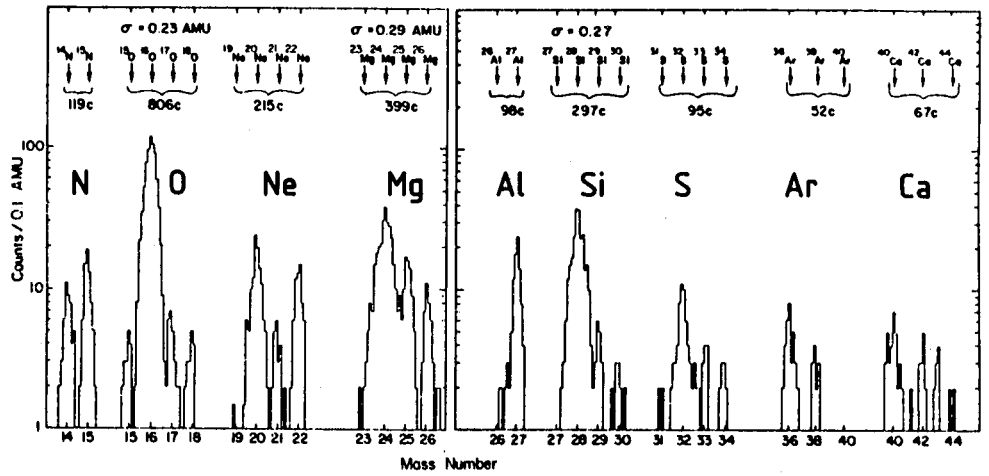

Fig. 2 *Cosmic-ray isotopes from N to Ca, as beautifully resolved by Webber et al. (2, 88).*

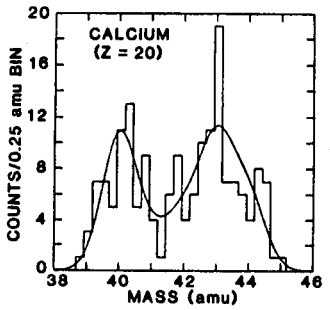

Fig. 3 *Isotopic analysis of cosmic-ray Ca, by Krombel and Wiedenbeck (2, 92).*

I-3. SPALLATION CROSS-SECTIONS

In response to a crucial need, and taking advantage of the facilities offered by the Berkeley Bevalac, a very massive effort is now being invested on spallation cross-section measurements. Let me insist on the materiality of the need : with the high accuracy now achieved in the cosmic-ray measurements, especially with the HEAO-C2 data, the check of the self-consistency and the refinement of the propagation models (truncation of the path length distribution ? distributed reacceleration ?), and a fortiori the determination of the source abundances of key largely secondary elements and isotopes (N, Na, ^{25,26}Mg, Al, ^{29,30}Si, P, Ar, Ca) are essentially limited by our knowledge of spallation cross-sections (§ II-1.2., III-2. and 4.1.). It is important to measure cross-sections for a great variety of energies and incident nuclei. In the interpretation of secondary nuclei abundances, it is indeed not worth having their production cross-sections from a few dominant parents determined with utmost accuracy, as long as the cross-sections for a large number of other contributing parents remain entirely unmeasured (Table 2). Measurement of spallation cross-sections on He are also becoming necessary now (Ferrando et al. 3, 61 ; § III-2.3.1.).

I-3.1. Measurements of spallation cross-sections on H

Following the early work of the Orsay group (e.g. Raisbeck and Yiou 1976) and the first studies on the Bevalac (Lindstrom et al. 1975 ; Olson et al 1983), in recent years the New Hampshire group has been leading the way as regards cross-section measurements (Webber and Brautigam 1982 ; Webber et al. 1983a,b ; Webber 1984 ; Webber and Kish 3, 87). Other groups are now joining the effort : Louisiana State U. - Berkeley collaboration (Guzik et al. 2, 80), Cal Tech (Lau et al. 1983 ; 3, 91), and the HEAO-C3 team in the Ultra-Heavy range (Brewster et al. 1983 ; Kertzman et al. 3, 95).

In the Be, B, C, N, O range, absolutely essential new data on the reactions $^{12}C \rightarrow$ Be, B and $^{16}O \rightarrow {}^{14,15}N$ have been provided by Webber and Kish 13, 87) and Guzik et al. 2, 80). They are summarized in fig.4. When these data are combined with those for $^{16}O \rightarrow$ B and $^{20}Ne \rightarrow {}^{14,15}N$ (Webber et al. 1983b), respectively $\sim$ 81%, 74% and 91% of the production of B, ^{14}N, ^{15}N between $\sim$ 0.3 and 2 GeV/n results from reactions whose cross-sections are measured (§ III-2.1. ; Table 2). While the very small errors quoted by the New-Hampshire group are sometimes questioned in view of the importance of their thick target correction, the agreement between the various data sets in fig. 4 shows that no large systematic error affects the data.

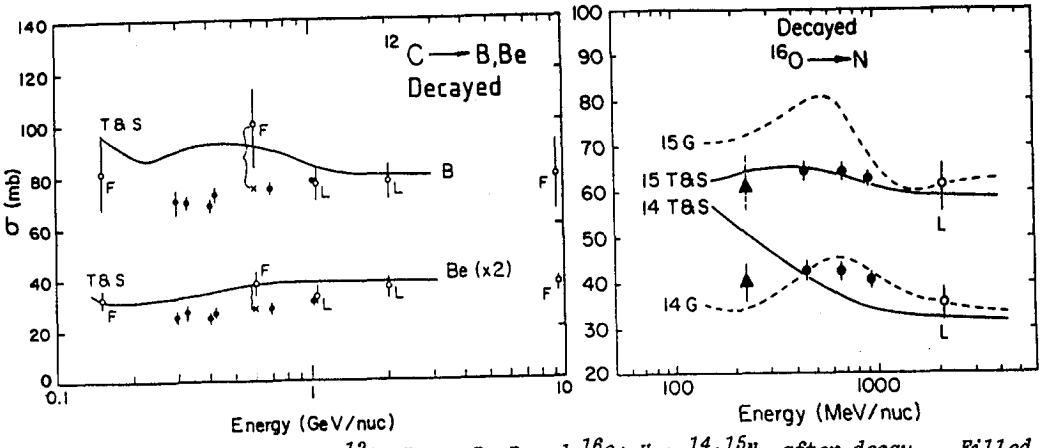

Fig. 4 Cross-sections for $^{12}C + H \rightarrow$ Be,B and $^{16}O + H \rightarrow {}^{14,15}N$, after decay. Filled circles : Webber and Kish (3, 87) (see also Webber 1984), and Webber et al. (1983b). Triangles : Guzik et al. (2, 80). Open circles : Lindstrom et al. (1975) (or Olson et al. 1983) and Fontes (1977). Curves : semi-empirical estimates by Tsao and Silberberg (1979) and Guzik (1981).

As regards the spallation of ^{56}Fe specifically, some of the discrepancies between the recent New-Hampshire data (Webber and Brautigam 1982 ; Webber et al. 1983a ; Webber 1984) and earlier studies (e.g. Perron 1976 ; Orth et al. 1976) are being removed by refined analysis of the recent data. Anyway, there is excellent agreement on the sum of the cross-section for formation of Sc+Ti+V+Cr. The new data on the energy dependence of the Fe cross-sections at low energy (down to 300 MeV/n ; Webber 1984 ; Lau et al. 3, 91) is of particular interest, and should allow a broad revision of the semi-empirical formulae for low energies.

Spallation cross-sections for ^{28}Si and ^{40}Ar between 500 and 1300 MeV/n have been measured by Webber and Kish (3, 87), who should also provide us soon with new cross-sections for spallation of ^{32}S, ^{40}Ca and ^{58}Ni. These measurements complement the above mentioned New-Hampshire data on ^{56}Fe spallation. For ^{40}Ar, and to some point ^{28}Si spallation, the new data imply that, at 650 MeV/n, the semi-empirical estimates (Tsao and Silberberg 1979) underestimate the cross-section, by factors of up to $\sim$ 1.9 for products with Z = 12 to 14 (fig. 5). If the same trend is present for other, neighbouring parent nuclei (which will be checked soon, ^{32}S, ^{40}Ca), it is of extreme importance, since it will decrease the estimate of the source abundances of Na, Al, $^{25,26}Mg$ and $^{29,30}Si$, which are at present critical issues (§ II-1.2.1. and 1.4., III-4.; figs. 14 and 29). The effect of such a correction on the determination of the source abundance of Al is illustrated in fig. 6 (from Webber et al. 3, 42).

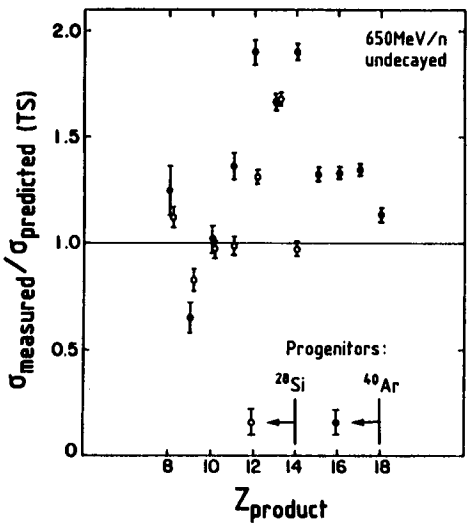

Fig. 5 Ratios of the charge changing cross-sections of ^{28}Si and ^{40}Ar on H measured by Webber and Kish (3, 87), to those estimated by Tsao and Silberberg (1979) (650 MeV/n, undecayed).

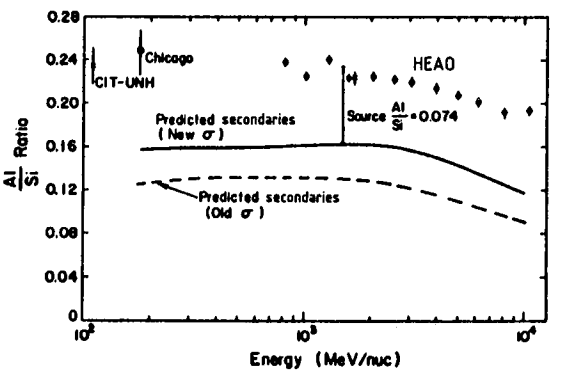

Fig. 6 Effect of the new ^{28}Si and ^{40}Ar cross-section measurements by Webber and Kish (3, 87) (fig. 5), extrapolated to neighbouring parent nuclei, on the derived Al source abundance (from Webber et al. 3, 42).

Relative cross-sections for spallation of ^{40}Ar and ^{56}Fe measured around 300 MeV/n by Lau et al. (1983; 3, 91) also give useful information to refine semi-empirical estimates. In particular, these authors note the effect of closed neutron shells: the cross-sections for formation of products with 1 neutron less than a magic number are found very small, probably because neutron emission out of a closed shell is difficult.

In the Ultra-Heavy (UH) range, beautiful new data on the spallation of $_{54}Xe$, $_{67}Ho$ and $_{79}Au$ around 1 GeV/n have been provided by Brewster et al. (1983) and Kertzman et al. (3, 95). Their measured total cross-sections σ_{tot} show that extrapolation of Westfall et al.'s (1979) formula for projectiles beyond Fe leads to slight overestimates for σ_{tot} (by 15% for $_{67}Ho$ on H). Figure 7 displays the measured charge yields on H. It shows that, when normalized to σ_{tot}, the charge yield is approximately a universal function of the charge change ΔZ, independent of the charge of the incident UH nucleus. Comparison with the semi-empirical estimates by Silberberg and Tsao (1979) (fig. 8) shows that the estimates are fairly good (generally to within a factor of 1.5) for the more important nearby products ($\Delta Z \lesssim 10$), but can underestimate by factors of up to 2 the smaller cross-sections for more distant products. Figure 8 also shows that the departures of the estimated cross-sections from the measured ones cannot be described by a unique pattern valid for all UH parent nuclei.

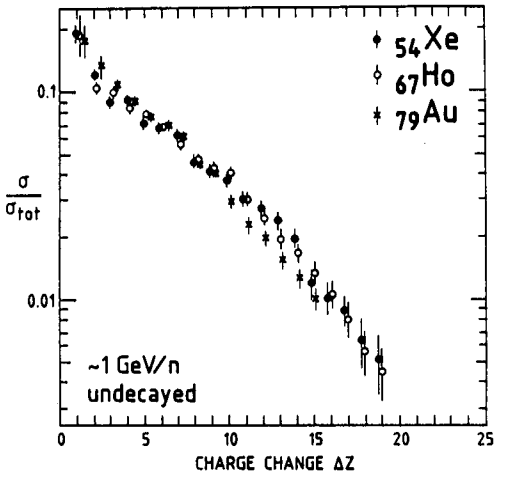

Fig. 7 Charge changing cross-sections for $_{54}Xe$, $_{67}Ho$ and $_{79}Au$ on H, as measured by Kertzman et al. (3, 95), normalized to the total cross-section ($\sim$1 GeV/n, undecayed). The values for Au have been revised since Brewster et al. (1983)'s study.

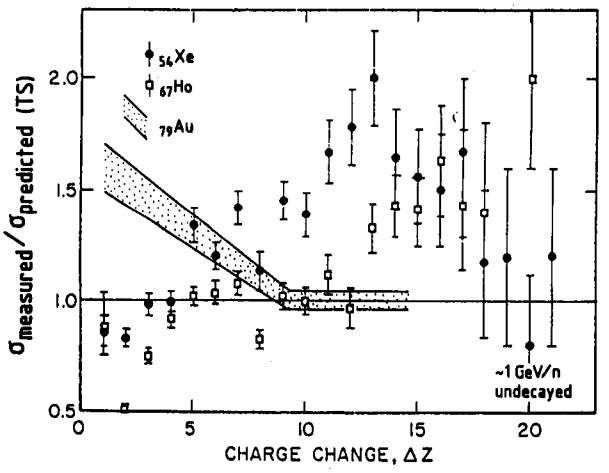

Fig. 8 Ratios of the charge changing cross-sections of $_{54}Xe$, $_{67}Ho$ and $_{79}Au$ on H measured by Kertzman et al. (3, 95), to those estimated by Tsao and Silberberg (1979) ($\sim$1 GeV/n, undecayed).

I-3.2. Semi-empirical estimates of spallation cross-sections on H

As regards semi-empirical estimates of unmeasured cross-sections (Silberberg and Tsao 1973a,b ; Silberberg et al. 1985 ; Tsao et al. 3, 103), it is clear that they will remain necessary. Estimating their accuracy is however still not easy: on the one hand, Letaw et al. (3, 46) give evidence that the errors on the semi-empirical cross-sections are uncorrelated and generally less than 35% below Fe at 4 GeV/n; on the other hand, recent cross-section observations show that the semi-empirical estimates for some major cross-sections are off by factors of up to ~ 2 around 0.6 GeV/n (fig. 5; § I-3.1.; Webber et al. 1983b ; Webber and Kish 3, 87). With the large body of recent and forthcoming measurements of cross-sections for the spallation of ^{12}C, ^{16}O, ^{20}Ne, ^{24}Mg, ^{28}Si, ^{32}S, ^{40}Ar, ^{40}Ca, ^{56}Fe, ^{58}Ni in the 0.3 to 1.7 GeV/n range by the New-Hampshire group, time will soon be ripe for a deep revision of the parametrization of the cross-section systematics, possibly including new physical effects (e.g., closure of neutron shells ; Lau et al. 3, 91 ; § I-3.1.). In particular, comparison of the data for ^{40}Ar and ^{40}Ca spallation will shed light on the effect of the neutron-richness of the parent nucleus. The detailed measurement of the behaviour of the Fe spallation cross-sections down to ~ 300 MeV/n (Webber 1984) is also an invaluable source of information (but one pending problem is to within which accuracy the cross-sections measured at Bevalac up to at most 1.7 GeV/n are constant beyond that energy ; see, e.g., Perron 1976). In the UH range, the new data by Kertzman et al. (3, 95) should also allow improved estimates. As a general rule, adjustment factors for individual cross-sections should, of course, be avoided, since they do not permit improved predictions for unmeasured cross-sections.

I-3.3. Nucleus-nucleus cross-sections

Since all the Bevalac measurements of spallation on H (§ I-3.1.) have actually been performed by comparing data for spallation on CH_2 and on C, they have also given information on nucleus-nucleus interactions. In addition Heinrich et al. (3, 99) have specifically addressed this problem, by performing measurements of ^{40}Ar and ^{56}Fe spallation on $C_{12}H_{18}O_7$ and Ag and discussing the scaling of the cross-sections as compared to cross-sections on H (see also their list of references). They are at present developing analytical expressions for nucleus-nucleus cross-sections. I shall not discuss this topic here, which is however important as regards nuclear physics, for atmospheric and instrumental corrections, and as giving hints on spallation cross-sections on He, which may become crucial for refined studies of interstellar propagation (truncation ; Ferrando et al. 3, 61; § III-2.3.1.).

I-4. OBSERVATIONS OF ULTRA-HEAVY (UH) NUCLEI

I-4.1. The HEAO-C3 and Ariel VI data

Improved data on UH nuclei (Z > 30) from the HEAO-C3 and Ariel VI spacecraft experiments have been presented at this conference by Newport et al. (2, 123), Klarman et al. (2, 127) and Waddington et al. (9,...), and by Fowler et al. (2, 115, 119).

The Ariel VI team has provided an improved analysis of their data for both $Z \lesssim 48$ (where only high geomagnetic cut-off portions of the orbit can be used, to avoid pollution by low-energy Fe nuclei) and $Z \gtrsim 48$ (where the entire orbit can be used) (Fowler et al. 2, 115, 119). Their "apparent charge" histogram for $Z \gtrsim 48$ is shown in figure 9; the median energy of these particles is fairly low, $\sim$ 2 GeV/n. From such histograms, elemental abundances are derived by deconvolution with an instrumental resolution function extrapolated from that of Fe. Corrections for interactions within the (rather thin) instrument are not large. The corrected abundances are plotted in figure 10 (for $Z \gtrsim 62$, grouped into broad ranges of elements, see also Table 1).

In the higher Z range $Z \gtrsim 50$, the HEAO-C3 team has also provided improved data for higher energy nuclei (recorded when the geomagnetic cut-off was > 5 GV; median energy $\sim$ 6 GeV/n) (Klarman et al. 2, 127; Waddington et al. 9,...). Their brutto "apparent charge" histogram is also shown in figure 9. Exploiting these data for $Z \gtrsim 62$, the authors felt it more realistic to give only abundances for broad ranges of elements, in view of the limited charge resolution and statistics. They are given in Table 1 and plotted in figure 10. These values have been approximately corrected for the interactions within the HEAO-C3 instrument, which is much thicker than Ariel VI (see caption of fig. 10).

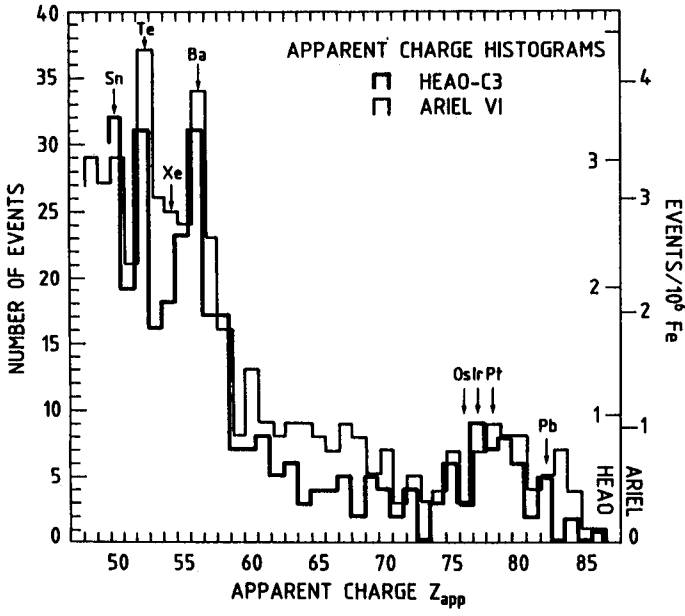

Fig. 9 The brutto "apparent charge" (Z_{app}) histograms prior to any correction for $Z \gtrsim 48$, obtained by both the HEAO-C3 and the Ariel VI experiments (Waddington et al. 9, ... ; Fowler et al. 2, 119). As can be seen, the charge resolution and the number of counts (Table 1) are comparable for both experiments in this charge range. There tends to be more Pb relative to Pt, and more secondaries with $Z \approx 62$-73 in the Ariel VI data. The latter point may be an energy dependent effect(see § I-4.2. and fig.11).

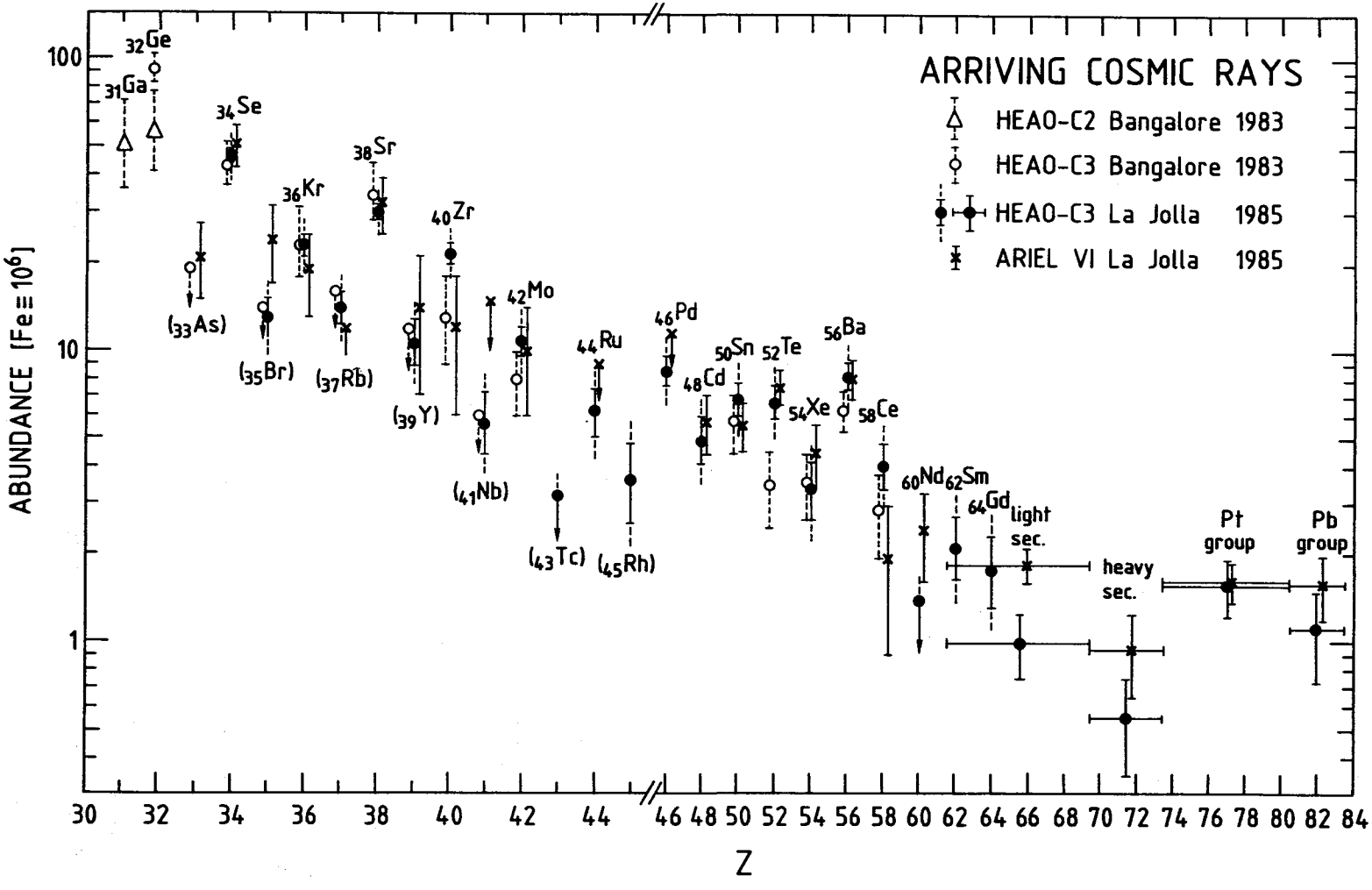
ARRIVING COSMIC RAYS
HEAO-C2 Bangalore 1983
HEAO-C3 Bangalore 1983
HEAO-C3 La Jolla 1985
ARIEL VI La Jolla 1985
ABUNDANCE [Fe≡10⁶]
Z
100
10
1
30 32 34 36 38 40 42 44 46 48 50 52 54 56 58 60 62 64 66 68 70 72 74 76 78 80 82 84
31Ga
32Ge
34Se
36Kr
38Sr
40Zr
42Mo
46Pd
48Cd
50Sn
52Te
54Xe
56Ba
58Ce
60Nd
62Sm
64Gd
(33As)
(35Br)
(37Rb)
(39Y)
(41Nb)
(43Tc)
(45Rh)
light sec.
heavy sec.
Pt group
Pb group

At lower Z = 34 to 64, the HEAO-C3 group is now developing a new technique of analysis in order to take advantage of their full statistics, by using the particles from the entire energy range covered by their detectors (Newport et al. 2, 123). Medium energy particles were previously excluded from the analysis, because their individual charge and velocity cannot be unambiguously determined from their ionization chamber and Cerenkov signals. The authors now perform a maximum likelihood adjustment of the elemental abundances, that accounts best for the entire ionization chamber-Cerenkov two-dimensional histogram. The useful statistics is thus almost doubled. But, of course, the method is delicate, and no conventional "charge histograms" can be produced.

Very preliminary elemental abundances obtained by this method are shown in figure 10, together with the "classical" earlier data presented at the Bangalore conference (Binns et al. 1983; Stone et al. 1983). These data have been presented at the Conference, but are not in the proceedings. The stated errors are only statistical ones within a given fitting model, and the final uncertainties will certainly be larger (E.C. Stone, private comm.; see caption of fig. 10).

Fig. 10 Abundances of arriving cosmic-rays with Z ≥ 31, deconvolved from the original "apparent charge" histograms or matrices (e.g. fig. 9). For Z ≤ 45 both even and odd-Z element abundances are given, but (except for $_{31}$Ga measured by the HEAO-C2 instrument with adequate resolution) none of the given odd-Z abundances should be considered really significant ; they are rather order of magnitude estimates that improve the estimate of the even-Z element abundances. For Z ≥ 46, only even-Z element abundances are given ; they include those of adjacent odd-Z elements (the systematic bias thus introduced is generally small with respect to the uncertainties). The HEAO-C2 points for $_{31}$Ga and $_{32}$Ge are from Byrnak et al. (1983b). The HEAO-C3 Bangalore Conference points are from Binns et al. (1983) and Stone et al. (1983). They are derived from charge histograms of a fraction of the data (see § I-4.1.). The new HEAO-C3 points up to Z = 64 are very preliminary results of a new two-dimensional analysis of the entire set of data (Newport et al. 2, 123). The stated errors are only statistical ones, within a particular fitting model ; the final errors will be larger (E.C. Stone, private comm.), which I have recalled by plotting an arbitrary dashed prolongation to the statistical error bars. This is in particular true for the odd-Z elements, whose abundances are highly dependent upon the fitting procedure; some of them were implausibly low in the authors' original graph. I have taken the liberty to raise them to a plausible level; the resulting corrections on the adjacent even-Z element abundances are not large (<18%). But I stress that the intrinsic charge resolution of the instrument is quite adequate to resolve even-Z elements (see Binns et al. 1983, 1984 ; Stone et al. 1983). The deconvolved Ariel VI data, with poorer intrinsic charge resolution below Z = 48, give comparable abundances for even-Z elements up to Z = 60 (Fowler et al. 2, 115, 119). For Z ≥ 62, where charge resolution and statistics are becoming poor in both experiments (fig. 9), I have followed the choice of the HEAO-C3 team and plotted only average abundances (per even-Z element) over broad, physically significant, ranges of elements (Table 1 ; Klarman et al. 2,127 ; Waddington et al. 9,...; Fowler et al. 2, 119). The normalisation to Fe of the HEAO-C3 data for Z ≥ 62 is not perfectly determined (corrections for interactions within the detector). Based on discussions, I have applied a global correction factor of 1.20 ± 0.15 to the HEAO-C3 figures relative to Fe (Table 1). For the sake of clarity, all error bars extending over a factor of ≥ 4 have been replaced by upper limits. The higher "secondary element" fluxes observed by Ariel between Z = 62 and 73 is probably an energy dependent effect (see § I-4.2. and fig. 11).

I-4.2. UH data, overview

The general picture apparent from fig. 10 can be described as follows. Up to Z ≈ 45, the intrinsic resolution of the HEAO-C3 instrument is significantly superior to that of Ariel VI (Binns et al. 1983, 1984 ; Fowler et al. 2, 115). The new two-dimensional analysis of the entire set of HEAO-C3 data (Newport et al. 2, 123) yields quite small statistical errors and is very promising, although the additional non-statistical errors have not yet been assessed. For even Z-elements, these new values are generally in good agreement with both the earlier HEAO-C3 analysis and the Ariel VI data, except for $_{40}$Zr, for which the earlier errors were very large. Tentative odd-Z-element abundances have been plotted in figure 10, but the instrument resolutions are such that none of them can be considered significant (except for $_{31}$Ga, observed with adequate resolution, though low statistics, by the HEAO-C2 experiment ; Byrnak et al. 1983b). Rough odd-Z-element abundance estimates are however useful to improve the fit of the even-Z-element abundances (which are not much affected by the associated uncertainties, except perhaps for $_{40}$Zr).

In the range Z = 46 to 60, where only even-Z-elements are given in figure 10, the resolution of the two experiments is becoming almost comparable (fig. 9). There is a very good agreement between the two experiments on the main s- and r-process peak elements from Z = 50 to 56 (in particular $_{52}$Te is no longer low in the HEAO-C3 analysis).

Beyond Z = 62, figure 9 clearly shows that in both experiments, neighbouring even-Z-elements are no longer well resolved (see, e.g., near Z = 75 and Z = 80), and that the statistics is low. There may, in addition, be small systematic shifts of the charge scale (see, e.g. $_{82}$Pb) (e.g., Newport et al. 3, 287). Accordingly, only abundances for the wide,

Table 1 - The data on UH nuclei with Z ≥ 62

Z_{app} [a]	Denomination	HEAO-C3 [b]				ARIEL VI [c]			
		brutto counts	relative corrected	normal.to Fe corrected		brutto counts	relative corrected	normal.to Fe corrected	
26	Fe	(9.6 ± 0.5).10^6	-	≡ 10^6	≡ 10^6	8.68.10^6	-	≡ 10^6	≡ 10^6
62-69	"Light Sec."	34	0.33 ± 0.06	4.0 ± 1.0	5.1 ± 1.1	63	0.44 ± 0.06	7.4 ± 1.0	9.3 ± 1.0
70-73	"Heavy Sec."	10	0.09 ± 0.03	1.1 ± 0.4		18	0.11 ± 0.04	1.9 ± 0.6	
74-80	"Pt group"	42	0.46 ± 0.07	5.5 ± 1.2	6.9 ± 1.5	46	0.34 ± 0.05	5.7 ± 0.9	7.7 ± 1.0
81-86	"Pb group"	10	0.12 ± 0.04	1.4 ± 0.5		22	0.12 ± 0.04	2.0 ± 0.5	
62-86	Sum Z ≥ 62	96	≡ 1.00	12.0 ± 2.3	12.0 ± 2.3	149	≡ 1.00	17.0 ± 1.4	17.0 ± 1.4
(62-73)/(74-86)	Sec/"PtPb"	-	0.73 ± 0.15	-	-	-	1.21 ± 0.20	-	-
(81-86)/(74-80)	"Pb"/"Pt"	-	0.25 ± 0.09	-	-	-	0.35 ± 0.10	-	-
≥ 87	Actinides	0.5 [d]	-	∿ 0.06	-	3	-	0.4 ± 0.2	-

[a] Z_{app} = "apparent charge", not including possible non-Z^2 effects in the real charge scale (e.g., Newport et al. 3, 287).
[b] Klarman et al. 2 , 127 ; Waddington et al. 9,... . The authors have applied a correction for the effect of nuclear interactions in their, comparatively thick, detector on the relative abundances of Z ≥ 62 nuclei. The effect of the interactions on the abundances with respect to Fe is not straightforward. Based on discussions, I have applied an additional global correction factor of 1.20 ± 0.15.
[c] Fowler et al. 2, 119. The corrections include deconvolution of the "apparent charge" histogram, and corrections for nuclear interactions in the, comparatively thin, detector.
[d] Fixsen et al. (1983) have observed 1 actinide nucleus for 17.4·10^6 Fe nuclei.

physically significant charge ranges defined by the HEAO-C3 team have been plotted in figure 10. They are defined in Table 1, which gives also key abundance ratios.

Figures 9 and 10 show that both experiments agree well on the "Pt-group" element abundances, and that Pb is better defined and somewhat higher in the Ariel VI data.

As regards secondaries, in the Z = 62-73 region, they are also higher in the Ariel VI data. Now, recall that the HEAO-C3 data are taken when the rigidity cut-off R_c is > 5 GV (median energy of the recorded particles ∿ 6 GeV/n), while the Ariel VI data include locations with much lower cut-off (median energy of the particles ∿ 2 GeV/n). When only location where R_c > 5 GV are selected in the Ariel VI data, the difference with respect to HEAO-C3 seems to disappear (fig. 11; P.H. Fowler, private comm.). So, the data simply seem to indicate an increase of the secondary/primary ratios towards lower energies. (See discussion in terms of a low energy increase of the grammage and especially cross-sections in § III-2.3.2.).

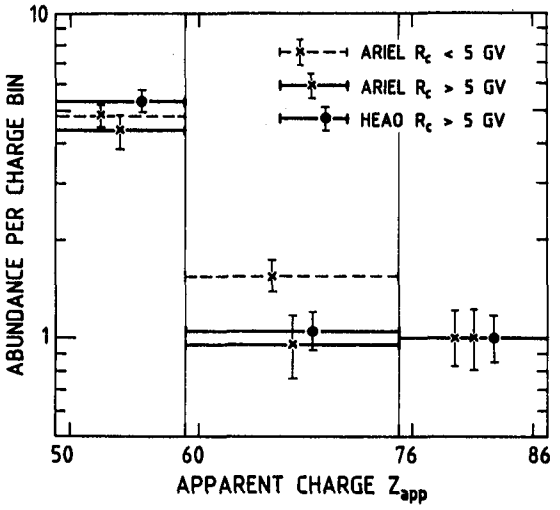

Fig. 11 Comparison between the Ariel VI data obtained at low cut-off rigidities R_c < 5 GV and the Ariel VI and HEAO-C3 data obtained at high R_c > 5 GV. Brutto data, averaged over wide charge ranges, are used. Normalized to the Pt-Pb region (Z_{app} = 76 to 86). Based on P.H. Fowler, private communication. The HEAO-C3 and Ariel VI data obtained at equal, high R_c agree.

The total abundance of nuclei with Z = 62-83, both primary and secondary, is marginally higher in Ariel VI (17.0 ± 2.6) than in HEAO-C3 (12.0 ± 2.0, relative to Fe = 10^6). These figures give a rough indication of (strictly, a lower limit to) the abundance of primary nuclei emitted at the sources). The small difference between Ariel VI and HEAO-C3 cannot be simply accounted for in terms of more spallation at low energy, which would produce the opposite effect. It might, however, have to do with the energy dependence of the shape of the mass yield (Kaufman and Steinberg 1980), on which the data of Kertzman et al. (3, 95) give information at 1 GeV/n only (§ I-3.1.; fig. 7).

As regards Actinides, the Ariel VI team has 3 candidates (Fowler et al. 2, 119). The HEAO-C3 team reported 1 candidate in Bangalore (Fixsen et al. 1983). See Table 1. The HEAO-C3 value for the ratio (Th+U)/(Pt+Pb group) is close to the LG value ∿ 10^{-2}, the Ariel value is ∿ 4 times higher.

I-5. DEUTERIUM, HELIUM-3 AND ANTI-PROTONS

Beatty (2, 56), Evenson et al. (2, 60) and Mewaldt (2, 64) have provided new data on low energy D and ^{3}He, which are purely secondary isotopes. The conclusion of the three studies is that most of the existing low energy D and ^{3}He data are readily accounted for by standard propagation and modulation models that account for the heavier nuclei abundances (escape length $\lambda_e \approx 6$ to 8 g.cm^{-2}). [2]

The high ^{3}He/^{4}He ratio $\approx 0.24 \pm 0.05$ at 6 GeV/n (Rigidity $\sim$ 13 GV) recently reported by Jordan and Meyer (1984) and Jordan (1985) is most probably an overestimate. The authors have indeed stressed that this result is highly sensitive to the value of the ^{4}He rigidity spectral index γ_R near Earth at the time of the observation (with $d\Phi/dR \propto R^{-\gamma_R}$), in the sense of a positive correlation between the derived value of ^{3}He/^{4}He and γ_R. To get the above value of the ^{3}He/^{4}He ratio, the authors have assumed that $\gamma_R = 2.65$ around 13 GV, near Earth, in April 1981. Now, Golden et al. (2, 1) have measured $\gamma_R = 2.58 \pm 0.05$ between 10 and 25 GV, in September 1976. [3] The value of γ_R near 13 GV in April 1981 can be only lower, because the spectrum is bent within the above rigidity range, and because of the much higher degree of solar modulation in 1981 (e.g. Lockwood and Webber 1984). Earlier measurements, as summarized by Smith et al. (1973) or Webber and Lezniak (1974), also clearly point towards lower values of $\gamma_R \sim 2.40$ to 2.50 at 13 GV, near Earth.

The standard leaky-box models fitting the B/C ratio with rigidity dependent escape yield ^{3}He/^{4}He $\approx 0.17 \pm 0.05$ at 6 GeV/n (scaled from Meyer 1974 ; Lagage and Cesarsky 1985). [4] Jordan (1985)'s observations lead to values of ^{3}He/^{4}He in this range for values of γ_R between 2.52 and 2.62, a perfectly plausible range for γ_R at the time of his observations. There is therefore no hint whatsoever for an anomaly.

Jordan (1985)'s data, together with the low energy data on D and ^{3}He, can be used to set lower limit to the intrinsic thickness of the thick sources invoked to explain a possible cosmic-ray anti-proton excess (Cowsik and Gaisser 1981 ; Cesarsky and Montmerle 1981 ; Tan and Ng 1983; Lagage and Cesarsky 1985 ; Tan 2, 346).

---

[2] There is, however, a problem for the high deuterium fluxes observed by Webber and Yushak (1983), which, like the earlier data of Hsieh et al. (1971), remain a mystery. Such data could be understood only if, at the time of the data taking, the interplanetary deceleration was so weak that the bulk of the deuterons due to the $p + p \rightarrow d + \pi^+$ process, with energies below $\sim$ 200 MeV/n in the interstellar medium, were still observable near Earth (Meyer 1975; Webber and Yushak 1983). This would be extremely difficult to accept, considering all evidences on solar modulation. In addition, Evenson et al. (2,60) noted the constancy of their observed D/^{4}He and ^{3}He/^{4}He ratios between 1978 and 1983 (a period which, however does not include extreme solar minimum conditions, e.g. Lockwood and Webber 1984).

[3] The larger value published by Golden et al. (2,1) in the proceedings is not that measured near Earth, but refers to the derived demodulated He spectrum. These results replace those published by Badhwar et al. (1979).

[4] With the assumption of rigidity dependent escape, the equilibrium ^{3}He/^{4}He ratio at a given energy/nucleon is 20% higher than predicted based on the formation rates only, because the residence time of ^{3}He in the galaxy is longer than that of ^{4}He at the same energy/nucleon. (Therefore, if the bulk of the grammage is spent near the sources, where the rigidity dependent escape takes place, the predicted ratio near Solar System is ^{3}He/^{4}He = 0.14 only.)

I-6. ENERGY SPECTRA OF PRIMARY NUCLEI

At this conference, a number of studies have been devoted to this subject : Golden et al. (2, 1) ; Engelmann et al. (2, 4) ; Webber et al. (2, 16) ; Derrickson et al. (2, 20) ; Burnett et al. (2, 32, 48) ; Sato et al. (2, 36); Streitmatter et al. (2, 40); Vernov et al. (2, 52).

Although I regard this subject as important, I will not discuss it here. [5]

I-7. ELECTRONS AND POSITRONS

Nishimura et al. (9, ...) have provided improved e^- spectra up to 2000 GeV (fig. 12). The presence of e^- fluxes at such high energies, where the e^- lifetime against synchrotron loss is $\lesssim 10$ years, implies that their sources are close by, within a few 100 pc. These data, confronted with the constraints from CR nuclei, also favour a nested leaky-box model for propagation, a standpoint already advocated by Nishimura et al. (1981), Tang and Müller (1983), Müller and Tang (1983), Mauger and Ormes (1983), and Tang (1984).

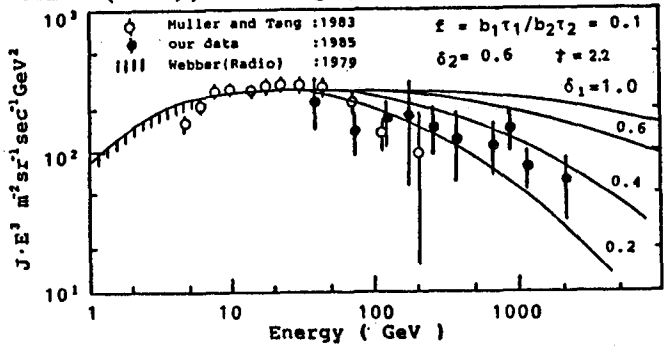

Fig. 12 New data on the high energy electron spectrum up to 2000 GeV by Nishimura et al. (9,...).

Golden et al. (2, 374) and Müller and Tang (2, 378) have provided new measurements of the $e^+/(e^+{+}e^-)$ ratio between 5 and 20 GeV (fig. 13). The high values observed for this ratio are probably due to a rapid decrease of the e^- flux above a few GeV.

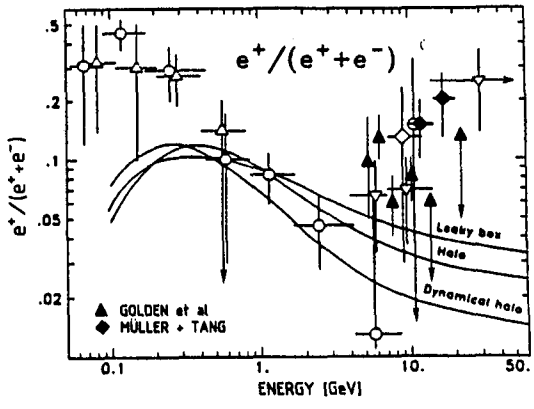

Fig. 13 The new observations of the $e^+/(e^+{+}e^-)$ ratio between 5 and 20 GeV by Golden et al. (2, 374) and Müller and Tang (2, 378), along with earlier data.

[5] This is the shortest paragraph in my report!

PART II

ASSESSING THE GALACTIC COSMIC-RAY SOURCE (GCRS) ELEMENTAL COMPOSITION CORRELATION WITH FIRST IONIZATION POTENTIAL (FIP)

II-1. GCRS ELEMENTAL COMPOSITION UP TO Z = 30

Up to Z = 30 the cosmic ray data are very reliable and a comparison is possible with Solar Energetic Particles (SEP) abundances. After having specified the Local Galactic (LG) abundances I shall use as a reference (§ II-1.1.), I am going to discuss the various available determinations of the elemental composition (fig.14) as to obtain an "adopted" GCRS composition (fig. 15 ; § II-1.2.). I shall then compare the GCRS, SEP and Solar Coronal compositions (fig. 17 ; § II-1.3.) and discuss their common properties (§ II-1.4.).

II-1.1. The Local Galactic (LG) reference abundances used

The LG abundances used for reference are mostly those of Meyer (1979a,b ; 1985a,b), generally in good agreement with recent analysis of Anders and Ebihara (1982) and Grevesse (1984a,b). For S, Cu and Zn, the improved agreement between the recent type I carbonaceous chondrite (hereafter C1) and photospheric determinations have led me to slightly modify the values and considerably reduce the error bars : S = 45 (1.15) [6], Cu = 0.047 (1.10), Zn = 0.124 (1.08) on the scale Si = 100. Note, however, that there is an apparently significant difference between C1's and photosphere for Fe, which seems higher by a factor of 1.45 ± 0.11 in the Photosphere than in C1's!!!. This is all the more a puzzle since the siderophile elements Cr, Co, Ni, Pd definitely do not show the same trend, and are found equally abundant in C1's and Photosphere (Grevesse 1984a). By contrast, there seems to be another significant discrepancy for Ti, a refractory, not siderophile element. As regards the C1 and photospheric abundances of volatile Ge and Pb, see Grevesse and Meyer (3, 5) and § III-3.5. .

In figures 14 and 15, I have kept the traditional C1 value to LG Fe, but have also indicated where Fe would lie if the photospheric value would be adopted as a reference instead.

II-1.2. GCRS composition up to Z = 30: the data and the adopted composition

Figure 14 gives up to date information on the GCRS/LG abundance ratios for elements up to Zn, versus First Ionization Potential (FIP). I have avoided, as much as possible, determinations based on low energy data ($\leqslant$ 500 MeV/n), whose interpretation may pose specific problems related to strongly energy dependent low energy cross-sections and possible distributed reacceleration (Silberberg et al. 1983). As will be shown in the discussion of the B vs. ^{15}N problem (§ III-2.1.), this hypothesis may have to be taken very seriously.

[6] Throughout this paper such figures between parentheses denote error factors: "within a factor of...".

II-1.2.1. Source abundances derived from elemental data

The basic determinations used are those from the HEAO-C2 experiment, derived from high energy observations between 1 and 25 GeV/n (Engelmann 1984 ; Lund 1984). At this conference, Webber et al. (3, 42) have reestimated the source abundances, based on the HEAO-C2 data specifically at 1.5 GeV/n, taking into account their new cross-section measurements up to $\sim$ 0.8 to 1.3 GeV/n (Webber and Kish 3, 87 ; see § I-3.1.). They have assumed that the trend for an enhanced production of secondaries with Z = 12 to 14 observed in the spallation of ^{28}Si and ^{40}Ar was also valid for other neighbouring parent nuclei. This leads, in particular, to a decrease of the estimated source Al abundance (fig. 6). Whenever different from the previous values, these new estimates of the GCRS/LG ratios have been given in fig. 14. HEAO-C3 data have also been used for Zn (Binns et al. 1984), as well as for Ar and Ca, for which the data of Jones et al. (2, 28) up to $\sim$ 200 GeV/n, i.e. at highest energies where the secondary component is much reduced, should in principle yield very accurate source abundances. However, for the reasons discussed in § I-1., I think these latter determinations should be considered preliminary at the present stage.

II-1.2.2. Source abundances derived for isotopic data

For N, Ar and Ca, we have also source abundance determinations based on low energy ($\sim$ 200 to 600 MeV/n) isotopic observations of ^{14}N, ^{36}Ar and ^{40}Ca, which are the predominant isotopes in the sources. These source abundance determinations should, in principle, be much more accurate than those based on elemental observations only, since the secondary component to be subtracted is comparatively much smaller.

As regards Ca, the cross-sections for secondary formation of ^{40}Ca are extremely small so that, while surviving primaries make up only 30 to 55% of arriving elemental Ca for energies from 1 to 25 GeV/n, they make up 95% of arriving ^{40}Ca at 0.6 GeV/n (fig. 16). ^{40}Ca is thus essentially a pure primary, and the Ca source abundances derived from ^{40}Ca isotopic data are therefore extremely clean (e.g., Krombel and Wiedenbeck 2, 92). They are essentially limited by the statistics of the isotopic observations (the mass resolution is generally adequate to separate mass 40 from $\geq$ 42, ^{41}Ca being very scarce; figs. 2 and 3). Following the summary by Krombel and Wiedenbeck (2, 92), I have plotted in fig. 14 the Ca GCRS/LG ratios resulting from the five available isotope measurements (Tarlé et al. 1979 ; Young et al. 1981 ; Webber 1981 ; Webber et al. 2, 88, source ^{40}Ca/Fe = 0.113 ± 0.027 derived by myself ; Krombel and Wiedenbeck 2, 92).

As regards Ar, the situation is less favourable: while surviving primaries make up $\sim$ 25 to 55% of arriving elemental Ar for energies from 1 to 25 GeV/n, they still make up only 50% of arriving ^{36}Ar at 0.6 GeV/n (fig. 16). So, the secondary contribution remains important, even for ^{36}Ar. The two available determinations (Webber 1981; Webber et al. 2, 88, source ^{36}Ar/Fe = 0.062 ± 0.024 derived by myself) thus give source Ar values which are sensitive to the conditions of propagation and secondary formation at low energy. I shall show in § III-2.1. that these conditions pose very serious problems.

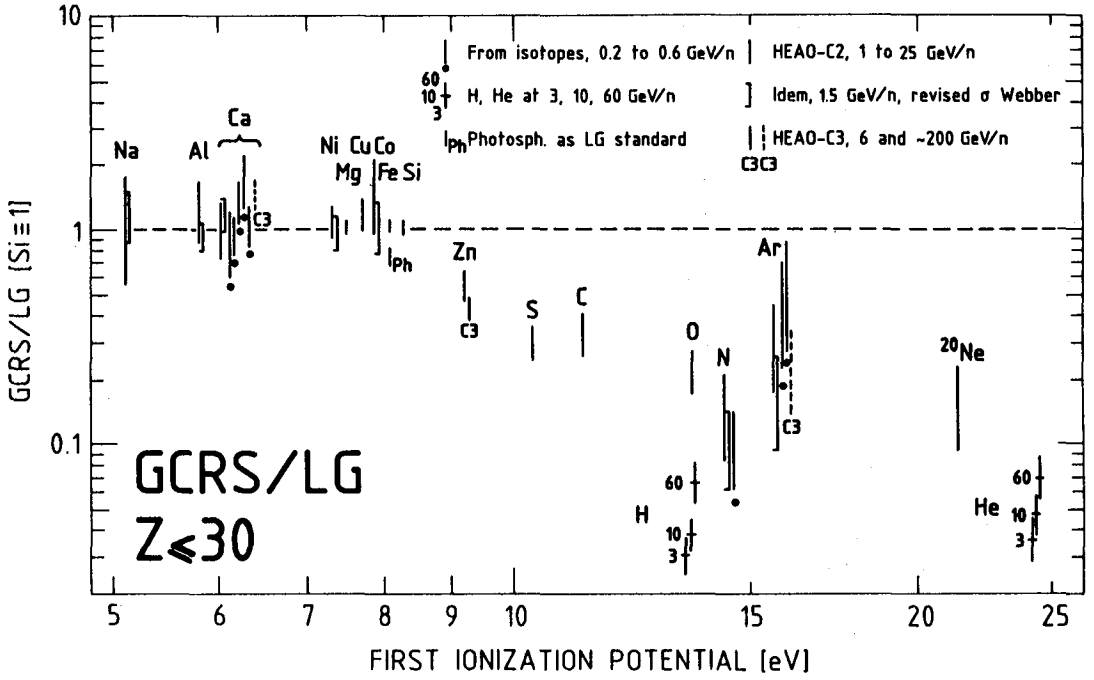

Fig. 14 GCRS/LG abundance ratios vs. FIP, for Z ≲ 30 : the various determinations. Normalized to Si. The errors are the quadratic sum of the GCRS and the LG errors (§ II-1.1.). For Fe, I have also plotted its GCRS/LG ratio if the photospheric value is taken as LG standard (marked by "Ph" ; § II-1.1.). For Ne, for which the minor isotope ^{22}Ne is greatly in excess (§ III-4.1. ; fig. 29), the plotted ratio refers to the dominant isotope ^{20}Ne only. [As regards Mg and Si, possibly also slightly isotopically anomalous (fig. 29), considering only the dominant isotopes ^{24}Mg and ^{28}Si would yield a negligible correction]. As regards H and He, they are given at a given energy/nucleon for three different energies (3, 10 and 60 GeV/n), based on the data compiled and propagated back to the sources by Engelmann et al. (1985) (see § II-1.2.3.). The various determinations of the GCRS abundances : for each element, the first bar on the left is the HEAO-C2 determination based on observations over the range from ∿ 1 to 25 GeV/n (Engelmann 1984 ; Lund 1984). Next comes, as a left-oriented bracket, the new estimate by Webber et al. (3, 42), based on the HEAO-C2 data at 1.5 GeV/n and on new cross-sections, especially from Webber and Kish (3, 87) (see § I-3.1. and II-1.2.1.). It is given only when the new estimate differs significantly from the original one. Next come, marked by a dot below the error bar, source abundances derived from low energy (∿ 200 to 600 MeV/n) isotope observations (see § II-1.2.2.). For Ca, they are, from left to right, due to Tarlé et al.(1979), Young et al. (1981), Webber (1981), Webber et al. (2, 88), and Krombel and Wiedenbeck (2, 92), and for Ar to Webber (1981) and Webber et al. (2, 88) (see discussion in § II-1.2.2. and III-2.1.). For N, the isotope bar summarizes a number of low energy isotope studies (see § III-2.1. and 2.2.). Finally, the bars marked "C3" result from the HEAO-C3 data, at GeV/n energies for Zn (Binns et al. 1984), and at ∿ 200 GeV/n for Ca and Ar (Jones et al. 2, 28) ; the latter two values, with dashed error bars, are still preliminary (see § I-1. and II-1.2.1).

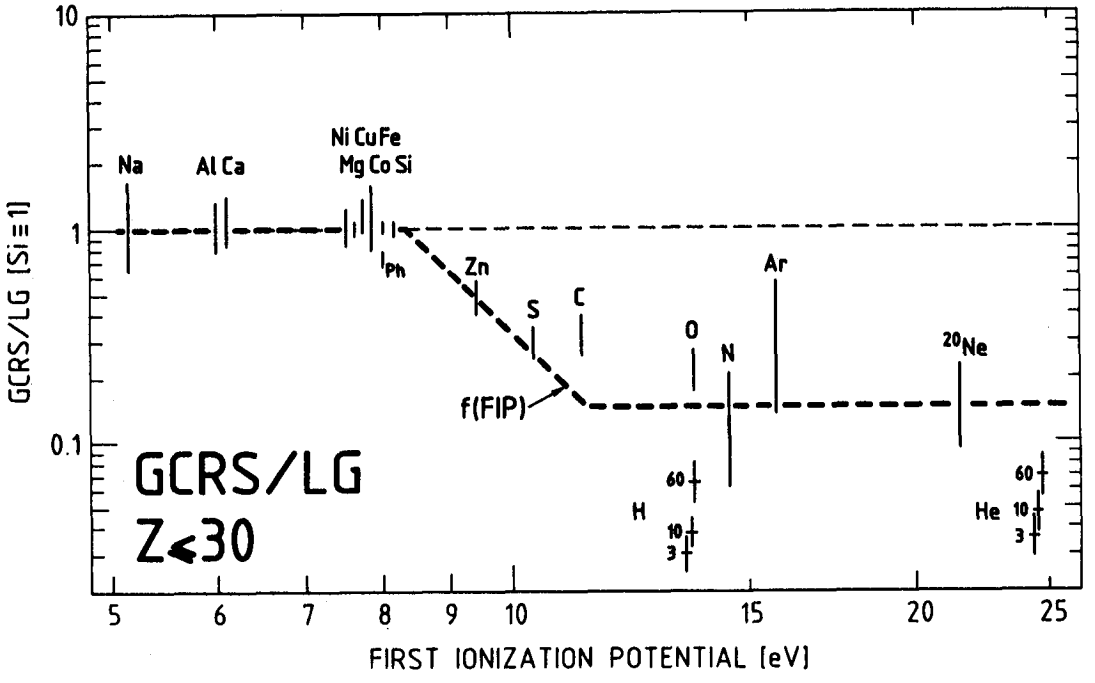

Fig. 15 GCRS/LG abundance ratios vs. FIP, for Z ≤ 30 : adopted values, derived from fig. 14. See caption of fig. 14, and text § II-1.2.4.. Also plotted is f(FIP) the adopted shape of the correlation between GCRS/LG vs. FIP for Z ≤ 30 (§ II-1.4.). As discussed in this §, f(FIP) does not fit C, O, H and He (see also fig. 17).

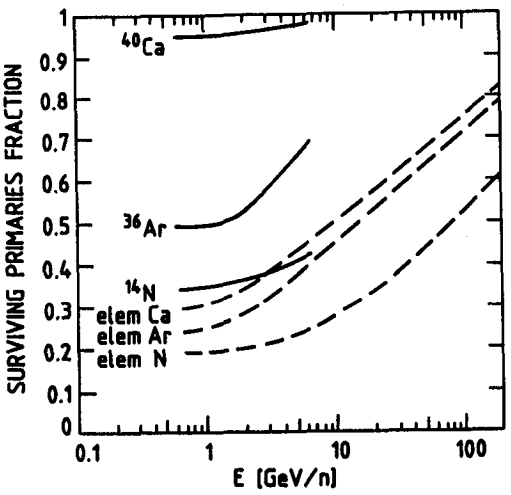

Fig. 16 Fraction of surviving primaries among arriving GCR's for elemental ^{14}N, Ar, Ca (dashed), and for isotopic ^{14}N, ^{36}Ar, ^{40}Ca (solid) as a function of energy (§ II-1.2.2. and III-2.2.). The assumed source ratios are ^{14}N/O = 6.0%, ^{36}Ar/Fe = 2.8%, ^{40}Ca/Fe = 6.3%.

The situation is even worse for N: surviving primaries make up $\sim$ 20 to 35% of arriving elemental N for energies from 1 to 25 GeV/n, but still make up only $\sim$35% of arriving ^{14}N at 0.6 GeV/n (fig. 16). Actually, the lower source N/O ratios ($\sim$ 3%) found from low energy isotopic ^{14,15}N data, and their contrast to higher values ($\sim$ 6%) derived from high energy elemental measurements have been discussed at length in recent years. I shall discuss that point in detail in § III-2., from a new standpoint.

II-1.2.3. Hydrogen and Helium at sources

Now consider H and He. According to current shock wave acceleration theories, the relevant parameter for acceleration is momentum per nucleon (or, equivalently, energy per nucleon), not rigidity (e.g. Krimsky 1977 ; Axford et al. 1977 ; Bell 1978a,b ; Blandford and Ostriker 1978 ; Axford 1981). It is therefore preferable not to discuss the source H/He ratio at a given rigidity, and I shall consider this ratio at a given energy/nucleon. But rigidity dependent escape from the galaxy (which acts differently on H and He at a given energy/nucleon) is essential in properly deriving the source H and He spectra from the observed ones. The study of Engelmann et al. (1985 ; see their fig. 12) shows that, when this is done, the H and He source spectra, in the range in which they are both precisely determined ($\sim$ 3 to 60 GeV/n), are such that : (i) The H/He ratio is remarkably constant and normal ($\approx$10); (ii) the abundance ratios of H and He to CNO are energy dependent; they increase by a factor of $\sim$ 2 (1.5) between 3 and 60 GeV/n (based on all existing data for the CNO spectrum, not merely those of HEAO-C2, which tend to be steeper than the other ones; Engelmann et al. 1985, and 2,4). Note that no significant energy dependence of any heavy element/heavy element source abundance ratio could ever be noticed between $\sim$ 0.5 and $\sim$ 25 GeV/n. This energy dependence of the H,He to heavier nuclei ratios has been shown in figs. 14 and 15.

II-1.2.4. "Adopted GCRS composition for Z $\lesssim$ 30

Based on the detailed data on GCRS composition presented in fig. 14, I derive an "adopted" set of elemental GCRS/LG ratios for Z $\lesssim$ 30, which is shown versus FIP in fig. 15. In these adopted abundances I have taken into account, though with some prudence, the trends associated with the new cross-section estimates by Webber and Kish (3, 87) and Webber et al. (3, 42), in particular as regards the lower Al abundance. For Ca, I have kept an error bar which is consistent with all elemental and especially isotopic determinations. For the more difficult cases of N and Ar, for which the interpretation of the isotopic data depends strongly on low energy propagation (§ III-2.1.), I have kept very large error bars, encompassing essentially the entire range of existing estimates. In fig. 15, I have also marked the position of Fe if the photospheric value is taken as a standard, instead of the C1 meteoritic value (§ II-1.1.; Grevesse 1984a) : Fe would then be deficient by a factor of $\sim$ 1.40 in GCRS, relative to Al, Mg, Si, Ca, Co, Ni, Cu.

II-1.3. Comparison with Solar Energetic Particles (SEP) and Solar Coronal compositions

Before discussing the properties of the obtained GCRS/LG correlation with FIP (§ II-1.4.), I want to compare the GCRS and the SEP abundances. It is now well established that the GCRS composition pattern versus FIP is remarkably similar to the basic pattern of SEP, as well as to the solar coronal composition, which differs from that of the photosphere and C1's ("Local Galactic") (Webber 1975, 1982b; Cook et al. 1979, 1980, 1984 ; Mc Guire et al. 1979, 1986; Mewaldt 1980 ; Meyer 1981a,b,c, 1985a,b ; Breneman and Stone 4, 213, 217). Using γ-ray line spectroscopy data, Murphy et al. (4, 249, 253) have, at this conference, found once again the same pattern of abundances in the upper chromosphere or lower transition region material (except for Ne, which is a problem!).

These similarities in composition, together with other arguments, led to the suggestion that SEP and GCRS compositions are, to first order, a reflection of the composition of solar-stellar coronae (F to M stars), out of which they have first been extracted (Meyer 1985b ; see also Montmerle, 1984). As regards the reason why the solar coronal composition is biased according to FIP, it is not known. Two scenarios are at present attempting to understand it, one in terms of a dynamical ionization model in spicules (Geiss and Bochsler 1984), the other in terms of gravitational settling of neutrals in the presence of the magnetic field within the chromospheric plateau (Vauclair and Meyer 4, 233).

Figure 17 compares the GCRS abundances to SEP abundances for $Z \lesssim 30$. Two sets of SEP abundances are taken: (i) the "mass-unbiased" baseline composition of Meyer (1981a, 1985a), which represents the composition of these events in which the abundances are least perturbed by rigidity (and hence, roughly Z -) dependent acceleration and propagation effects, as judged from their Fe/Mg,Si ratio [7] ; in these events the correlation of abundances with FIP, presumably an image of their coronal source material, is cleanest. (ii) the new 10-flare average presented at this conference by Breneman and Stone (4, 213, 217), who suggest that, on the average, rigidity dependent acceleration-propagation effects do not entirely cancel out in SEP's, so that the average SEP composition is slightly biased as a function of A/Q (or, roughly, Z) with respect to the original coronal composition (where Q = mean effective charge). (This conclusion however depends somewhat upon the adopting of the photospheric, rather than C1, value as a standard for Fe; the properties of this average over 10 flares will also have to be confirmed by a much broader averaging).

I now discuss the GCRS/SEP ratios plotted in fig. 17:

(i) Fig. 17 confirms that the two compositions are very similar. The strong dependence of the GCRS/LG ratio upon FIP (fig. 15) has to first order disappeared in the GCRS/SEP plot.

[7] Using the photospheric instead of the C1 value as a standard for Fe would only slightly modify the derived "mass-unbiased" baseline SEP composition (Meyer 1985a).

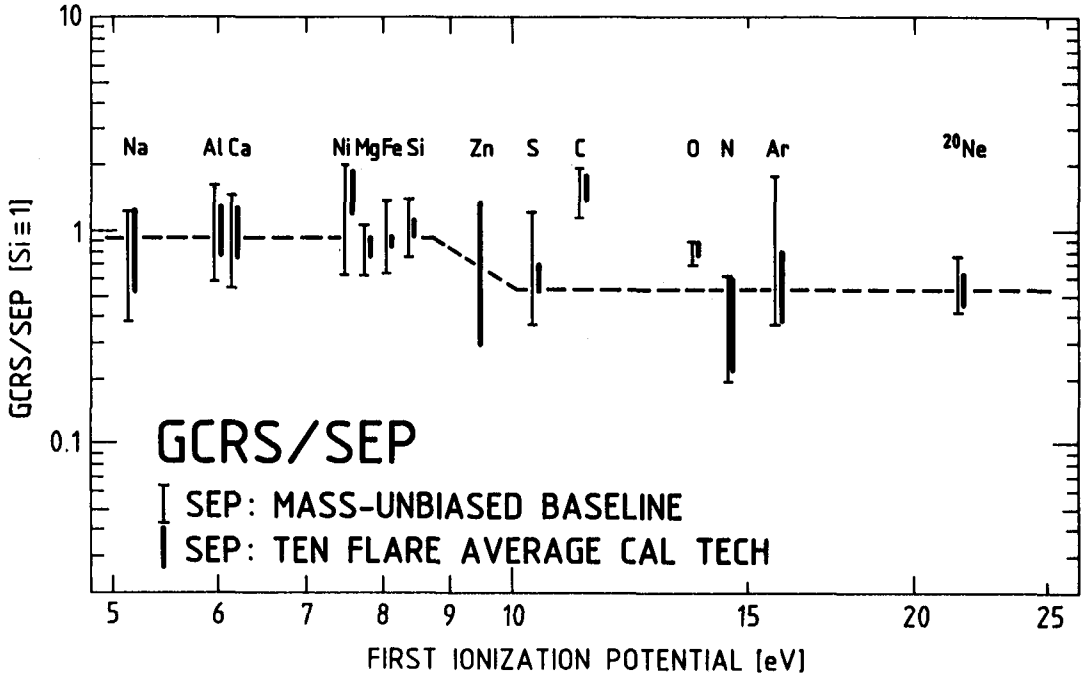

Fig. 17 GCRS/SEP abundance ratios, vs. FIP, for Z ≤ 30 (§ II-1.3). The GCRS values are those adopted in fig. 15 (with the errors on the LG denominator taken out). The SEP values are (i) the "mass-unbiased baseline" defined by Meyer (1985a), and (ii) the 10-flare average reported at this conference by Breneman and Stone (4, 213, 217). To zeroth order, the FIP-dependent bias has disappeared here. However the line, drawn to guide the eye, suggests that the depletion of high-FIP elements relative to low-FIP ones is slightly more pronounced in GCRS than in SEP's (by a factor of ∿ 1.5 ; Meyer 1985b ; Webber et al. 3, 42). C, and probably O, are above the correlation, i.e. are distinctly in excess in GCRS relative to SEP.

(ii) Fig. 17 shows that C (and, to a lesser extent, possibly O) is much above neighbouring "high-FIP" elements (FIP > 9 eV). In particular, the C/O ratio itself, extremely well determined in both GCRS and SEP's, is about twice as high in GCRS as in SEP's. See discussion in terms of the GCRS excess of ^{22}Ne and ^{25,26}Mg in § III-4.

(iii) Based on the other "high-FIP" elements ^{20}Ne, Ar, N and S, fig. 17 suggests that the depletion of "high-FIP" elements relative to "low-FIP" elements (FIP < 9 eV) is somewhat higher (a factor of ∿ 6 instead of ∿ 4) in GCRS than in SEP. This point, already noted by Meyer (1985b) is confirmed by the analysis of the new SEP data by Webber et al. (3, 42).

(iv) In this context the GCRS N abundance is very critical : if the correlation of GCRS/LG with FIP (fig. 15) and the similarity with SEP (fig. 17) are to hold, the GCRS/LG and GCRS/SEP ratios for N may not be lower than those for Ar and especially ^{20}Ne. This condition requires that N/O ≳ 6% at GCRS. It requires that the actual GCRS N abundance lies in the upper part of the adopted error bar, in agreement with the abundances derived from the high energy elemental observations (1-15 GeV/n), but in conflict with those derived from low energy (30 to 600 MeV/n) isotopic data (see discussion in § III-2.).

II-1.4. Shape of the GCRS/LG correlation with FIP for Z ≤ 30

At this conference, many papers have discussed the shape of the correlation between the GCRS/LG abundance ratio and FIP, based on data for Z ≤ 30 (Jones et al. 2, 28 ; Krombel and Wiedenbeck 2, 92 ; Webber et al. 3, 42) or for Z > 30 (Fowler et al. 2, 115 and 119 ; Klarman et al. 2, 127 ; Waddington et al. 9,... and 3, 1; Binns et al. 3, 13 ; Letaw et al. 1984).

As regards elements with Z ≤ 30, figs. 14 and 15 show that the Al and Ca abundances seriously tie down (to a factor of ≤ 1.4) any possible systematic excess of elements with lower FIP relative to elements with FIP ≈ 8 eV. In SEP's, in which no correction is required for spallation, there is not either any indication for such an excess (Meyer 1985a,b; Breneman and Stone 4, 213, 217; Mc Guire et al. 1986).

All exponential fits of the GCRS/LG pattern versus FIP are inadequate, as illustrated in fig. 18. They are totally unable to reproduce the steep drop in the Si, Zn, S, C, O, N region, together with the flat behaviour of GCRS/LG at lower and higher FIP's. Relative to Mg, Si, Fe (FIP ≈ 8 eV), exponential fits, either (i) fit more or less Zn, S, C, O, N and are much too low for Ar and Ne and too high for Na, Al, Ca, or (ii) fit Ar and Ne and are much too high over the entire region from Zn to N (fig. 18). The fit proposed by Letaw et al. (1984) is more adequate, but also somewhat high in this region.

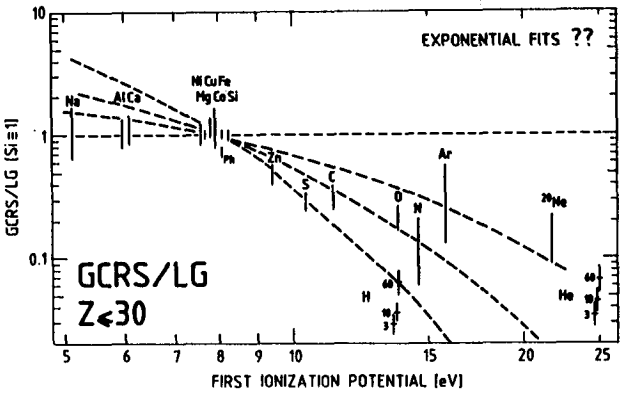

Fig. 18 Same as fig. 15, except that, instead of f(FIP), various exponential functions, normalized to the Mg Fe Si region, are tested to fit the behaviour of GCRS/LG vs. FIP for Z ≤ 30. None of them works (§ II-1.4.).

It seems to me that the obvious shape of the pattern of the GCRS/LG ratio versus FIP is that indicated as f(FIP) in fig. 15 : two plateaus at low and high FIP, with a narrow intermediate region (Zn, S). C and O, the two elements that are overabundant with respect to SEP's (fig. 17 ; § II-1.3.) have been left above the correlation curve f(FIP) ; such an excess of ^{12}C and ^{16}O is actually quantitatively predicted in connection with the ^{22}Ne and $^{25,26}Mg$ excesses, if the latter are due to the presence of a small fraction of He-burning material in GCRS, possibly originating in Wolf-Rayet stars (§ III-4. ; Meyer 1981c, 1985b ; Cassé and Paul 1982 ; Maeder 1983 ; Prantzos 1984a,b ; Prantzos et al. 1983 and 3, 167 ; Arnould 1984). The N abundance problem, mentioned in § II-1.3., will be discussed in § III-2.. H and He, whose abundances relative to

heavier elements vary with energy (§ II-1.2.3.) and which do not behave like heavier elements in SEP's (e.g., Mason et al. 1983 ; Meyer 1985a), are also left out of the correlation.[8]

This two-plateau structure of f(FIP) resembles that found in SEP's and solar corona (e.g. Cook et al. 1984 ; Meyer 1985b ; Breneman and Stone 4, 213, 217). Physically, it cannot be easily understood as representing simply the ionized fraction in a gas at a single temperature or with a monotonic distribution of temperatures (Arnaud and Cassé 1985 ; Meyer 1985b). It rather suggests a situation where ions and neutrals are selected with different efficiencies out of a plasma at ∿ 6000 K (Meyer 1985b ; Geiss and Bochsler 1984 ; Vauclair and Meyer 4, 233) (see § II-1.3.).

II-2. GCRS ELEMENTAL COMPOSITION FOR Z > 30 ("ULTRA-HEAVY" NUCLEI, UH)

II-2.1. The Local Galactic (LG) reference abundances used for UH nuclei

The LG abundances used for $Z \lesssim 30$ have been discussed in § II-1.1. For Z > 30, the C1 meteoritic values of Anders and Ebihara (1982) have been adopted; their error is usually much smaller than the GCRS error. Photospheric abundances, which are certainly a more undisputable image of the abundances in the protosolar nebula, are often lacking or still very inaccurate for UH nuclei; but, whenever they are accurately determined, they generally agree well with the C1 values (Grevesse 1984a,b). This may, however, not be always true, especially for volatile elements, and Grevesse and Meyer (3, 5), at this conference, have found possibly significant differences between C1 and photospheric abundances for Ge and Pb (§ III-3.5.).

As regards C2 meteorites, which are a mixture of 50% C1-like material, plausibly unfractionated, and of 50% highly fractionated "pebbles", there is no reason whatsoever to believe that their bulk composition might have any relevance as a standard (Anders 1971 ; Meyer 1979a,b ; Ebihara et al. 1982 ; Anders and Ebihara 1982). And C2 abundances indeed yield strange discontinuities at $_{46}$Pd-$_{47}$Ag refractory-volatile junction (Meyer 1979a). As regards the noble gases $_{36}$Kr and $_{54}$Xe, their abundances are interpolated, and the associated error difficult to assess.

II-2.2. The GCRS composition of UH nuclei

In fig. 10 (§ I-4.), I have summarized the recent observations of arriving UH nuclei. From these data, I have derived rough values of the source abundances of selected elements in the range Z = 31 to 58. The resulting GCRS/LG ratios have been plotted versus FIP in fig. 19, together with the data for $Z \lesssim 30$ and with the correlation f(FIP) adopted for these lighter elements (fig. 15). The case of Pt and Pb, for which, like most authors, I dare not derive some abundances relative to Fe or Si, will be discussed later (§ III-3.1.).

---

[8] In § III-4. and 5. and in the Appendix, f(FIP) will be expressed as f_{ik}(FIP), denoting the value of f(FIP) for species i normalized to that for a reference species k.

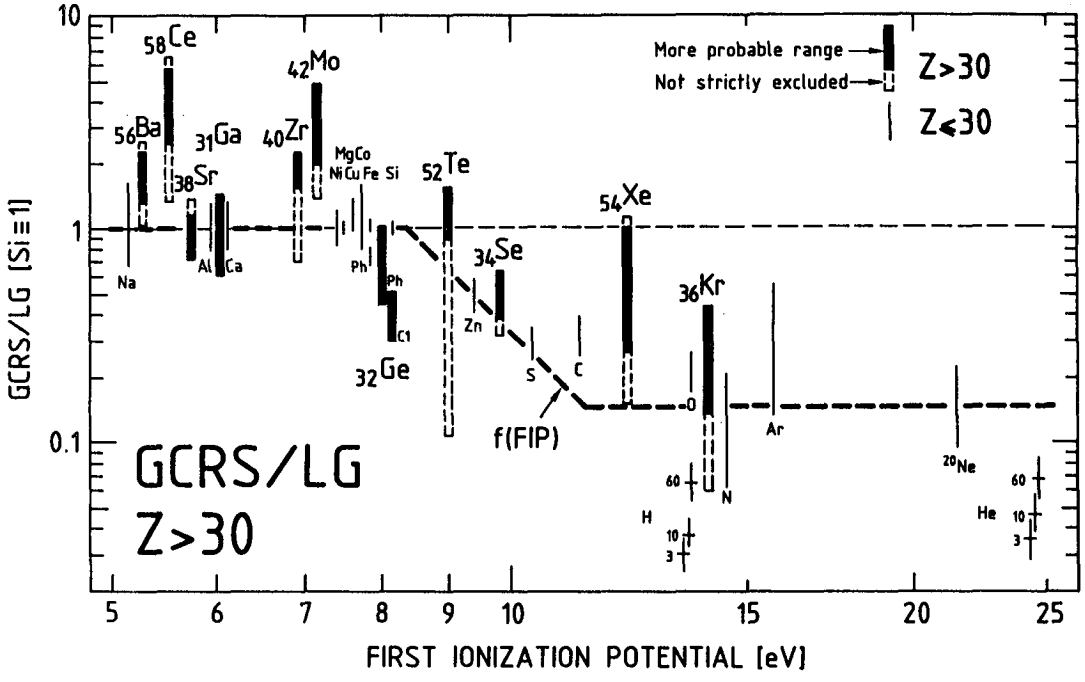

Fig. 19 GCRS/LG abundance ratios vs. FIP, for Ultra-Heavy (UH) elements with Z > 30 (thick bars), and for elements with Z ≤ 30 (thin bars, from fig. 15). The correlation f(FIP) defined in fig. 15 based on the data for Z ≤ 30 (§ II-1.4.) has also been reproduced. See caption of fig. 14. For UH elements, the thick, solid bars indicate the more probable ranges, based on the new, preliminary analysis of the HEAO-C3 data by Newport et al. (2, 123) and on conservative estimates of the spallation correction (cf. Israel et al. 1983). The dashed, white prolongations give ranges that cannot yet be strictly excluded, considering all the data in fig. 10 (Ariel VI data, Fowler et al. 2, 115,119; earlier analysis of the HEAO-C3 data ; see § I-4.) and broader assumptions for the spallation correction (§ II-2.2.). For Ge and Fe, the values of the GCRS/LG ratio is also given if the photospheric measurement ("Ph") is adopted as LG standard, instead of the more usual meteoritic value ("C1") ; see footnote # 10 (§ II-1.1., 2.1. ; III-3.5.).

The solid error bars for UH elements in fig. 19 correspond to what I believe to be the more probable range for their source abundances, based on the new, preliminary analysis the HEAO-C3 data by Newport et al. (2, 123) [9], and on conventional corrections for spallation adapted from those of Israel et al. (1983). For many elements the results of Newport et al. (2, 123) are actually in good agreement both with the earlier analysis of the HEAO-C3 data and with the Ariel VI data (fig. 10 ; § I-4.). For many elements too, the spallation corrections are not very large, so that they cannot be a major source of uncertainty.

For a few elements, however, there are large differences between sets of data (especially $_{40}Zr$, $_{52}Te$, $_{58}Ce$) and/or large spallation corrections which could be very significantly altered by slightly different

[9] To account for possible systematic errors in the fitting procedure, a standard 20% error has been quadratically added to the purely statistical errors of Newport et al. (2,123) (§ I-4.1.).

propagation models or cross-sections ($_{36}$Kr, $_{54}$Xe, possibly $_{52}$Te). Taking into account all data in fig. 10 and allowing for more extreme spallation corrections, the solid error bars in fig. 19 (giving the more probable range of source abundances) have been prolongated by dashed white bars representing ranges that, though much less likely, cannot yet be entirely excluded.

For Ge, I have plotted two values in fig. 19, one relative to the usual C1 value, one relative to the photospheric value as a LG standard (Grevesse and Meyer, 3, 5 ; § III-3.1. and 3.5.) [10].

II-2.3. Discussion – UH nuclei, correlated with FIP ?

This discussion will be based on the more probable GCRS abundances indicated by the solid bars in fig. 19, the dashed bars giving only indications as to what is really definite and what might possibly still change.

When compared to the quite orderly pattern of GCRS/LG ratios versus FIP for elements with $Z \lesssim 30$ (fig. 15), the points for UH nuclei in fig. 19 give an impression of disorder. Clearly, the same simple correlation with FIP found for $Z \lesssim 30$ does not entirely account for the UH nuclei data. But the general pattern with FIP nevertheless seems to some extent present : higher-FIP $_{34}$Se, $_{54}$Xe, $_{36}$Kr do seem depleted relative to lower-FIP elements.

The general picture is that, while a few UH elements lie on the correlation established for $Z \lesssim 30$, many of them lie above (with only $_{32}$Ge being perhaps below, depending upon whether one uses the C1 or the photospheric value as a standard; § III-3.5.). It is particularly clear that four low-FIP elements are overabundant (certainly $_{58}$Ce and $_{42}$Mo, seemingly by factors of $\sim$ 3 to 4 ; and most probably $_{56}$Ba and $_{40}$ Zr). The striking point is that these excesses are not at all correlated with FIP. [11,12]

---

[10] One should not mechanically couple the choices of a C1 or of a photospheric value as LG standard for Ge (and Pb) and for Fe (figs. 19 and 20). The problems involved in the photospheric and C1 determinations are totally different and uncoupled for Fe and Ge (and Pb). Both problems are, independently, open.

[11] The case of $_{42}$Mo is especially compelling. Its FIP (7.1 eV) is close to those of Mg, Si, Fe; when the earlier data from both HEAO-C3 and Ariel VI repeatedly indicated a high abundance for Mo, we (or at least, I) did not pay too much attention to them, surmising that with improved statistics and data treatment, its abundance would gently fall off and get normal. The improved data from both HEAO-C3 and Ariel VI (fig. 10 ; § I-4.) now confirm and even slightly increase the apparent Mo excess. Note also that Mo is a refractory element for which there exists both good C1 data [Mo = 2.52 (1.05), for Si = 10^6] and reliable photospheric data [Mo = 2.32 (1.12)], which agree perfectly (Anders and Ebihara 1982; Grevesse 1984a,b). So, the LG abundance of Mo cannot be questioned. The spallation correction, taken into account in the Mo value plotted in fig. 19, is not either very important (e.g., Israel et al. 1983). Similarly, the $_{40}$Zr LG abundance cannot be questioned [Zr = 10.7 (1.12) in C1's and 10.1 (1.12) in the Photosphere], and its spallation correction is small.

[12] Only the slightly high $_{56}$Ba could be interpreted as an indication of a slight slope of the low-FIP elements plateau. But aside from Al and Ca, UH $_{38}$Sr and $_{31}$Ga would not confirm this view.

Actually, the UH elements that are clearly above the correlation with FIP valid for $Z \lesssim 30$ tend to be the heavier ones ($Z \gtrsim 40$), while lighter $_{31}Ga$, $_{32}Ge$ (?), $_{34}Se$, $_{36}Kr$, $_{38}Sr$, both low-FIP and high-FIP elements, are roughly conistent with the correlation f(FIP).

To try to separate FIP-dependent from other, e.g. Z-dependent effects, I am going to correct the GCRS/LG ratios of all elements for the bias with FIP, i.e. plot the ratio [GCRS/LG]/f(FIP) versus Z. [13] This procedure yields fig. 20 (in which Pt and Pb are still lacking, see § III-3.1.). Fig. 20 represents enhancement factors for each element in GCRS, relative to a "normal", or "main" CR component assumed to obey the correlation f(FIP) (cf. § III-4. and 5.). For completeness the GCRS excesses of the minor isotopes ^{22}Ne, $^{24,25}Mg$ and $^{29,30}Si$ relative to standard LG isotope ratios have also been plotted (fig. 29; § III-4.1.).

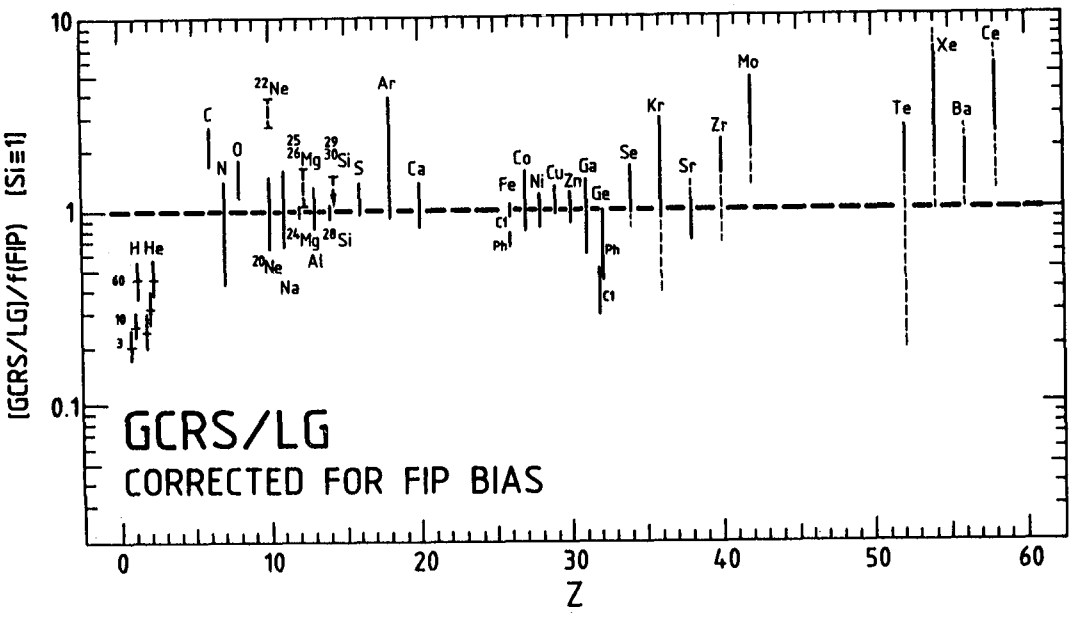

Fig. 20 [GCRS/LG]/f(FIP) ratio vs. Z for elements between Z = 1 and Z = 58 (as derived from fig. 19 ; § II-2.3.). Normalized to ^{28}Si (see fig. 14 caption). It represents the GCRS/LG ratios corrected for the bias with FIP, as described by f(FIP) which characterizes the data up to Z = 30 (figs. 15, 19 ; § II-1.4.). It also represents the excess for each species in GCRS, relative to a "normal" or "main" CR component assumed to obey the correlation f(FIP) [i.e. the quantity $E_{ik}^{*}{}_{,CR}$ in the notations of the Appendix ; § III-4. and 5.]. For Ne, Mg, Si, the elemental abundances are replaced by those of the dominant isotopes ^{20}Ne, ^{24}Mg, ^{28}Si. The excesses of the minor isotopes ratios have been plotted as dashed bars (fig. 29 ; § III-4.1. ; see footnote # 27). For H and He, the excess is energy-dependent, and given at 3, 10 and 60 GeV/n (§ II-1.2.3. ; figs. 14, 15). For Fe and Ge, two ranges are given, corresponding to the adoption of the more usual meteoritic ("C1") or to the photospheric ("Ph") value as LG reference ; see footnote # 10 (§ II-1.1., 2.1. ; III-3.5.). For $Z \gtrsim 34$, the error bars include a more probable range (solid), and a broader range which, though much less likely, cannot be entirely excluded (dashed) (fig. 19 ; § II-2.2.). The Pt-Pb region is absent from this plot, and will be treated separately (§ III-3.1., 3.5.).

[13] I recall that f(FIP) is the function describing the correlation of GCRS/LG with FIP for $Z \lesssim 30$ (figs. 15,19 ; § II-1.4.).

PART III

THE PROBLEMS WITH THE GALACTIC COSMIC RAY SOURCE COMPOSITION AND PROPAGATION - BEYOND THE CORRELATION WITH FIRST IONIZATION POTENTIAL -

To first order, the GCRS composition is characterized by its correlation with FIP. The question I am going to ask now is : what is beyond ? Where does the correlation with FIP not work ? Or, at least, where is it insufficient to account for the data ?

In fig. 20, the deviations of the ratio [GCRS/LG]/f(FIP) from the value 1, when really significant, indicate the nuclei for which the FIP-dependent filtering is insufficient to account for the data (for the Pt-Pb region, see § III-3.1.). I see five areas of problems in fig. 20, which I classify in three types:

a - The Hydrogen and Helium deficiency, which is a very specific problem (§ III-1.).

b - Excesses of heavy nuclei. They can in principle be accounted for by the presence of minor components highly enriched in specific nuclei, highly diluted in a dominant component that obeys the FIP correlation. (The abundances of the other nuclei may thus remain unaffected by the presence of the minor components). I see two areas of this kind: the C, O, ^{22}Ne, ^{25,26}Mg, ^{29,30}Si area (§ III-4.) and the $Z \geqslant 40$ area (§ III-5.).[14]

c - Depletions of heavy nuclei. They cannot be accounted for in the same way. The depletion of a single, isolated heavy species, if really proven, would imply that the bulk of GCR's originate in a medium specifically depleted in that species. Such an evidence would be sufficient to question the relevance of the entire apparent correlation with FIP and of the similarity with SEP and Solar Coronal compositions. I see three possible areas of this kind: Nitrogen (which will lead me to discuss the problems of CR propagation; § III-2.), and Germanium and Lead, which will be discussed together (§ III-3.).[15]

I am now going to discuss these various areas of problems in turn.

---

[14] Ar and Kr, with their large error bars, are also just consistent with the value 1 in fig. 20. I do not think we have to worry there. The errors are large, both on the spallation correction and on the LG value.

[15] I shall not discuss here the problems that arise if the photospheric value is adopted for LG Fe (figs. 15,20). Note that a deficiency of a group of neighbouring elements might be accounted for by (A/Q) dependent effects at high temperatures, superimposed on the correlation with FIP (as present in daily SEP composition, e.g. Meyer 1985a, and possibly in the average SEP composition, Breneman and Stone 4, 213,217). But, relative to a photospheric standard, GCRS Fe would be underabundant relative to its neighbours Co, Ni, Cu as well as to Mg, Si (figs. 15, 20), so that the above type of explanation would not work.

III-1. THE HYDROGEN AND HELIUM DEFICIENCY PROBLEM

III-1.1. H and He source spectra, and behaviour in SEP's

As shown in § II-1.2.3., the GCR observations, propagated back to the sources using a rigidity dependent escape length λ_e, imply:

- that the He/H-ratio at the sources is remarkly constant and normal ($\sim$ 10%), at least between $\sim$ 3 and $\sim$ 60 GeV/n, when taken at a given energy/nucleon (the relevant parameter according to current shock wave acceleration theory ; e.g., Krimsky 1977 ; Axford et al. 1977 ; Bell 1978a,b ; Blandford and Ostriker 1978 ; Axford 1981);

- that the roughly common spectral shape of H and He differs from that of heavier nuclei (CNO), which is steeper in this range (3 to 60 GeV/n). Meanwhile, no significant difference in source spectral shape between any two heavy nuclei has ever been found, over the range $\sim$ 0.5 to 25 GeV/n.

These facts are expressed in our plot of the abundances of H and He relative to heavies at three different energies (3, 10 and 60 GeV/n) in figs. 14,15,19,20,21,22.

In SEP's, H and He do not follow the orderly dependence on FIP and (A/Q) of all heavier species. This is in particular true for the variations of their abundances with time, a crucial parameter we have access to in SEP's, not in GCR's ! (e.g. Mason et al. 1983 ; Meyer 1985a).

So, H and He, the dominant elements, behave distinctly differently from the trace heavy elements we are studying, both in SEP's where their variations do not correlate with those of heavies, and in GCRS where they have a different spectrum. I therefore do not worry if they do not fit in the abundance pattern for the trace elements. Clearly, other phenomena are going on.

III-1.2. Deficiency of H and He : direct injection out of the Hot Interstellar Medium (HIM) ?

Attempts have been made to account for the low H and He abundances, assuming direct rigidity dependent injection of GCR's out of the HIM (Eichler 1979 ; Ellison 1981, 1985 ; Ellison et al. 1981 ; Eichler and Hainebach 1981). At this conference Binns et al. (3, 13) have tried to test this hypothesis by plotting the GCRS/LG ratios versus the ratio (A/Q_{120}) for all available elements way up to Z = 58, where Q_{120} is the approximate charge of the ions in a $\sim 10^6$ K plasma (Q_{120} is estimated by assuming that all electrons with ionization potential < 120 eV have been

removed). Their plot, shown in fig. 21 (updated), shows that the heavy element abundances are not at all organized in terms of (A/Q_{120}). This confirms earlier studies based on more accurate calculations of the charge Q in hot plasmas, but limited to $Z \leqslant 30$, by Cesarsky et al. (1981; 1985, quoted by Cassé 1983), which showed (fig. 22) that, for temperatures between 10^5 and 10^6 K, the GCRS/LG ratios plotted versus A/Q are characterized by discontinuities which cannot be accounted for by the smooth A/Q dependence of the composition predicted by the models assuming direct injection out of the ISM. These models would also have trouble in accounting for a normal He/H ratio (fig. 22).

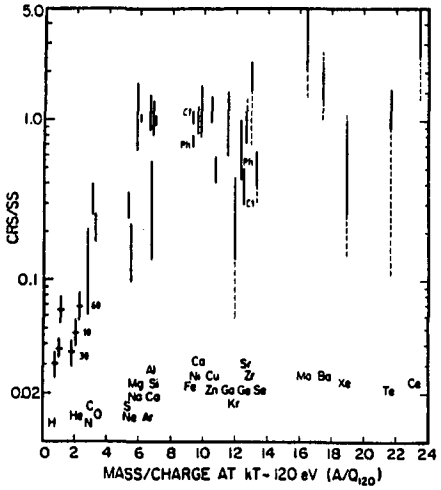

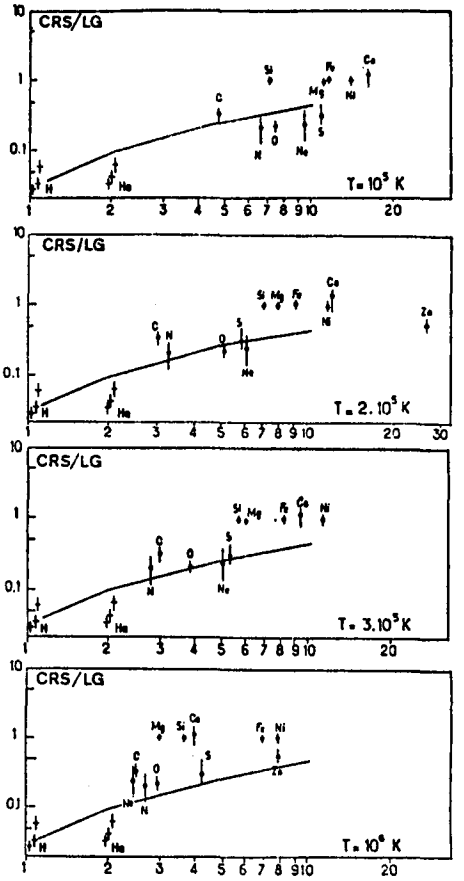

Fig. 21 GCRS/LG ratio for elements between Z = 1 and 58, versus mass to charge ratio A/Q in a 10^6 K plasma, after Binns et al. 3, 13 (updated). The charge Q = "Q_{120}" is roughly estimated by assuming that all electrons with ionization potential < 120 eV have been removed from the atoms. As regards the GCRS/LG ratios given in ordinates, I have updated them, using the values of fig. 19. See captions of figs. 14 and 19. Like in these figures H and He are given at 3, 10 and 60 GeV/n, Fe and Ge are given referred to both C1 and Photospheric LG abundances, and the error bars for UH nuclei include a more probable and a less probable range. Following the authors, I conclude that mass to charge ratio in a 10^6 K plasma does not order the data. This is a difficulty for models assuming direct injection of the particles out of the hot ISM plasma (§ III-1.2.).

Fig. 22 GCRS/LG ratio for elements between Z = 1 and 30, versus mass to charge ratio A/Q in 10^5, $2 \cdot 10^5$, $3 \cdot 10^5$ and 10^6 K plasmas, after Cesarsky et al. (1981 ; 1985, quoted by Cassé 1983). I have updated the graph for H and He, plotted at 3, 10 and 60 GeV/n. The charges Q are mean charges resulting from refined models of ionization equilibrium by Arnaud and Rothenflug (1985). The curves, normalized to H at ∿ 10 GeV/n are the enhancements predicted by Eichler and Hainebach (1981), very similar to those of Ellison (1981), assuming direct injection of the particles out of the hot ISM plasma. As can be seen, they do not account for the "observed" discontinuities of GCRS/LG vs. A/Q (§ III-1.2.).

III-2. THE NITROGEN DEFICIENCY PROBLEM - COSMIC RAY PROPAGATION - THE B - ^{15}N CONTRADICTION - DISTRIBUTED REACCELERATION ? TRUNCATION OF THE PLD ?

Is N depleted in GCRS relative to other high-FIP species, as compared to LG and/or to SEP abundances ? The best high-FIP species to which N can be compared is ^{20}Ne, since Ar is poorly determined and C and O are enhanced in SEP's relative to GCRS's, most probably because they are synthesized in large quantities together with the excess ^{22}Ne and ^{25,26}Mg (§ III-4.). The most stringent condition comes from the comparison with SEP (in which N/^{20}Ne is better determined and a bit higher than in LG matter, see figs. 15 and 17). The condition that N be not deficient relative to ^{20}Ne in GCRS, as compared to SEP, is equivalent to the condition that N/O $\gtrsim$ 6% in GCRS.

As noted in § II-1.2.2., most of the low energy studies based on isotopic observations of ^{14}N yield source N/O ratios $\sim$ 3%, which would imply that the correlation with FIP and the similarity with SEP's are not relevant, while high energy elemental studies yield N/O $\sim$ 6%, and thus make no problem (low energy isotope data : Pretzler et al. 1975; Wiedenbeck et al. 1979 ; Guzik 1981 ; Mewaldt et al. 1981 ; Webber 1982a,1983b; Webber et al. 2, 88 ; high energy elemental data : Goret et al. 1981 ; Webber 1982b ; Engelmann 1984 ; Lund 1984 ; Dwyer and Meyer 1985 ; Webber et al. 2,16; further discussions : Mewaldt 1981; Silberberg et al., 1983; Wiedenbeck 1984 ; Meyer 1985b ; Guzik et al. 2, 80 ; Webber et al. 3,42).

The surviving primary fraction is $\sim$ 34% among arriving low energy isotopic ^{14}N, and ranges from $\sim$ 19 to $\sim$ 31% (average $\approx$ 23%) for the high energy elemental N observed between $\sim$ 1 and $\sim$ 15 GeV/n by the HEAO-C2 instrument (fig. 16 ; assuming N/O = 6% at sources). So, the superiority of the low energy isotopic data as regards surviving primary fraction is not overwhelming. But the relevant cross-sections are most precisely measured at low energy, up to $\sim$ 1 GeV/n (fig. 4 ; § I-3.1.), so that the high energy estimates of the source N/O ratio require an extrapolation of the cross-sections to higher energies. Although the cross-sections are known not to vary much in the GeV range for such light nuclei (which is confirmed by the existing higher energy measurements, fig. 4), we do not know to within which accuracy this is true.

The HEAO-C2 isotopic data points for ^{14}N/O at high energy (E = 2.5 to 6 GeV/n; fig. 25), obtained from different subsets of events with various methods of geomagnetic isotope analysis, are at present too scattered to be decisive (Goret et al.1983 ; Byrnak et al. 1983a; Ferrando et al. 2, 96 and priv. comm. ^{15}N/N = 0.49 $\pm$ 0.06). Let me just note that the region of marginal agreement of all HEAO-C2 error bars on ^{14}N/O in fig. 25 (1σ errors are plotted) corresponds to N/O = 6% at the source; [while the corresponding data range for ^{15}N/O, fig. 24, agrees with the ^{15}N/O ratios predicted from the high energy B/C ratios].

I am now going to discuss cosmic ray propagation at low energy.

III-2.1. Low energy cosmic ray propagation - The B-^{15}N contradiction - Distributed reacceleration ?

Figs. 23 and 24 compare observed data to the result of propagation calculations for two (presumably) pure secondary to primary ratios: B/C and ^{15}N/O. The species considered are close in mass, so that the compared predictions for the two ratios are not sensitive to the exact shape of the Path Length Distribution (PLD; which may be truncated or not).

The PLD's used throughout figs. 23,24,25,26 are the pure exponential distributions with rigidity dependent escape length λ_e used by Soutoul et al. (2, 8). They are adjusted to best fit the observed B/C ratio, with the most up to date cross-sections. At high energy, they fit the HEAO-C2 data of Engelmann et al. (1983), with the relevant modulation parameter ϕ = 600 MV. [To fit the B/C ratios just obtained by Webber et al. (2, 16), slightly lower grammages would be required]. At lower energies, below R = 5.5 GV or E $\approx$ 2 GeV/n, two behaviours of λ_e are considered : λ_e = cst = 7.7 gcm^{-2}, and λ_e = 7.9 β gcm^{-2} (pure H). Two levels of modulation are also considered, ϕ = 350 and 490 MV. Actually λ_e = cst and ϕ = 350 MV on the one hand, and $\lambda_e \propto \beta$ and ϕ = 490 MV yield about the same results.[16] The value ϕ = 490 MV is probably more adequate for the Chicago IMP-8 data, so that their data on B/C tend to favour $\lambda_e \propto \beta$ (fig. 23). But the important point here is that the dispersion of the curves that encompass the plausible fits to the low energy B/C data points is not large, neither in fig. 23, nor in figs. 24,25 and 26.

I have also included in figs. 23,24,25,26 an estimate of the uncertainty on the calculated curves due to the cross-section uncertainties around 600 MeV, based on the figures given in Table 2. I have distinguished the errors associated with measured cross-sections, for which I have used the published uncertainties, from those associated with unmeasured cross-sections for which I have attributed a standard 35% error to the semi-empirical estimates.[17] I have simply linearily summed the two contributions.

Comparison of figs. 23 and 24 shows that the propagation models (values of λ_e) that fit the purely secondary B/C ratio do not at all fit the nearby purely secondary ^{15}N/O ratio at low energies.[18] This is another way of expressing the problem earlier addressed by Guzik (1981) and Guzik et al. (2, 80).

---

[16] For a higher degree of interplanetary deceleration ϕ, the low energy particles observed near Earth had originally higher energies in interstellar space. In the few 100 MeV/n $\sim$ 1 GeV/n range in interstellar space, higher energy particles have higher B/C ratios. Therefore a higher value of the modulation parameter ϕ yields higher B/C ratio near Earth.

[17] This 35% error may seem large since the sum of a large number of unmeasured cross-sections is involved, whose errors should largely compensate each other on the average (e.g., Letaw et al. 3, 46). On the other hand, recently measured cross-sections often deviate much more than expected from the semi-empirical estimates (e.g., Webber and Kish 3, 87) (fig. 5 ; § I-3.).

[18] The lower B/C ratios just obtained by Webber et al. (2, 16), plotted in fig. 23, would require still lower values of λ_e, thus amplifying the contradiction.

Table 2 - Contribution of various parents (fraction f) and associated cross-section errors (when unmeasured, adopted error = 35%) to the formation of secondary B, ^{14}N, ^{15}N, Sc-Cr around 600 MeV/n

Daughter / Parent	B			^{14}N			^{15}N			Sc-Cr		
	f	% error	Product	f	% error	Product	f	% error	Product	f	% error	Product
C	0.554	2.6%	1.4%	-	-	-	-	-	-	-	-	-
N	0.111	35.0%	3.9%	0.179	35.0%	6.3%	-	-	-	-	-	-
O	0.252	8.2%	2.1%	0.648	4.9%	3.2%	0.810	3.5%	2.8%	-	-	-
F,Ne	0.084	35.0%	2.9%	0.095	10.3%	1.0%	0.103	8.4%	0.9%	-	-	-
≥ Na				0.078	35.0%	2.7%	0.087	35.0%	3.0%	-	-	-
Mn, ^{54,55,57,58}Fe,Co,Ni	-	-	-	-	-	-	-	-	-	0.260	35.0%	9.1%
^{56}Fe	-	-	-	-	-	-	-	-	-	0.740	3.0%	2.2%
Fraction yielded by measured σ	0.806	-	-	0.743	-	-	0.913	-	-	0.740	-	-
∑ errors measured σ	-	-	3.5%	-	-	4.2%	-	-	3.7%	-	-	2.2%
∑ Errors Total	-	-	10.3%	-	-	13.2%	-	-	6.7%	-	-	11.3%

The contradiction is cleanest in the ∿ 300 to 500 MeV/n range, where we have in fig. 24 four independent solid points for $^{15}N/O$ by Webber and coworkers, obtained with good to excellent instrumental isotope resolution (fig. 2; § I-2.), which lie ∿ 30% above the predictions that fit B/C. The interpretation of the data in terms of solar modulation in this energy range is also less critical than for the lowest energy points (≲ 100 MeV/n), which, however, point toward the same problem (Guzik 1981; Guzik et al. 2,80). This energy range is also the one where the cross-sections have been best measured recently (§ I-3.1. ; fig. 4). It is clear from figs. 23 and 24 (Table 2) that the discrepancy is far beyond those permitted by reasonably estimated combined cross-section errors (± 13%).

Again, changes in the exact shape of the PLD (truncation) will not remove the contradiction for such nearby nuclei. So, unless there are gross, unknown errors, either in the CR data, or in the measured cross-sections for B and/or ^{15}N - which seems improbable -, I can imagine no way of understanding simultaneously the low energy B/C and $^{15}N/O$ observations within the classical propagation framework.

At this state, I can think of only two ways out [19] :

(i) A special propagation history for C (and O?) nuclei ?

The first one is very speculative, certainly difficult to check, but should still be kept in mind as a possibility. According to our current knowledge, ∿ 50% of the GCR C nuclei originate, together with the ^{22}Ne excess, in special environments, plausibly Wolf-Rayet stars (§ II-1.3. and III-4. ; figs. 17, 20 and 30). It is not impossible - although there is no particular astrophysical justification for this

[19] Here I exclude the hypothesis that a significant fraction of the ^{15}N be primary. This would imply an excess of ^{15}N by a factor of ∿ 100 in GCRS, as compared to excesses by factors of ∿ 2 to 2.5 for ^{12}C and ∿ 3.2 for ^{22}Ne. A strong dilution of the ^{15}N-rich material with normal material would then be difficult to accept. Most CR's probably ought to originate in the ^{15}N-rich material.

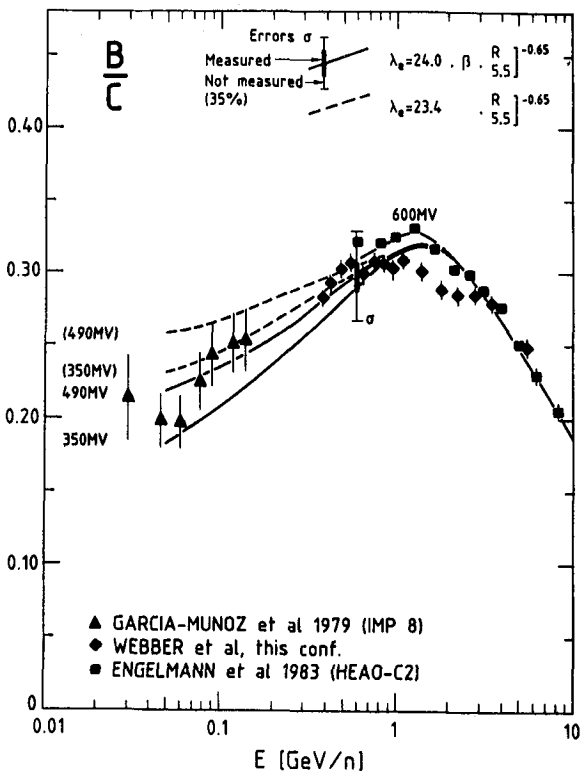

Fig. 23 *The B/C ratio, vs. energy. Observations are from : Garcia-Munoz et al. 1979 (IMP-8) ; Webber et al. 2, 16 ; and Engelmann et al. 1983 (HEAO-C2). The calculated curves are adjusted as to best fit the observed ratios. They refer to pure exponential PLD's with λ_e = f(R) or f(R,β) as indicated on the figure, based on Soutoul et al. (2, 8) [λ_e in g cm^{-2} of pure H ; R in GV ; the bracket with R and 5.5 indicates that for R < 5.5 GV, the R dependence ceases, and R is to be replaced by 5.5]. The full curves include a β-dependence, the dashed curves do not. Three values of the modulation parameter φ are considered ; 600 MV is believed to be adequate for the HEAO-C2 data, and 490 MV for the low energy IMP-8 data, thus favouring a β-dependence of λ_e. An estimate of the uncertainty on the curves due to cross-section (σ) errors is given around 600 MeV/n ; I have indicated separately the errors associated with the measured cross-sections and those due to the unmeasured ones, taken as 35% (§ III-2.1., Table 2).*

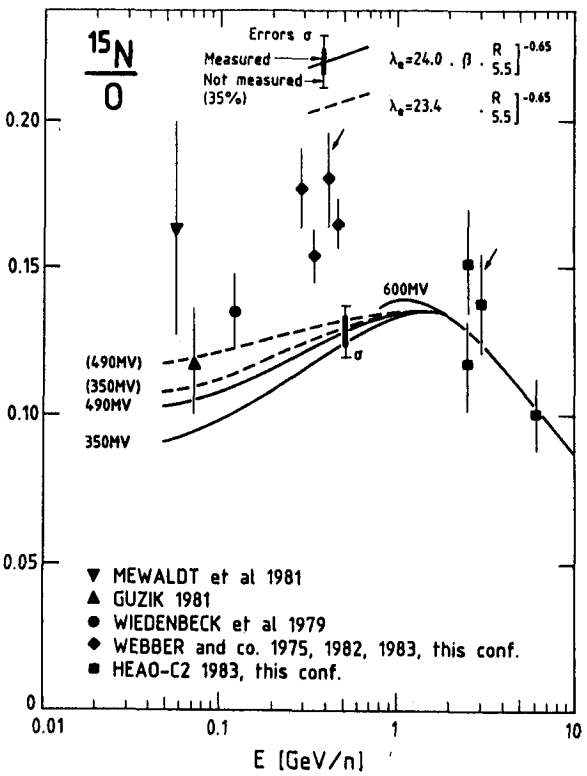

Fig. 24 *The ^{15}N/O ratio, vs. energy. Observations are from : Mewaldt et al. 1981 (ISEE 3) ; Guzik 1981 (IMP 7-8) ; Wiedenbeck et al. 1979 (ISEE 3) ; Pretzler et al. 1975 ; Webber 1982a, 1983b ; Webber et al. 2, 88; Goret et al. 1983 (HEAO-C2) ; Byrnak et al. 1983a (HEAO-C2) ; Ferrando et al. 2, 95 and priv. comm. (HEAO-C2). New data presented at this conference are marked by an arrow. Calculated curves, adjusted as to best fit the B/C ratio : see caption of fig. 23.*

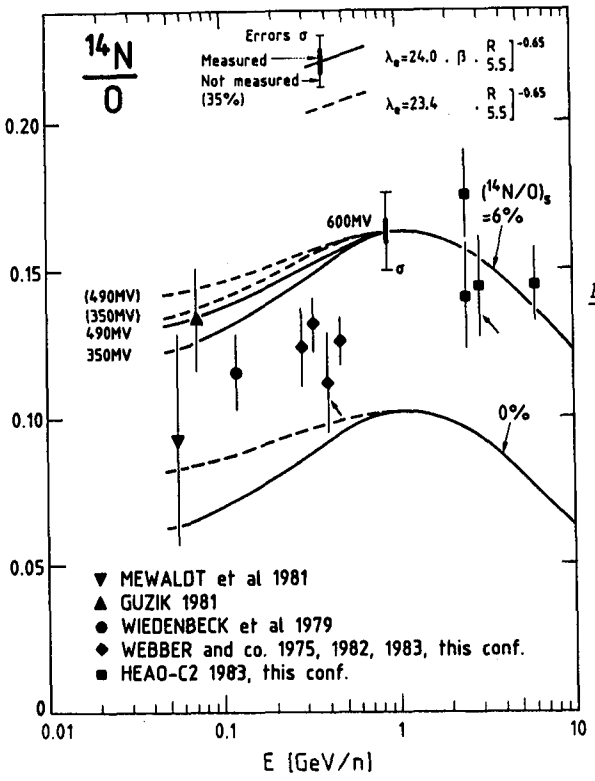

Fig. 25 The $^{14}N/O$ ratio, vs. energy. References for the observations : same as in fig. 24. Calculated curves, adjusted as to best fit the B/C ratio : see caption of fig. 23. The curves are given for source ratios $(^{14}N/O)_s$ = 0% and 6% and would scale linearly in between.

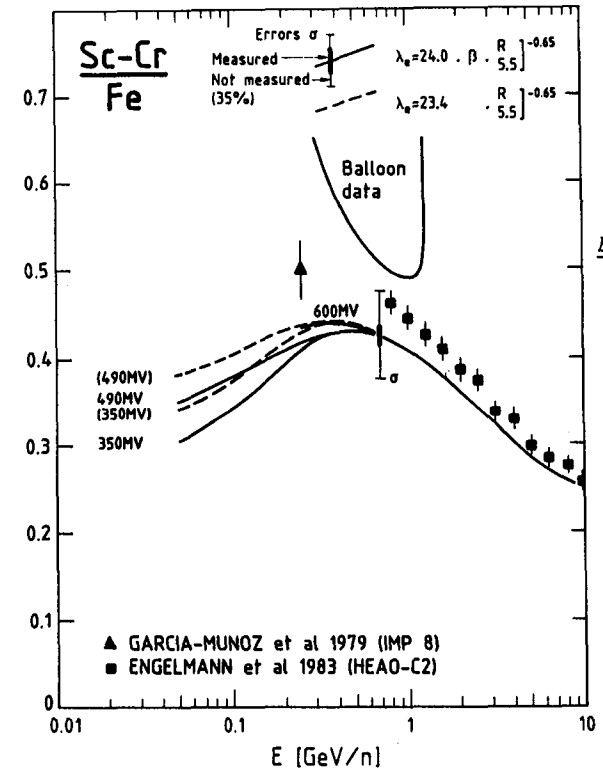

Fig. 26 The Sc-Cr/Fe ratio, vs. energy. Observations are from Garcia-Munoz and Simpson 1979 (IMP-8) and Engelmann et al. 1983 (HEAO-C2). An envelope is given for various earlier balloon data, which often yield ratios above those calculated for $\lambda_e = \infty$. Calculated curves, adjusted as to best fit the B/C ratio : see caption of fig. 23. [LG abundances have been assumed for the source abundances of Sc, Ti, V and Cr, all low-FIP elements, relative to Fe].

hypothesis - that these nuclei have a propagation history different from that of the bulk of the CR nuclei and traverse on the average significantly less matter, thus yielding comparatively low B/C ratios. The B/C ratio would then not be a good cornerstone to discuss propagation in general. An immediate argument against this hypothesis would be that, in the same framework, it is expected that $\sim$ 30% of the O also originates in Wolf-Rayet stars (fig. 30), so that the difference in propagation history is not so large for the daughters of C and of O. [This figure of $\sim$ 30% of O from Wolf-Rayet stars is, however, probably more model dependent than the 50% for C]. When good cross-sections become available, study of almost purely secondary Fluorine may be very instructive in this context.

(ii) Distributed reacceleration ?

The second way-out I can think of at the moment is less speculative, and certainly more liable to check : it is the hypothesis of distributed reacceleration. In this hypothesis, the CR's we observe in the few 100 MeV/n range have earlier been propagating a long time at lower energy (say, $\lesssim$ 100 MeV/n), before they got boosted up in energy by factors of a few units by passing weak supernova shocks (Silberberg et al. 1983, and 3,238 ; Letaw et al. 1984 ; Simon et al. 3,230). The relevant cross-sections for secondary formation are then largely thecross-sections below 100 MeV/n, which sometimes show strong peaks followed by a steep decrease down to threshold. Silberberg et al. (1983) have noted several problems with CR composition, specifically at low energy, which might be solved if distributed reacceleration is at work.

At high energy, distributed acceleration has less effect on composition, because the cross-sections are much more constant with energy. Note that, at this conference, Simon et al. (3, 230) have shown that distributed reacceleration is not in conflict with the observed decrease of the secondary/primary ratios at high energies ($\sim$ 2 to 200 GeV/n).

A serious difficulty with the hypothesis that the particles have traversed a lot of matter at E $\lesssim$ 100 MeV/n before we observe them at a few 100 MeV/n, arises from the strong energy loss and its Z^2 dependence at low energy, which may well kill selectively heavier nuclei such as Fe and especially UH elements. [This is the problem first posed by Eichler (1980) and Epstein (1980a) regarding the injection problem; at very low energies $\lesssim$ 3 MeV/n, however, the pick-up of electrons by heavier nuclei is sufficient to cancel the Z^2 dependence of the energy loss (Meyer 1985b) ; but this is no longer true in the 10-100 MeV/n range where the nuclear interactions involving the low energy cross-sections are supposed to take place]. Small reaccelerations must be frequent enough that Fe and UH nuclei do not get preferentially thermalized. This is a problem.

Anyway, I think that the lower energy B-^{15}N contradiction is perhaps a clear case for distributed reacceleration. To check this hypothesis, I recommend: (i) measurement of key unmeasured spallation cross-sections below $\sim$ 100 MeV/n, down to threshold ; (ii) detailed analysis of the consistency of our data on secondary ^{6}Li, ^{7}Li, ^{7}Be, ^{9}Be, ^{10}B, ^{11}B, ^{15}N, ^{17}O, ^{19}F at low energy, with and without distributed reacceleration; (iii) studies of the energy loss problem for heavier nuclei: can it be overcome ?

III-2.2. The ^{14}N source abundance from low and high energy data

Fig. 25 is the twin-figure to fig. 24, for $^{14}N/O$. Here, of course, a significant source component is expected, and I have plotted the $^{14}N/O$ ratios expected from the purely secondary production, $(^{14}N/O)_S = 0\%$, and for source $(^{14}N/O)_S = 6\%$. In between, calculated curves would scale roughly linearly with $(^{14}N/O)_S$.

As well known, the bulk of the low energy points indicate $(^{14}N/O)_S \approx 3\%$, if the values of λ_e that fit the B/C ratio (fig. 23) are adopted. Of course, if one were to increase the low energy λ_e's so as to fit the $^{15}N/O$ ratio instead, the predicted secondary yields for ^{14}N would increase accordingly and the ^{14}N source values derived from the low energy points correspondingly decrease down to values close to zero.

I think that, as long as the low energy B-^{15}N contradiction is not solved, we cannot say anything serious on the ^{14}N source abundance as derived from low energy data. Assuming that the CR data are correct, some cross-sections ought to be wrong : those for B formation ? for ^{15}N formation ? and then, how about those for ^{14}N formation ? As mentioned above, I do not think the recent cross-section measurements for production of these very species from their principal progenitors can be that wrong. Errors on estimates of other, not measured cross-sections are not either likely to make the difference (Table 2 ; figs. 23 and 24). That is why I think some other ingredient must interfere. The most likely one I can think of at the moment is distributed reacceleration. The relevant cross-sections could then largely be those below $\sim$ 100 MeV/n, and we would indeed be using wrong cross-sections at present ! And before the very low energy cross-sections are known (those for Li, Be, B formation have been largely investigated, e.g. Read and Viola 1984, but not those for $^{14,15}N$) and propagation with distributed acceleration has been modelled, only God knows whether this hypothesis solves the B-^{15}N contradiction (while being consistent with the data on ^{7}Be, ^{9}Be, ^{10}B, ^{11}B, ^{15}N, F), and which source ^{14}N abundance it yields.

At high energies (where, anyway, distributed reacceleration would not significantly affect the composition), the marginal consensus of the various HEAO-C2 isotope analysis around 3 GeV/n and the point at 6 GeV/n yield $^{15}N/O$ ratios which are consistent with the predictions from the B/C ratio, and converge on $(^{14}N/O)_S \approx 6\%$ (figs. 24 and 25; plotted are 1σ errors).

6% is also the value for $(^{14}N/O)_S$ derived from the N/O elemental data between $\sim$ 1 and 15 GeV/n (HEAO-C2 data, Engelmann 1984, Lund 1984; in excellent agreement with the new data of Webber et al. 2, 16 and of Dwyer and Meyer 1985).

III-2.3. Truncation of the exponential Path Length Distribution (PLD) ?

A truncation at low pathlengths of the roughly exponential PLD of CR's in the galaxy means a dearth of particles having traversed a small amount of matter, say ≤ 1 gcm^{-2}, between source and earth. The simplest interpretation of such a dearth is that many sources are surrounded by dense matter, in which newly accelerated CR's are trapped before escaping into the general galactic medium: this is the nested leaky-box model (Cowsik and Wilson 1973).

Whether the PLD is truncated or not can be decided by comparing observed secondary to primary ratios, for groups of nuclei with widely different nuclear destruction lengths λ_{nucl} (some with $\lambda_{nucl} \gtrsim \lambda_e$, others with $\lambda_{nucl} << \lambda_e$, where λ_e is the escape length from the Galaxy; e.g., Webber et al. 1972). The PLD may actually be truncated for some energies, and not for others. At this conference, a number of investigators have addressed this problem, at both high and low energy, based either on data for $Z \leq 30$ (Soutoul et al. 2,8 ; Margolis 3,38 ; Webber et al. 3,42; Letaw et al. 3, 46 ; Ferrando et al. 3, 61 ; see also Garcia-Munoz et al. 1984), or on data for UH nuclei (Fowler et al. 2, 119 ; Klarman et al. 2, 127 ; Waddington et al. 3,1 ; Giler and Wibig 3,17 ; see also Brewster et al. 1983 and Letaw et al. 1984). In view of the very small value of λ_{nucl} for UH nuclei, the latter studies should in principle be the most powerful tool to investigate a possible dearth of short pathlengths.

I shall discuss in turn the evidence for and against truncation (i) at high energy ($\gtrsim 1$ GeV/n) based on elements with $Z \leq 30$; (ii) at high energy, based on UH elements; and (iii) at low energy (< 1 GeV/n), based on elements with $Z \leq 30$.

III-2.3.1. Truncation of the PLD in the GeV/n range - Data for $Z \leq 30$ - The role of interstellar He

From the comparison of the B/C and Sc-Cr/Fe ratios, there is a general agreement that no significant truncation is required beyond 1 or a few GeV/n. This is, in particular, illustrated in the comparison of figs. 23 and 26, based on Soutoul et al. (2, 8). The purely exponential PLD that best fits B/C also fits almost perfectly Sc-Cr/Fe at high energy (and certainly within the cross-section errors). The fit is, however, slightly low, and a limited amount of truncation cannot be excluded either.

Ferrando et al. (3, 61) have suggested that the need for truncation may be reenforced when interstellar He is included in the propagation calculations in a physical way (i.e. using as much as possible real cross-sections on He; not just scaling the cross-sections on H, which is merely equivalent to a change of "units" for λ_e). Referred to the total cross-section, the spallation of Fe on He yields less nearby products (Sc-Cr) than its spallation on H, while the spallation of C yields about as much Be on He as on H. When interstellar He gets properly taken into account, one may therefore expect a decrease of the calculated yield for Sc-Cr as compared to that for Li Be B. Then more truncation of the PLD will be required. I think that this idea must be studied more precisely, based on all available data on spallation on He (or, for lack of such

data, on spallation on heavier targets such as Be and C). Also, production of B, for which we have much better CR data, should be considered, rather than of Be. [B will probably be comparatively less produced than Be in the spallation of C on heavier targets, more like Sc-Cr; the above effect should therefore be smaller for B than for Be; on the other hand, as much as $\sim$ 45% of B is produced out of parents heavier than C (Table 2), for which B is not a nearby product]. Anyway, this problem requires measurements of spallation cross-sections on He.

III-2.3.2. Truncation of the PLD in the GeV/n range - UH nuclei data

As regards UH nuclei, Klarman et al. (2, 127) have in particular compared the observations to the predictions for purely exponential PLD's for two mainly secondary/primary ratios : (Z = 62 to 69)/"Pt Pb" and (Z = 70 to 73)/"Pt Pb", where "Pt Pb" stands for (Z = 74 to 83) (fig. 27). The predictions are obtained using a cross-section systematics derived from the latest cross-section measurements by Kertzman et al. (3, 95) at 1 GeV/n (fig. 7 ; § I-3.1.). Fig. 27 shows that the agreement between the HEAO-C3 measurement and the predictions is excellent. It may, however, be coincidental. The HEAO-C3 data indeed refer to a median energy of $\sim$ 6 GeV/n, while the new cross-sections measurements have been performed at $\sim$ 1 GeV/n. Now, the study of Au spallation by Kaufman and Steinberg (1980) shows that, for $\Delta A \leqslant 40$, spallation cross-sections peak around 1 GeV/n and decrease by factors of $\sim$ 2 between 1 and 6 GeV/n [20]. So, the secondary yields at 6 GeV/n predicted for a pure exponential PLD could well be twice lower than apparent in fig. 27, which would be a case for truncation. In addition, the Ariel VI group finds higher fluxes of secondary nuclei (figs. 27 and 9, 10). They refer to lower energies than the HEAO-C3 data, and the difference is believed to be real (fig. 11). Their median energy, $\sim$ 2 GeV/n, is actually much closer

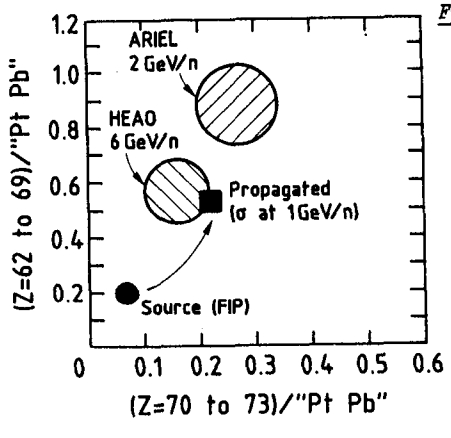

Fig. 27 Cross plot of the two mainly secondary to primary ratios (Z = 62 to 69)/"Pt Pb" vs. Z = 70-73/"Pt Pb", where "Pt Pb" stands for (Z = 74 to 83), adapted from Klarman et al. (2 127) [see also Binns et al. 1985]. The source ratios assume LG abundances biased according to f(FIP) (fig. 15). The propagated ratios have been obtained assuming a pure exponential PLD, and using cross-sections derived from the latest measurements by Kertzman et al. (3, 95) at 1 GeV/n (fig. 7 ; § I-3.1.). The observed ratios are those of the experiments HEAO-C3 around 6 GeV/n and Ariel VI mainly around 2 GeV/n (figs. 9, 10 ; § I-4.). It is important to note that a subset of the Ariel VI data around 6 GeV/n agrees well with the HEAO-C3 point at the same energy (fig. 11). See discussion in § III-2.3.2..

[20] This behaviour is not simple. Both the energy at which the cross-section peaks (it falls again at lower energy) and the relative amplitude of the peak depend on ΔA (Kaufman and Steinberg 1980).

to the energy at which the cross-sections have been measured, so that these Ariel VI data, together with the above mentioned calculation [21], could provide further support for truncation (fig. 27).

The above arguments are valid, unless distributed reacceleration, working at higher energy as well, makes the cross-sections at 1 GeV/n relevant for 6 GeV/n ! (we might then also have problems in explaining the high secondary fluxes in the Ariel data at lower energy !).

III-2.3.3. Truncation of the PLD in the few 100 MeV/n range

Below 1 GeV/n, comparison of the data for B/C and Sc-Cr/Fe [22] in figs. 23 and 26, shows that the purely exponential PLD's that fit B/C indeed do not produce as much Sc-Cr as observed at low energy. However, the discrepancy is only marginal, when considering the uncertainty on the prediction associated with the unmeasured cross-sections (taken to be good to within 35%, perhaps somewhat pessimistically; fig.26, Table 2).[23]

Much more important, the low energy discrepancy between B/C and Sc-Cr/Fe (figs. 23 and 26), which we tend to interpret in terms of a truncation of the PLD, is much smaller than that between B/C and $^{15}N/O$ (figs. 23 and 24), which is totally not understood (and certainly not due to truncation)!!! [24] So, I think that, as long as the B-^{15}N contradiction is not understood, it would be very imprudent to draw any conclusion regarding truncation of the PLD at low energy.

III-2.3.4. Summary on the truncation of the PLD

At high energy ($E \gtrsim 1$ GeV/n) there is a consensus that the data up to Fe do not suggest any significant truncation of the PLD. They should actually allow to place strict limits to acceptable truncations. However, a realistic introduction of spallation in interstellar He might increase the need for truncation. The UH data, which are extremely sensitive to truncation, are difficult to interpret because of probable energy dependence of the cross-section. They might well favour some truncation. Distributed reacceleration, if present, may further complicate the picture.

At low energy, ($E \lesssim 1$ GeV/n) no conclusion can be drawn before the B-^{15}N contradiction is solved (§ III-2.1.).

---

[21] These UH secondary/primary ratios, while very sensitive to a truncation of the PLD, are very insensitive to the exact value of λ_e (which is anyway >> λ_{nucl}), and to its $\sim$ 50% increase between 6 and 2 GeV/n.

[22] At low energy, I shall consider essentially the IMP 8 data from the U. of Chicago. There exists a large body of diverging balloon data, most of which are above the saturated Sc-Cr/Fe ratio (corresponding to no escape at all) (Soutoul et al. 2,8).

[23] The discrepancy between B/C and Sc-Cr/Fe may appear larger when expressed in terms of the λ_e's for pure exponential PLD's required to fit both ratios (Soutoul et al. 2,8). But this λ_e is not a good parameter since a small increase of Sc-Cr/Fe, obtained by a small amount of truncation of the short pathlengths, would require a large increase of λ_e in a purely exponential framework (since λ_e >> λ_{nucl}).

[24] Actually, a larger λ_e at lower energy that would fit $^{15}N/O$ would roughly fit Sc-Cr/Fe.

III-3. THE GERMANIUM-LEAD DEFICIENCY PROBLEM

I shall discuss together the Ge and Pb deficiency problems, because both may be volability indicators, and because for both the Cl meteoritic abundance standard might have to be questioned (see below § III-3.4. and 3.5.).

III-3.1. Defining the Ge and Pb/Pt anomalies

It is immediately apparent in figs. 19 and 20 that Ge is low in GCRS as compared with elements with similar FIP (Fe, Mg, Si), when referred to the standard Cl meteoritic value as LG abundance (§ II.1.1. and 2.1.).

Pt and Pb have not been plotted in the above figures, because their source abundances relative to Fe or Si cannot yet be reliably determined. Even the even-Z elements are not individually resolved in this range, neither on HEAO-C3, nor on Ariel VI (fig. 9), so that charge groups have had to be defined "Pt-group" $\equiv$ (Z = 74 to 80) and "Pb-group" $\equiv$ (Z = 81 to 86) (§ I-4 ; fig. 10 ; Table 1). Second, extrapolation to the sources of the observed abundances relative to Fe or Si is still very uncertain, model dependent (truncation of PLD, § III-2.3. ; cross-sections, § I-3.1.) (e.g. Giler and Wibig 3, 17). I shall therefore discuss only the "Pb-group"/"Pt-group" ratio, without reference to Fe or Si. And, rather than deriving this ratio at the sources from the observations, I shall follow most authors and more prudently investigate which source abundances may, or may not, be consistent with the observed ratio. I recall that the observed "Pb-group"/"Pt-group" ratios are 0.25 ± 0.09 and 0.35 ± 0.10 from the HEAO-C3 and Ariel VI experiments respectively (Table 1 ; Waddington et al. 9,... ; Fowler et al. 2, 119). These observed ratios have been plotted on fig. 28. Possible non-Z^2 effects in the HEAO-C3 instrument might further slightly reduce the ratio (fig. 28 ; Waddington et al. 9,... ; Newport et al. 3, 287).

I shall now ask the question : are the observed "Pb-group"/Pt-group" ratios consistent with what would be predicted by the simplest model : source abundances following standard meteoritic Cl values biased according to FIP, and later modified by standard pure leaky-box propagation in the galaxy ?

Fig. 28 addresses this question. Based on standard Cl values, the LG ratio "Pb-group"/"Pt-group" = 1.00 (1.11) (Grevesse and Meyer, 3, 5). Correction for FIP bias according to the pattern f(FIP) adopted in fig. 15 increases this ratio by a factor of $\sim$ 1.55 (1.15), since FIP(Pb) = 7.4 eV and FIP(Os, Ir, Pt) $\approx$ 8.9 ± 0.2 eV. We thus get "Pb-group"/"Pt-group" = 1.55 (1.19) at the sources, after bias with FIP. The modification of this ratio during propagation is not small, because a large fraction of the interacting "Pb-group" elements is transformed into one of the numerous "Pt-group" elements. With the best-available scalings of cross-sections (§ I-3.1.) ; Kertzman et al. 3, 95 and priv. comm.) and a simple leaky-box model, propagation reduces the "Pb-group"/"Pt-group" ratio by a factor of $\sim$ 0.48 (1.20) (my estimate of the error, perhaps quite optimistic ; § I-3.1. and III-2.3.2. and 3.2.). The clear conclusion of fig. 28 is that the "Pb-group"/"Pt-group" ratio is indeed anoma-

lously low, based on the most standard assumptions, and in particular starting from standard C1 values as LG abundances.

Of course, since we are unable to provide a reliable link with the abundances of much lighter elements, we cannot tell whether Pb is underabundant or Pt overabundant !

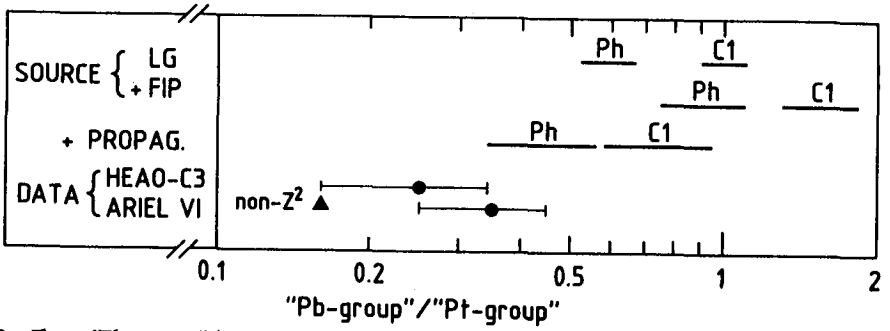

Fig. 28 The "Pb-group"/"Pt-group" abundance ratio (see Table 1 for def.), studied in the framework of the standard cosmic-ray model. Based on Waddington et al. (9,...) and Grevesse and Meyer (3, 5). From top to bottom : LG abundance ratio, equal to 1.00 (1.11) based on C1 meteoritic data (C1), and equal to 0.59 (1.14) based on solar photospheric data (Ph) (§ III-3.5.). If the usual bias with FIP applies, the presumable GCRS ratio is increased by a factor of 1.55 (1.15) relative to its LG value (§ III-3.1. ; fig. 15). Pure leaky box propagation between sources and Earth in turn decreases the ratio by a factor of 0.48 (1.20) (§ III-.3.1. ; on the figure, these various uncertainties have been summed quadratically). The two bottom lines give the data observed by the HEAO-C3 and Ariel VI experiments (Waddington et al. 9, ... ; Fowler et al. 2, 119 ; § I-4. ; Table 1 ; figs. 9, 10). Possible non-Z^2 effects on the HEAO-C3 charge scale might displace the HEAO-C3 point to the position of the triangle (e.g., Newport et al. 3, 287). The clear conclusion of this figure is that the observed "Pb-group"/"Pt-group" ratios are definitely inconsistent with the most standard CR model if C1 meteoritic abundances are adopted as a LG basis, but are not inconsistent if the solar photospheric values are adopted instead.

III-3.2. The low Pb/Pt ratio : probably not explainable in terms of a truncation of the PLD

It is clear from § III-2.3.2. that the question of a limited truncation of the PLD, to which UH elements would be extremely sensitive, is still open. The main problem is here the energy dependence of the relevant cross-sections, which are measured at 1 GeV/n (§ I-3.1.) and are used at 6 and 2 GeV/n, a range in which they are likely to significantly decrease with energy (Kaufman and Steinberg 1980). If too large cross-sections are actually used, truncation is actually needed.

But this trade-off between cross-sections and truncation is about the same when considering the (Z = 62-73)/"Pt Pb" ratio and the effect of secondaries on the "Pt-group"/"Pb-group" ratio. Fig. 27 shows that, with the cross-sections used as they are and no truncation, the (Z = 62-73)/"Pt Pb" data of HEAO-C3 and Ariel VI (high energy part of the data, identical to those of HEAO-C3 ; see fig. 11) are well fitted. Therefore not much can be changed by some trade-off between cross-sections and truncation as regards the calculated "Pt-group"/"Pb-group" ratio.

III-3.3. The low Pb/Pt ratio - Interpretations in terms of nucleosynthesis

It is well known that in ordinary matter Pb is primarily a s-process element while elements of the Pt group are mainly formed by the r-process. On this line Giler and Wibig (3, 17) have proposed a model in which the parameters governing nucleosynthesis of UH elements in GCR material differ from those for ordinary, "solar-mix", material : for GCR material, neutron fluences and densities, temperatures and time scales are adjusted in such a way that the s-process does not reach beyond Z = 58, and the shape of the GCR Pt-Pb peak is reproduced by a specific type of r-process. [25]

On the other hand, Margolis and Blake (3, 21) note that, in "solar-mix" material, the standard s-process that fits s-nuclides up to ^{204}Pb (1.5% of Pb) underproduces the dominant, heavier Pb isotopes. It is generally believed (Clayton and Rassbach 1967 ; Beer and Macklin 1985) that most of the missing Pb is produced in specific sites with particularity intense neutron exposures ("recycling s-process"), which are identified as low mass stars ($M < 1\ M_\odot$). The sites for production of most Pb being different from those for lighter s-nuclides, a deficiency of Pb in GCR's would be explained if the nucleosynthetic yield of these sites, i.e. stars with $M < 1\ M_\odot$, was underrepresented in GCR's as compared to "solar mix". [26]

The difficulty with such explanations of the deficiency of a specific element in terms of nucleosynthesis is always the same : they imply that the vast majority of GCR's must originate in specific sites of current nucleosynthesis, while their bulk composition resembles so much the "solar-mix" modified by simple atomic selection effects (the same selection effects found present in the solar Corona and SEP), and correlates so poorly with the outcome of the major cycles of nucleosynthesis and with the calculated pre-supernova and supernova compositions (Arnould 1984 ; Meyer 1985b).

Of course, there remains the possibility that Pb be not low, but that "Pt-group" elements be high, as a specific excess of r-nuclides (see § III-5.3.).

---

[25] This adjustment is also tuned as to reproduce other features of the UH source abundances for lower Z (some of which are, however, in my opinion, very unreliably derived from the abundances observed near Earth). Selection according to FIP is assumed to apply for s-process elements, not for r-process species.

[26] Käppeler et al. (1982) had erroneously attributed to r-process the entire difference between the observed Pb abundance and that estimated for conventional s-process, thus forgetting about the important contribution of the "recycling s-process" (Käppeler et al., private circular ; Beer and Macklin 1985). On this erroneous track, Fixsen (1985) has reevaluated a r-process Pb abundance, which is also much too high (as noted by Fixsen himself, by comparison with the neighbouring r-process components of Tl and Bi). This high r-process Pb abundance is however the one adopted by Binns et al. (1985) and Waddington et al. (9,...) ; I shall not consider it further in my discussion. These authors, however, note that the CR data may be consistent with a "Pb-poor r-process" (similar to the more standard one considered by Giler and Wibig 3, 17).

III-3.4. Ge and Pb as volatility indicators

It is now well known that, for most elements, the degree of volatility is (positively) correlated with the value of the FIP so that the apparent correlation of abundances with FIP might as well be interpreted as a correlation with volatility (Cesarsky and Bibring 1980 ; Epstein 1980a ; Bibring and Cesarsky 1981). Only a few low-FIP, though volatile, elements that are exceptions to the general rule permit to distinguish between the two types of correlation. Two indicators, Cu and Zn, though not entirely clear-cut, tend to favour FIP. But the best available indicators are at present Ge and Pb (Meyer 1981d ; Grevesse and Meyer 3, 5).

The fact that Ge and Pb are simultaneously found underabundant is striking ! At face value, it implies in this context that volatility, not FIP, is the relevant ordering parameter, and that GCR's are primarily interstellar grain destruction products. This is an interesting possibility, but not an easy one to live with ! The models of grain destruction and preferential injection in shock waves, while accounting fairly easily for the relative abundances of the refractory and volatile reactive heavy elements and for the low abundances of H and He, have a hard time in accounting for the roughly normal abundances of heavier noble gases (Ne, Ar, Kr, Xe) relative to O. Note also that, if GCR's are grain destruction products, their similarity in composition with SEP and Solar Corona is purely fortuitous.

III-3.5. Questioning the LG reference abundances for Ge and Pb

LG reference abundances have been discussed in § II-1.1. and 2.1.. As mentioned there, I think that C2 meteoritic abundances are irrelevant as a standard, which does not mean that C1's are necessarily perfectly representative of the protosolar nebula for all elements.

The study of Grevesse and Meyer (3, 5) shows that the C1 meteoritic abundances are well defined for both Ge and Pb.

As regards the solar Photosphere, this study shows that the Ge abundance can be reliably determined from 2 lines, and that of Pb from 1 line. This represents very few lines indeed ! However, with the quality presently reached by the solar atmospheric models, it is no longer unreasonable to determine the abundance of an element based on 1 or 2 lines only. A critical treatment of the errors in the photospheric abundance determinations, especially on the log gf values, leads to the conclusion that, to the best of our present knowledge, there is a significant discrepancy between the C1 and the photospheric abundances of Ge and Pb, both being found lower by a factor of ~ 1.6 in the Photosphere. If the photospheric values are adopted, there is no longer any significant underabundance of Ge relative to Fe, Mg, Si (figs. 19 and 20) and of Pb relative to Pt (fig. 28).

Can one meaningfully pick-up specifically two elements and adopt for them photospheric rather than C1 meteoritic values ? Once again, C1 values are better measured, but their relevance as representative of the abundances of the protosolar nebula is not straightforward, especially for volatile elements (§ II-2.1.). And we are specifically considering two volatile elements (especially Pb, which is extremely volatile) ! Consideration of fig. 2 in the review by Grevesse (1984a) shows that there is still some leeway for limited differences between photospheric and C1 abundances among volatile and highly volatile elements (not to speak of the problems with siderophile Fe and refractory Ti ; § II-1.1.).

III-3.6. Summary on the Ge-Pb deficiency problem

The low Ge and Pb abundances in GCRS seem at first to indicate that volatility, rather than FIP, is the parameter governing GCR abundances, and that GCR's are primarily grain destruction products. (However other, less clear-cut indicators, Cu and Zn, do not confirm this view). This hypothesis is not easy to live with : it has difficulties in explaining the noble gas abundances in CR's ; in addition, it would imply that the similarity between GCRS, SEP and solar coronal abundances is fortuitous.

On the other hand, models based on specific nucleosynthetic processes have been proposed to account for the low Pb. These are, in my view, not appealing. They would, indeed, require the entire cosmic radiation to originate in sites of specific nucleosynthetic processes. This seems highly improbable, in view of the similarity of the main features of GCRS composition to LG, SEP and solar coronal composition, and of its dissimilarity to predicted outcome of the main nucleosynthetic cycles and to calculated global pre-supernova and supernova compositions.

A more acceptable possibility, to be kept in mind, would be a specific excess of the r-nuclides around Pt, with respect to which a normal Pb abundance would appear low (see § III-5.3.).

One possible way-out is to question the C1 meteoritic standard used for reference. If the - apparently significantly - lower photospheric values were used as a standard, Ge and Pb would no longer appear depleted in GCR's. The question is open.

III-4. THE C, O, ^{22}Ne, $^{25,26}Mg$, $^{29,30}Si$ EXCESSES

The C, and to a lesser extent, O excesses in GCRS are most conspicuous when the GCRS composition is compared to that of SEP's, the two compositions being otherwise quite similar (fig. 17 ; § II.1.3.). In particular the C/O ratio itself, extremely well determined in both populations, is about twice as high in GCRS as in SEP's. I surmise that these excesses relative to SEP's are highly meaningful ; and the shape of f(FIP), the basic FIP-dependent pattern of GCRS relative to LG composition defined in fig. 15, has been chosen accordingly : f(FIP) does not try to fit the GCRS/LG values for C and O, which are in excess, like in fig. 17 (§ II-1.4.). In addition such C and O excesses are known to be expected, associated with the ^{22}Ne and $^{25,26}Mg$ excesses, if these are due to a small fraction of He-burning material appearing in GCR's.

But let me first review the evidences for or against the existence of ^{22}Ne, $^{25,26}Mg$ and $^{29,30}Si$ excesses is GCRS.

III-4.1. Estimating the ^{22}Ne, $^{25,26}Mg$, $^{29,30}Si$ excesses in GCR Sources

Fig. 29 summarizes our knowledge on the Ne, Mg and Si isotopic composition. I have plotted the estimated composition from Wiedenbeck's (1984) summary at Graz, which is mainly based on low energy data (< 600 MeV/n), the new data brought at this conference by Webber et al. (2, 88) around 500 MeV/n, and a summary of the high energy HEAO-C2 data between 2.5 and 6 GeV/n, including those presented at this conference (Ferrando et al. 2, 96 ; Herrström et al. 2, 100) (§ I-2.).

In this figure, I have given both the isotope ratios measured near Earth and those derived for the sources, thus evidencing the crucial importance of the correction for secondaries in estimating the $^{25,26}Mg$ and $^{29,30}Si$ excesses (or absence of excess !!!) at the sources. These corrections differ somewhat from calculation to calculation. An important new point is that the cross-sections for secondary production of Mg and Si isotopes out of ^{28}Si and ^{40}Ar just measured by Webber and Kish (3, 87) are higher than was expected (§ I-3.1. ; fig. 5). These higher cross-sections, when extrapolated to other neighbouring parent nuclei (the question is of course : how to extrapolate ?), yield significantly higher secondary production, hence lower source abundances, for $^{25,26}Mg$ and $^{29,30}Si$ (as for Al, illustrated in fig. 6). In fig. 29, these higher cross-sections are applied to the data of Webber et al. (2, 88), but I have not modified the other corrections accordingly.

Extreme prudence is in addition required since, except for the HEAO-C2 data (which are conclusive, neither for Mg, nor for Si), all estimates are based on low energy studies. But we have shown in § III-2.1. that the B-^{15}N contradiction suggests that we understand poorly propagation at these energies, and that distributed reacceleration possibly completely blurrs the picture there. If this were the case, the corrections for secondary formation of ^{22}Ne, $^{25,26}Mg$ and $^{29,30}Si$ might have to be based on the cross-sections below 100 MeV/n, which are unknown.

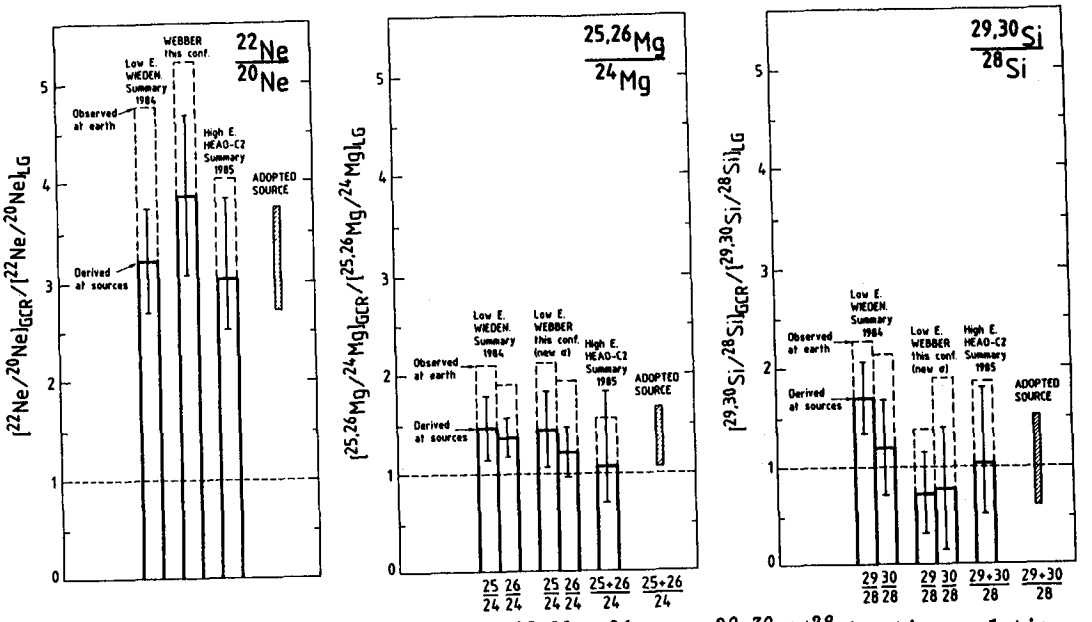

Fig. 29 Excesses in the GCR $^{22}Ne/^{20}Ne$, $^{25,26}Mg/^{24}Mg$ and $^{29,30}Si/^{28}Si$ ratios, relative to standard LG (see footnote # 27). For each set of data, I give the excess as observed at Earth (dashed ; error bar omitted for clarity) and that derived at source after correction for secondary production as derived by the authors (solid). From left to right in each plot : (i) Wiedenbeck's (1984) summary of the data existing in 1984, based mainly on low energy data (E < 600 MeV/n) ; (ii) the new data by Webber et al. (2, 88) around 500 MeV/n, the correction for secondary production being based on new, larger cross-sections, recently measured or estimated (§ I-3.1. ; figs. 5, 6) ; (iii) a summary of the HEAO-C2 data at high energy, mainly near 2.5 GeV/n but up to 6 GeV/n, based on Byrnak et al. (1983a), Goret et al. (1983) ; Ferrando et al. (2, 96) and Herrström et al. (2, 100) ; (iv) an "adopted" source excess. For Mg and Si, the various ratios plotted are indicated at the bottom of the figure.

An important point in fig. 29 is the low abundance of $^{29,30}Si$ observed near Earth by Webber et al. (2, 88), with an excellent resolution and a decent statistics (fig. 2 ; § I-2.). Together with the increased correction for spallation, it yields very low $^{29,30}Si/^{28}Si$ source ratios. Considering all the data for Si together, there may be a slight excess of $^{29,30}Si$ at the sources, but the data are also perfectly consistent with a totally normal source $^{29,30}Si/^{28}Si$ ratio.

As regards $^{25,26}Mg$, the data do suggest on excess in GCRS, but are not really compelling in view of all the uncertainties on the secondary correction. And, even if real, the excess could be very small.

Only the ^{22}Ne excess is established beyond any doubt, and is rather precisely determined.[27]

The adopted GCRS excesses of $^{22}Ne/^{20}Ne$, $^{25,26}Mg/^{24}Mg$ and $^{29,30}Si/^{28}Si$ have been plotted in fig. 20.

[27] No error has been associated with the LG $^{22}Ne/^{20}Ne$ isotope ratio, taken on the basis of SEP's (Meyer 1985b). If the Solar Wind value turned out to be more representative (e.g., Geiss 1985), the GCRS excess would be slightly larger.

III-4.2. The common and new wisdom on He-burning and weak s-process in Wolf-Rayet stars

It is now common wisdom that the simultaneous conspicuous ^{22}Ne and C excesses in GCRS (relative to LG and especially SEP abundances) are an indication that a small fraction GCR's originates in He-burning material. The smaller excesses of $^{25,26}Mg$ and O, if confirmed, indicate a more limited contribution from the subsequent stage of nucleosynthesis where ^{22}Ne is turned into $^{25,26}Mg$ and ^{12}C into ^{16}O. It is also well known that Wolf-Rayet (WR) stars, in which the nucleosynthetically active core has been bared by huge stellar winds which disperse the newly "cooked" material, are a very plausible site for providing this processed component without further alteration.

More precisely, it has been shown that the ^{22}Ne-C and possible $^{25,26}Mg$-O excesses are explained if material from WC-WO type stars (the WO stage is very rapid) is diluted in GCR's in $\sim$ 50 times as much nucleosynthetically standard, solar-mix material (to be precise, this dilution factor applies to high-FIP species that are unaffected by the local nucleosynthesis, such as ^{20}Ne ; see § III-4.3. and footnote # 29). If one considers material from the entire WR stars sequence, which includes 40% of WN stars (which are not enriched in ^{12}C, ^{22}Ne), one GCR ^{20}Ne nucleus out of $\sim$ 30 should originate in a WR star of any type (Meyer 1981c, 1985b ; Cassé and Paul 1981, 1982 ; Maeder 1983 ; Blake and Dearborn 1984 ; Arnould 1984 ; Prantzos 1984a,b ; Prantzos et al. 1983 ; 3, 167).

Note that a high abundance of Ne (presumably ^{22}Ne) has indeed been recently observed by IRAS in the atmosphere of a WC star (Van der Hucht and Olnon 1985).

One strong conclusion from the above studies is that, while $^{25,26}Mg$ can be produced in the destruction of ^{22}Ne, there is no way of producing $^{29,30}Si$ in the same context. To explain excesses of $^{29,30}Si$, additional, extrinsic hypothesis would have to be invoked, such as supermetallicity (i.e. CR's coming from far away in the inner galaxy), or galactic evolution, which are not straightforward (Woosley and Weaver 1981 ; Cassé 1981, 1983). The new observations by Webber et al. (2, 88) (§ I-2 and III-4.1. ; fig. 2 and 29) indicating that there may well be no $^{29,30}Si$ excess at all, if confirmed, would greatly simplify the situation.

In addition, liberation of neutrons at the time of the ^{22}Ne destruction by the $^{22}Ne(\alpha, n)\ ^{25}Mg$ process leads to the predicted formation of other n-rich species (weak s-process), which have been estimated quantitatively in the framework of a consistent WR evolution scheme by Prantzos et al. (1983), Prantzos (1984a,b) and at this conference by Prantzos et al. (3, 167) who have integrated over the contribution of WR stars with initial masses > 50 $M_\odot$. The predicted excess of these other n-rich species in GCRS can be related to the ^{22}Ne excess through the time scales of the WR star evolution and the dilution factor required for ^{22}Ne. These results will be discussed in the next § III-4.3. (figs. 30 and 31).

Note that a possible N excess originating in WN-stars (largely lower mass stars, < 50 $M_\odot$) has not been studied quantitatively in the same framework. Recall, however, that, even at the end of CNO cycle, N

is overabundant by a factor of at most ~ 17 (to be compared to 120 for ^{22}Ne in the He-burning phase) (Prantzos 1984a ; Meyer 1985b). Quite small dilution factors for the WN star material would be required to produce an observable N excess in GCRS, while only $\sim 40\%$ of WR stars are of type WN, 60% of them being of type WC-WO.

III-4.3. Relating the excesses in GCRS to those in the (WR) processed component material. FIP effects in the dilution

This is all nice, but there is a problem.

In order to characterize the sources of the processed material, we have to correctly relate the excesses in that processed component to those in GCRS as derived from the observations. The key point here is to properly take into account the dilution of the processed component in the main component, for each particular element.

The studies performed up to now have, in my view, not dealt with this point correctly. As pointed out in Meyer (1985b), it has been forgotten that, in the main component in which the processed material is believed to be diluted, low-FIP elements such as Mg are overabundant by factors of ~ 6 relative to high-FIP C, O, Ne. Then, while we do not know what atomic selection effects might affect the processed component, two simple cases should be considered (see formalism in the Appendix) :

(i) The processed component is affected by the same bias with FIP as the main component

Then, of course, all elements are diluted by the same factor ; and the existing studies, that simply ignore differences in dilution factor between elements, give correct results (Meyer 1981c, 1985b ; Cassé and Paul 1981, 1982 ; Maeder 1983 ; Blake and Dearborn 1984 ; Arnould 1984 ; Prantzos 1984a,b ; Prantzos et al. 1983 ; 3, 167). Then, as shown in the Appendix, the classical formula applies :

$$E^{*}_{ik,CR} = 1 + p_k \cdot E_{ik,proc,nucl} \qquad \text{(A3)}$$

where (see Appendix)

$E^{*}_{ik,CR}$ = enhancement in GCRS relative to LG after correction for bias with FIP, i.e. [GCRS/LG]/f(FIP), the quantity plotted in fig. 20, for species i relative to a reference species k which is not affected by the nuclear processing.

$E_{ik,proc,nucl}$ = enhancement in the processed component material relative to LG, due to nuclear effects only, for species i relative to the same, unaffected, reference species k.

p_k = fraction of the unaffected species k originating in the processed component ($1/p_k$ = dilution factor for species k).

I regard this situation as astrophysically implausible. It would indeed be quite odd to have the same filtering according to FIP occur independently in the main component and in the processed component, which certainly originates in a cahotic environment ; the proposed

favourable objects, Wolf-Rayet (WR) stars, are very hot, so that all elements are ionized on their surface and FIP does not have a chance to play a role.

The only way-out would then be : the filtering according to FIP should occur after mixing of the main and the processed components (i.e. at a common injection or acceleration phase).

But the presence of the refractory, condensable elements in the main GCR component and its bias with FIP seem to reflect the composition of coronae of solar-like F-M stars (as well as that of SEP's), which are likely to be the injection sites of this main component (Meyer 1985b). The cause for the bias with FIP of the main component therefore probably lies in the composition of the medium they have been extracted from, not in later, distant injection or acceleration processes. [28]

Note however that the above formula ignoring any differences in dilution between elements gives, anyway, correct results when applied only to elements on the same FIP-plateau, e.g. ^{20,22}Ne, C, O, for which it has actually been first used (see Appendix).

In the top graph of fig. 30, the data on the GCRS excesses (from figs. 20,29 and Wiedenbeck 1984) are compared to the excesses predicted for GCRS, based on Prantzos et al. (3, 167)'s He-burning and weak s-process calculations in 50-100 $M_\odot$ WO-WC star atmospheres, and on the above eq.(A3) to describe the dilution of this processed component. The dilution factor ($p_{^{20}Ne} \approx 1/50$ for the WC-WO material) [29] is adjusted as to fit the GCRS ^{22}Ne excess of ≈ 3.2 (figs. 20,29). The depicted species are those produced in WC-WO stars, whose excess in GCRS is, or may become observable (as a reminder ^{29,30}Si, which is not produced in this context, has also been plotted).

In the top graph of fig. 31, the enhancement factors in the source medium of the processed component, as derived from the GCRS data using eq.(A3), are compared with those directly predicted by the stellar evolution codes for WC-WO atmospheres. The same value $p_{^{20}Ne} = 1/50$ is used to adjust the excesses derived from the GCRS data to the ^{22}Ne enhancement calculated for time averaged WC-WO atmospheres.

---

[28] I believe that we definitely have two completely different injection sites for the main and the processed component. The final, high energy accelerations may take place, either (i) prior to mixing of the two components, in different environments; for instance, the WR component might be specifically accelerated by the WR's own stellar wind terminal shock, or (ii) after mixing of the two injected suprathermal populations, by a common agent. The lack of detectable difference between the source spectral shapes of C, O, ^{22}Ne and other heavy nuclei between ~ 1 and ~ 20 GeV/n (Engelmann et al. 1985 ; Herrström and Lund 2, 100) is consistent with the second hypothesis, but not necessarily inconsistent with the first one. Of course, search for such differences in spectral shapes should continue, especially at higher energies.

[29] Choosing ^{20}Ne as the reference species k unaffected by the local nucleosynthesis is not strictly adequate, since a small amount of ^{20}Ne is produced at the end of the WO stage (Prantzos et al. 1983 ; Prantzos 1984b ; time integrated excesses : ^{20}Ne : 1.6 ; ^{22}Ne : 108). But after dilution, the ^{20}Ne excess is completely negligible, and we can forget about it.

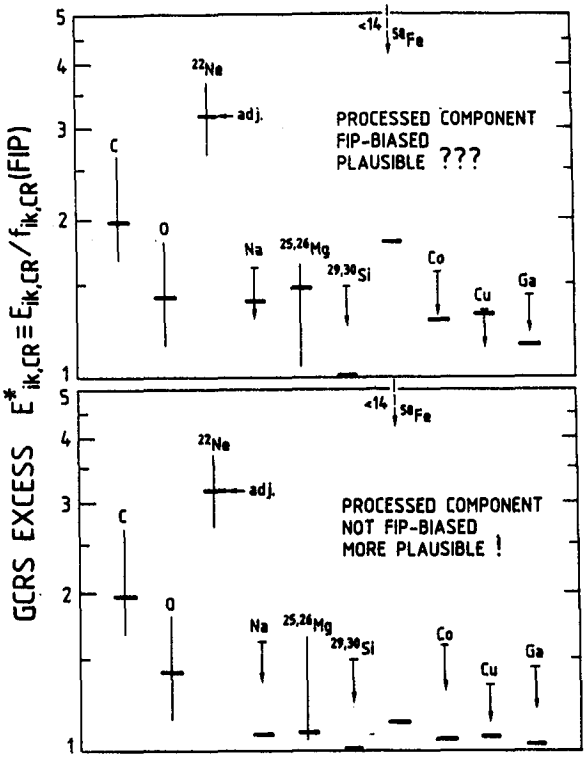

Fig. 30 *Plotted are excesses $E^*_{ik,CR}$ in GCRS, relative to the FIP-pattern $f_{ik}(FIP)$ describing the main GCRS component (cf. fig. 20) (§ III-4.3. and 4.4. ; Appendix). The species plotted are those formed by He-burning and weak s-process, for which excesses in GCRS are, or may become, observable (as a reminder $^{29,30}Si$ which is not produced in this context, has also been plotted). Vertical error bars, identical in both graphs : GCRS excesses derived from the observations (figs. 15, 20, 29). Thick horizontal marks : predictions based on Prantzos et al. (3, 167)'s model of He-burning and weak s-process in WC-WO stars, diluted in the main component by a factor of $1/p_k$ = 50 for ^{20}Ne (adjusted as to fit the "observed" GCRS $^{22}Ne/^{20}Ne$ excess). Top graph : the processed WC-WO component is assumed to be FIP-biased like the main component, so that all species are diluted by the same factor ; this assumption has been made in existing studies, but is not very plausible. Bottom graph : the processed component is not FIP-biased, so that its low FIP elements are ∿ 6 times as diluted as its high-FIP elements ; this hypothesis is much more plausible.*

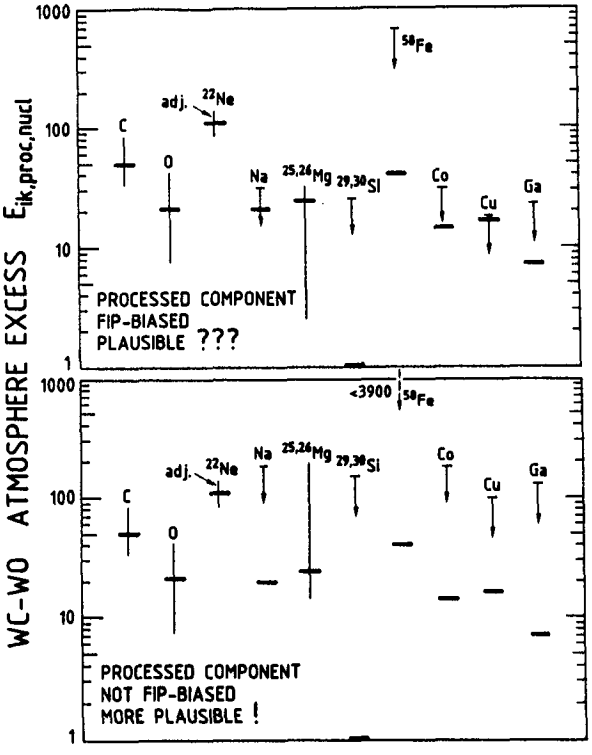

Fig. 31 *Plotted are excesses $E_{ik,proc,nucl}$ in the surface material of WC-WO stars, relative to LG composition (§ III-4.3. and 4.4. ; Appendix). Thick horizontal marks, identical in both graphs : excesses directly predicted by Prantzos et al. (3, 167)'s model of He-burning and weak s-process in WC-WO stars. Vertical error bars : excesses in the processed component source material, as derived from the "observed" GCRS excesses, assuming a dilution in the main component by a factor of $1/p_k$ = 50 for ^{20}Ne (adjusted as to fit the calculated ^{22}Ne excess in WC-WO stars). Top graph : the processed component is FIP-biased. Bottom graph : it is not FIP-biased. See caption of fig. 30.*

(ii) The processed component is not affected by atomic selection effects.

We now consider the situation in which the processed component is not affected by the same bias with FIP as the main component. As just discussed, this is the more plausible situation. Other atomic selection effect, unrelated to FIP, may of course be present in the processed component ; but in the absence of any information on them, we can only ignore them and take for the processed component the composition given directly by the local nucleosynthesis.

Then we have, as shown in the Appendix :

$$E^{*}_{ik_{CR}} = 1 + \frac{p_k}{f_{ik}(FIP)} \cdot E_{ik,proc,nucl} \qquad (A4)$$

with the notations defined above for eq.(A3) and $f_{ik}(FIP)$ being the value of f(FIP) for species i normalized to that for species : $f_{ik}(FIP) = f_i(FIP)/f_k(FIP)$.

Here $f_{ik}(FIP) = 1$ for high-FIP species (reference species k = ^{20}Ne), and $f_{ik}(FIP) \approx 6$ for low-FIP species (fig. 15). Equation (A4) thus simply expresses the 6-fold higher degree of dilution of "processed" low-FIP species as compared to high-FIP species (Meyer 1985b). The dilution factor $p_{^{20}Ne} = 1/50$ relevant for high-FIP species becomes 1/300 for low-FIP species.

When eq.(A4) is used to describe the dilution, the new connections between the excesses in GCRS and those in the WC-WO processed component are depicted in the bottom graphs of figs. 30 and 31.

III-4.4. Discussion : types of dilution, observed and predicted excesses

Figs. 30 and 31 include only three high-FIP species, C, O and ^{22}Ne, all heavier species being low-FIP elements. Comparison of the top and bottom graphs shows that :

- as regards the high-FIP species, the top and bottom graphs are, of course, identical (since the dilution is adjusted as to fit the high-FIP $^{22}Ne/^{20}Ne$ ratio). As has been known for a while now, the same degree of dilution of the WC-WO material fits simultaneously the ^{22}Ne, C and O excesses.
- For all other, low-FIP, species, the 6-fold higher degree of dilution in the bottom graphs (in which the processed component is no longer assumed to be affected by the bias with FIP) decreases the expected excesses at GCRS by that same factor of 6 (fig. 30). [Conversely, it increases the excesses in the processed material, required to fit the observed GCRS excesses (fig. 31)].
- As regards specifically $^{25,26}Mg$, produced together with O, the predicted GCRS excess drops from ~ 1.48 if the WR component is biased with FIP (as usually implicitely assumed up to now), down to ~ 1.08, i.e. a minute enhancement, in the much more probable opposite case. The present data (fig. 29) do not really exclude either of the possibilities. We really need higher statistics observations and safe, accurate secondary corrections.

- As regards the other low-FIP species, produced by the weak s-process (Prantzos et al. 3, 167), their predicted enhancements are also very small if the WR component is not biased with FIP (fig. 30, bottom). Even in the unlikely case that this component were FIP-biased, the predicted excesses would still be below all present upper limits to the GCRS excess (fig. 30, top). The most promising species that might set limits in this case are, first, Ca, and then Na, Co, Ga. Present upper limits on ^{58}Fe are still very far up.
- Note finally that, if the processed component is not FIP-biased, the existing data on Mg and Si isotopes in GCRS do not exclude equal excesses of ^{22}Ne, ^{25,26}Mg and ^{29,30}Si in the material of the processed component (fig. 31, bottom). This leaves the door slightly open for the proponents of the supermetallicity hypothesis to explain the ^{22}Ne, ^{25,26}Mg, ^{29,30}Si excesses (Woosley and Weaver 1981). It would remain to see how the C and O excesses would then fit into the picture.

III-4.5. Excess ^{22}Ne : preferential injection at the decay of ^{22}Na ?

A shrewd, totally new mechanism to explain the ^{22}Ne excess has been proposed at this conference by Yanagita (3, 175). Although I am not too convinced that it will finally work out as a very plausible scenario for ^{22}Ne, I think it deserves attention becauses it contains a lot of new ideas which may be fruitful in this, or other occasions.

The idea is that, at the moment of β-decay, the daughter nucleus gets both ionized and selectively heated, hence "injected", by the recoil energy of the electron emission. The mechanism therefore concerns nuclear species which originate from the β-decay of some other, directly synthesized progenitor. Now, it is well known from Ne-E in meteorites that some ^{22}Ne is produced via β-decay of ^{22}Na, which is itself largely synthesized by explosive H-burning in novae and possibly massive supernova envelopes (e.g., Arnould and Norgaard 1978,1981 ; Arnould et al. 1980 ; Hillebrandt and Thielemann 1982). This ^{22}Ne could be preferentially injected, hence be in excess in GCRS.

Now, among the various species thus formed via β-decay from some other directly synthesized nuclide, why should only ^{22}Ne be enhanced in GCRS ? Yanagita (3, 175) remarks that the mechanism does not work for radioactive progenitors other than ^{22}Na ($\tau_{^{22}Na}$ = 2.6 yr) because, either they are too short-lived so that the decay occurs within a stellar medium, inappropriate for acceleration, or they are rapidly locked in grains. Only ^{22}Na both has a long enough period and remains volatile in space.[30]

Many questions remain to be solved with this scenario : (i) the suprathermal ^{22}Ne must be picked up by an accelerating shock wave before it gets thermalized, which takes about 1 year ; (ii) the total production of ^{22}Ne via ^{22}Na in novae can be estimated through the observed ^{26}Al γ-ray line emission, provided most of the ^{26}Al is indeed produced by

[30] There might however be another possibility with fission products (Xe) formed in supernovae.

explosive H-burning in novae (Arnould et al. 1980 ; Hillebrandt and Thielemann 1982), which is not obvious [31] ; even then, the process requires that as much as 6% of all the ^{22}Na nuclei ejected by novae get accelerated and become cosmic-ray ^{22}Ne ; this would be a very high efficiency indeed ! (iii) the energetics remains to be precisely worked out.

Of course, this interesting mechanism, when applied to GR ^{22}Ne suffers from an additional weak point : it takes care only of the ^{22}Ne excess, so that an independent cause must be found for the C excess, as well as for the weak $^{25,26}Mg$ and $^{29,30}Si$ excesses, if they exist (figs.29 and 20 ; § III-4.1.). [32]

III-5. THE EXCESS OF ELEMENTS WITH Z ⩾ 40

The conspicuous really new event in fig. 20 is the probable excess of all of the six nuclei with Z ⩾ 40 for which GCRS abundances have been estimated (see also fig. 19). As discussed in § II.2.2., the solid error bars in fig. 20 indicate the more probable ranges for the excesses of UH nuclei, while their dashed prolongations indicate ranges which cannot yet be entirely excluded, but are by far less likely. As can be seen, the excesses seem certain for $_{42}Mo$ and $_{58}Ce$, and probable for $_{40}Zr$, $_{52}Te$, $_{54}Xe$, $_{56}Ba$. The discussion that follows is based essentially on the solid bars, and thus assumes that all six excesses are real. The dashed bars however tell us where there is still a slight degree of doubt.

The excesses appear roughly comparable in magnitude for elements in the ranges Z = 40-42 and Z = 52-58, and also for predominantly s ($_{40}Zr$, $_{42}Mo$, $_{56}Ba$, $_{58}Ce$) and for predominantly r ($_{52}Te$, $_{54}Xe$) elements But this point will have to be discussed more seriously in § III-5.2..

A very striking feature is that there is no trend for an excess up to Z = 38 : the excess starts abruptly at Z = 40. It is true that $_{34}Se$ and $_{36}Kr$, with their large error bars on fig. 20, could apparently be also in excess ; but further analysis will show that this possibility is only apparent (§ III-5.1.2.). As regards $_{38}Sr$, a refractory element for which good C1 meteoritic data agree with the photospheric value (Anders and Ebihara 1982 ; Grevesse 1984a), which is well measured in CR's (fig. 10), and for which the spallation correction is negligible (e.g., Binns et al. 1983), it is definitely not in excess (see also fig. 19). By contrast, most probably $_{40}Zr$, and definitely $_{42}Mo$ are in excess. For these two elements the LG values and the spallation corrections cannot either be questioned (see footnote # 11). [33]

---

[31] There are other, competing processes for ^{26}Al formation, in red giants (Norgaard 1980) and in Wolf-Rayet stars (Dearborn and Blake 1985 ; Prantzos and Cassé 1985).

[32] For these weak excesses, galactic evolution effects or the supermetallicity hypothesis might do the job (Cassé 1981, 1983 ; Woosley and Weaver 1981).

[33] Atomic selection effects are not good candidates to explain the jump. As regards FIP-dependent effects (actually taken out in fig. 20), $_{38}Sr$, $_{40}Zr$ and $_{42}Mo$ have very similar low values of FIP (fig. 19). In a 10^6 K plasma, fig. 21 shows that they also behave quite alike. Only in a very specific temperature range between ∿ 15000 and ∿ 80000 K would $_{38}Sr$ (in its Kr-like state) behave differently from $_{40}Zr$ and $_{42}Mo$.

III-5.1. Estimating the excesses in the processed component material - FIP effects in the dilution

III-5.1.1. The dilution problem

Before discussing the possible significance of the excesses in fig. 20, we must make sure that we understand them correctly. We are indeed faced with the same problem as in the study of the ^{22}Ne and its associated excesses in § III-4.3.. Most likely, we have again a processed component, highly enriched in specific species, which is highly diluted in the FIP-biased main CR component. We need to derive the nuclear anomalies in the source material of this processed component from the GCRS excesses in fig. 20. This requires to properly take into account the differences in degree of dilution of the various elements of the processed component, due to the FIP-bias in the composition of the main component itself (cf.§ III-4.3.).

We shall, again, start from the fundamental eq.(A2) of the Appendix, explicited for $E_{ik,proc,nucl}$:

$$E_{ik,proc,nucl} = \frac{E^{*}_{ik,CR} - 1}{p_k} \cdot \frac{f_{ik(FIP)}}{f_{ik,proc(atom)}} \qquad (A2')$$

with the notations of § III-4.3. and of the Appendix [$f_{ik,proc}(atom)$ describes any atomic selection effects in the processed component]. This equation is valid for $p_k << 1$ (high degree of dilution) and $E_{ik,proc,nucl} >> 1$.

The situation however differs from the one we had when studying the ^{22}Ne anomaly : here we have no model at hand to theoretically estimate $E_{ik,proc,nucl}$ and therefore have no way to know the dilution factor $1/p_k$ (which I just assume to be large). $E_{ik,proc,nucl}$ can therefore be derived only to within an unknown factor. This is why fig. 32, otherwise similar to fig. 31, is labelled in arbitrary units (actually normalized to the $_{42}Mo$ excess $\equiv 10^n$, where n is an unknown, non integer, number).

Like in § III-4.3., we have two choices :

(i) the processed component has gone through the same FIP-filtering as the main component ; then all differential effects on dilution cancel out ; $f_{ik,proc}(atom) = f_{ik}(FIP)$, and the second factor in eq.(A2') vanishes (fig. 32 ; top) ; for the reasons developed in § II-4.3., I consider this situation as implausible ;

(ii) the processed component did not go through the same FIP filtering ; other atomic selection effects may of course be at work, probably not related with FIP ; in the absence of any information on them, we can only ignore them and set $f_{ik,proc}(atom) = 1$; we are thus left with a factor $f_{ik}(FIP)$ in eq. (A2'), which just describes the lower degree of dilution of the processed species belonging to elements which are underabundant in the main component (fig. 32, bottom) ; this should be a better approximation to reality.

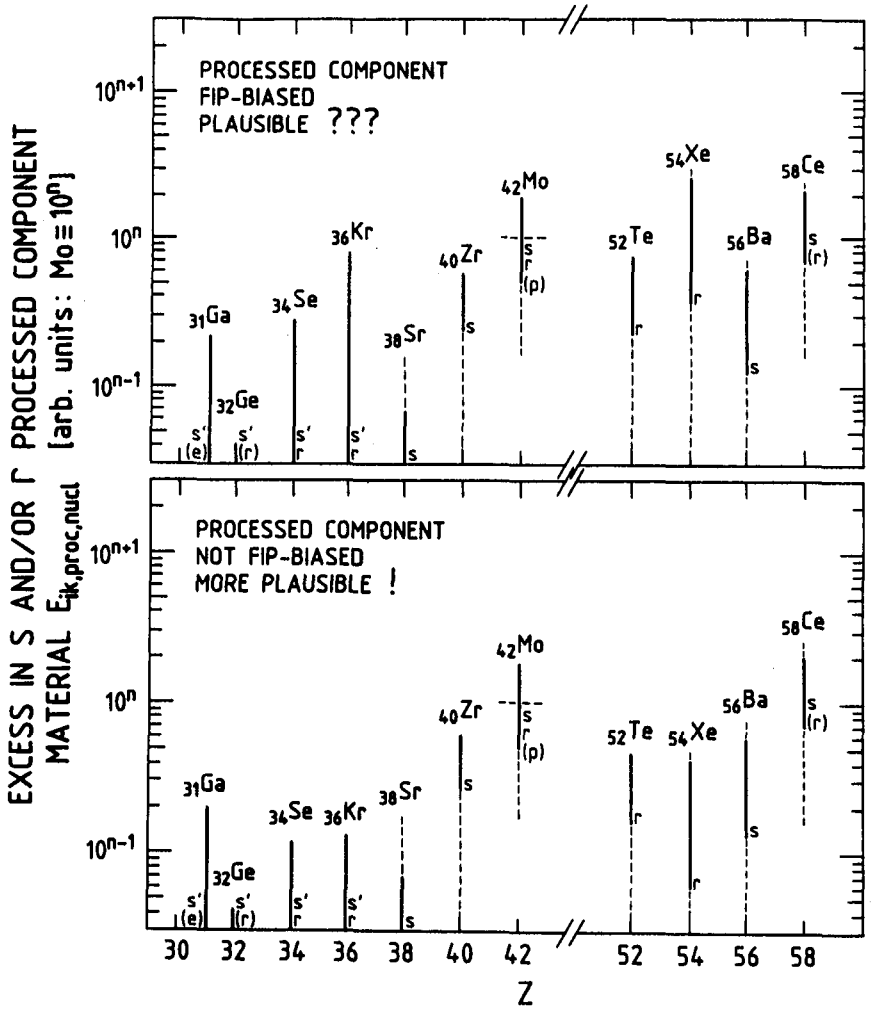

Fig. 32 *Plotted are excesses $E_{ik,proc,nucl}$ in the s and/or r-processed component material, relative to LG composition (§ III-5.1. ; Appendix). This figure is similar to fig. 31. The excesses in the processed component are those derived from the GCRS composition (figs. 19, 20 ; § II-2.2.) ; they are known only to within an unknown dilution factor for the processed component ($1/p_k$, assumed large), so that only relative values of the excesses are given (normalized to the $_{42}$Mo excess ≡ 10^n). For each element, the thick, solid error bar gives the more probable range, and its thin, dashed continuation a range that is much less likely, but cannot yet be entirely excluded (figs. 19, 20 ; § II-2.2.). Of course, bars reaching the bottom lines are only upper limits, consistent with no enhancement at all. Also given are the main processes responsible for the synthesis of the various elements in the "solar mix" : e, s, r, p processes, and s' = s due to the weak component of the neutron irradiation (see footnote # 35). One symbol plotted : ≥ 80% one process ; two symbols : two processes contribute about equally ; second symbols in parenthesis : contributes about 1/3 of total. Top graph : the processed component is assumed to be FIP-biased like the main component, so that all species are diluted by the same factor ; this assumption is quite implausible. Bottom graph : the processed component is not FIP-biased, so that in GCRS its low-FIP elements have been more diluted than its high-FIP elements ; it is the more plausible hypothesis.*

III-5.1.2. Consequences of differential dilution

Introducing the differential effects of dilution changes the picture in some respects, which are apparent when comparing figs. 20 and 32, top and bottom. In fig. 32, I have marked the predominant nucleosynthetic processes responsible for the formation of the various elements in the usual "solar mix" (Käppeler et al. 1982 ; Fixsen 1985 ; Binns et al. 1985).

Elements $_{34}Se$, $_{36}Kr$ and $_{38}Sr$ are all three consistent with no enhancement at all (fig. 20). Figs. 20 and 32 (top), however, do not exclude the possibility that $_{34}Se$ and $_{36}Kr$, with their large upward error bars be in excess, while $_{38}Sr$ is definitely not. Since about half the $_{34}Se$ and $_{36}Kr$ are formed by r-process while $_{38}Sr$ is almot pure s, one could have considered a specific enhancement of r-nuclides in this range [however the enhancement of $_{40}Zr$, also almost pure s, would have poorly fitted into the picture]. When differential dilution is included (fig.32, bottom), this possibility of an enhancement of $_{34}Se$ and $_{36}Kr$ relative to $_{38}Sr$ in the source material of the processed component disappears.

In the $_{52}Te$ $_{54}Xe$ $_{56}Ba$ $_{58}Ce$ quartet, introduction of differential dilution specifically reduces the excesses of the two r-elements $_{52}Te$ and especially $_{54}Xe$ (which happen to be high- or intermediate-FIP elements, fig. 19) in the processed component material (fig. 32).

III-5.2. Evidences for s and/or r-process excesses

I am now going to discuss the excesses in the processed component material, under the most plausible assumption that this component has not gone through the FIP-dependent filter of the main component (§ III-4.3. and 5.1.). Fig. 32 (bottom) will therefore serve as the main basis for the discussion.

III-5.2.1. What happens at Z = 40 ?

As noted earlier, and obvious from figs. 20 and 32 (top as well as bottom), the most striking feature in the data is the sharp onset of the excesses, specifically between Z = 38 (no excess) and Z = 40 (provided the $_{40}Zr$ excess is confirmed, § II-2.2.).

At Z = 38 to 40, we are right at the neutron magic number N = 50 (fig. 33) ! This fact very strongly suggests an s-process anomaly. $_{38}Sr$ and $_{40}Zr$ are almost pure s elements, while $_{42}Mo$, for which the excess is best established, is about 44% s, 32% r and 24% p (Käppeler et al. 1982 ; Fixsen 1985 ; Binns et al. 1985).

As shown in fig. 33, all isotopes of Sr have $N \leqslant 50$ neutrons ; but one isotope dominates by far, ^{88}Sr (82%), which has N = 50 neutrons. As regards Zr, all its isotopes have $N \geqslant 50$ neutrons ; the most abundant isotope, ^{90}Zr, which makes up 52% of Zr, has also N = 50 neutrons. Both ^{88}Sr and ^{90}Zr lie right near the bottom of the first precipice of the σN_S curve (e.g., Ward and Newman 1978 ; Käppeler et al. 1982). So, ^{88}Sr is definitely not enhanced in GCRS, while ^{90}Zr, with the same magic number of neutrons N = 50, may be enhanced, or not. The responsibility for the enhancement of elemental Zr might indeed rest only with its isotopes with $N \geqslant 51$, which make up 48% of elemental Zr.

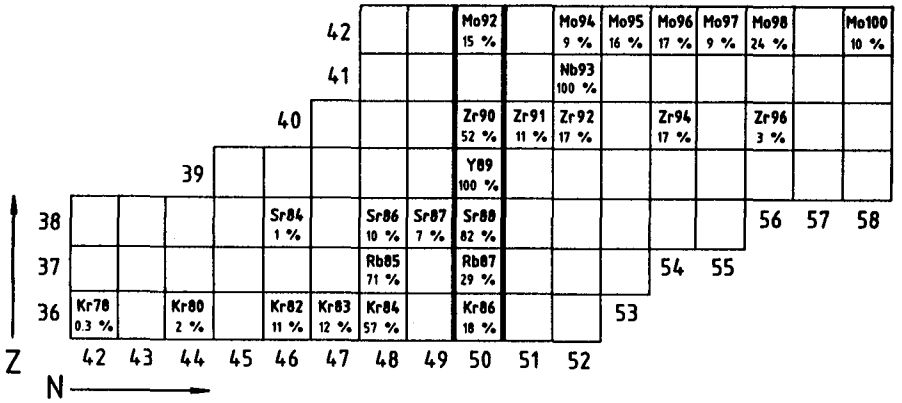

Fig. 33 The critical part of the chart of the nuclides around Z = 40, i.e. around magic N = 50 neutrons (§ III-5.2.1.). Only stable nuclides are given. The percent contribution of each isotope to the elemental abundance in the "solar mix" is indicated. For the contribution of the various processes to each nuclide, see Käppeler et al. 1982, Fixsen 1985, Binns et al. 1985 (see also fig. 32). The CR data indicate that $_{40}$Zr and $_{42}$Mo are probably enhanced in CR sources, while $_{36}$Kr and $_{38}$Sr are not (figs. 10, 19, 20, 32 ; § II-2.3. and III-5.). This may suggest that nuclides with N ≳ 51 neutrons are specifically in excess in GCRS.

So the enhancement of s-species precisely from Z = 40 upwards might mean that only species with N ≳ 51 neutrons, beyond the magic N=50, are enhanced in GCRS. [34] This would imply that products of comparatively strong s neutron irradiations, with average number of neutrons captured per Fe nucleus $n_c \gtrsim 54$, are overrepresented in GCR's (e.g., Clayton 1968, Fig. 7-22). Some material having undergone specifically such strong irradiations should be injected in the CR accelerating machine ! A very important conclusion indeed ! [which however depends on the confirmation of the [35] $_{40}$Zr excess ; $_{42}$Mo lies beyond N = 50, and is almost as much r as s].

III-5.2.2. The $_{52}$Te $_{54}$Xe $_{56}$Ba $_{58}$Ce quartet

In the r- and s-peaks region between Z = 52 and 58, we have evidence for enhancement of all four studied elements, by comparable amounts for predominantly r $_{52}$Te and $_{54}$Xe and for predominantly s $_{56}$Ba and $_{58}$Ce (figs. 20 and 32, bottom).

The best established enhancement is that of $_{58}$Ce, which is 65% s and 35% r in "solar mix" material. Almost pure s $_{56}$Ba is probably also enhanced.

---

[34] In this context, a reliable determination of the CR abundance of the single isotope pure-s element $^{89}_{39}$Y, which has also 50 neutrons, would be worth a very specific effort, if feasible at all.

[35] For A ≲ 86 (i.e. from $_{36}$Kr downwards) an additional frequent weak neutron irradiation is required to account for the s-species abundances, which are higher than predicted by the main irradiation law which make up all s-species up to ^{204}Pb (Ward and Newman 1978 ; Käppeler et al. 1982). Elements largely produced by this extra irradiation, i.e. $_{31}$Ga, $_{32}$Ge, $_{34}$Se, $_{36}$Kr, denoted by s' in fig. 32, are clearly not enhanced in CR's. One could imagine that the enhancement starts right beyond this zone, when the main irradiation law sets in. But the limit would then lie between $_{36}$Kr and $_{38}$Sr, not between $_{38}$Sr and $_{40}$Zr as it does.

The data as they stand tell us that r-nuclides in this range are enhanced by comparable factors (fig. 32, bottom). But the two predominantly r elements we have, $_{52}$Te and $_{54}$Xe are not among the nuclides whose excesses are best established (fig. 19). The HEAO-C3 data for $_{52}$Te have changed a lot between the earlier and the new analysis, which however agrees with the Ariel VI data (fig. 10). $_{54}$Xe is poorly resolved between more abundant elements in both HEAO-C3 and Ariel VI experiments (fig. 9) [not to speak of the question of the $_{54}$Xe LG abundance]. For both elements, secondary formation by spallation is not negligible, so that a limited downward revision of the observed abundance can result in a large revision of the source abundance. Finally, both excesses are sensitive to the exact choice of f(FIP), which is of course also subject to an uncertainty, especially in the relevant intermediate- and high-FIP region (fig. 19).

For these reasons, the r-process excess in the Z = 52-54 peak, while suggested by the data, should still be taken with caution.

III-5.3. UH element excesses - Summary and overview

There is no enhancement of, either s, or r nuclides for $Z \leqslant 38$ (fig. 32, bottom).

There is quite convincing evidence for s-process enhancements beyond Z = 38, from (fig. 32, bottom) : (i) the jump between the almost pure s elements $_{38}$Sr, not enhanced, and $_{40}$Zr, probably enhanced, right at the limit N = 50 (magic) ; (ii) the well established excesses of largely s $_{42}$Mo and $_{58}$Ce (which have, however, also very significant r components in the "solar mix") ; (iii) the probable excess of almost pure s $_{56}$Ba. This implies that some specific material having undergone strong s neutron irradiations (average number of neutrons captured/Fe nucleus $n_c \geqslant 54$, Clayton 1968) is probably present in CR's.

There is evidence for comparable excesses of r-nuclides in the Z = 52-54 r peak (fig. 32, bottom), but it is weaker : it rests on two elements, $_{52}$Te and $_{54}$Xe whose excesses are probable, but not very strongly established.

It must be stressed that the real strength of the evidence for a s-process excess rests on the sharp jump right at N = 50 (fig. 33), i.e. on the reality of the $_{40}$Zr excess, which becomes our cornerstone. Its LG abundance is very reliable. But as can be seen in fig. 10, its excess is observed only in the new analysis of the HEAO-C3 data. It needs confirmation.

If this $_{40}$Zr excess happened not to be confirmed, the entire picture would be much more ambiguous : all elements $_{42}$Mo, $_{52}$Te, $_{54}$Xe, $_{58}$Ce have significant r contributions, and a predominant excess of r nuclides could not be excluded [36]. Only $_{56}$Ba, whose excess is not very strongly established, would definitely not fit in. Recall, too, that the low "Pb-group"/"Pt-group" ratio (§ III-3.), usually discussed in terms of a low Pb abundance, can also be interpreted in terms of an excess of the r elements forming the "Pt-group".

[36] Although it would then seem odd to have the almost pure r elements $_{52}$Te and $_{54}$Xe apparently less enhanced than the mixed elements $_{42}$Mo and $_{58}$Ce (fig. 32, bottom).

PART IV

SUMMARY AND RECOMMENDATIONS

IV-1. SUMMARY

A few key new observations have been brought at the La Jolla Conference : observation of sub-Fe nuclei up to 200 GeV/n (§ I-1. ; fig. 1) ; improved isotopic data, which are especially important for Si (§ I-2. ; figs. 2, 3) ; a whole bunch of results from continuing efforts on systematic spallation cross-section measurements (§ I-3. ; figs. 4 to 8) ; a breakthrough in the accuracy of the Ultra-Heavy (UH) nuclei abundance measurements up to $Z \approx 60$ (§ I-4. ; figs. 9 to 11) ; improved data on low energy deuterium and ^{3}He, and evidence (related to new spectral measurements) that the recently claimed high ^{3}He fluxes at high energy is probably an overestimate (§ I-5.) ; energy spectra of primary nuclei (§ I-6. ; not discussed) ; improved observations of e^- fluxes up to 2000 GeV and of e^+ around 10 GeV (§ I-7. ; figs. 12, 13).

From these and earlier data, the Galactic Cosmic Ray compositions at Sources (GCRS) can be inferred. This implies correcting for the effects of interstellar propagation, which I discuss now.

As regards CR propagation, we have two strong facts :

(i) At very high energies, observations of sub-Fe nuclei have shown beyond doubt that the escape length λ_e continues to decrease, at roughly the same rate, up to at least 200 GeV/n (§ I-1 ; fig. 1).

(ii) While in the GeV/n range, the observations of secondary nuclei yield a reasonably consistent picture of CR propagation, at low energies ($\lesssim$ 600 MeV/n) we have a flat contradiction between two presumably pure secondary to primary ratios : B/C and ^{15}N/O. They cannot be fitted simultaneously with classical propagation models (§ III-2.1. ; figs. 23 and 24). The contradiction is well beyond reasonable errors on both the CR data and the cross-sections, which happen to be particularly well measured for the relevant nuclei and at these energies (§ I-3.1.; fig.4 ; Table 2). The nuclei concerned are also too close in mass for refinements of the propagation model (truncation of the PLD) to have any chance to solve the problem.

One way out would be to have ^{15}N enhanced by a factor of $\sim$ 100 in CR sources, but it does not sound plausible to me (footnote # 19). I therefore think that some really new ingredient must be introduced in our understanding of low energy CR propagation.

One may note that a large fraction of C_2 (and a smaller one of O) is believed to originate, together with the ^{22}Ne excess, in a specific

environment, plausibly Wolf-Rayet stars (§ III-4.2.). One cannot exclude that these nuclei might have a propagation history different from that of the bulk of other CR's, and traverse on the average less matter. This hypothesis cannot be strictly ruled out, but it is completely speculative, ad hoc, and difficult to check (§ III-2.1.).

The only other way-out I can think of at this point is the hypothesis of distributed reacceleration, in which CR's still increase their energy by a factor of a few units while propagating, as they meet extended weak SN shock waves. This idea, which is much less far-fetched and more liable to check, was first advocated by Silberberg et al. (1983) to ease various problems in cosmic ray composition, especially below a few 100 MeV/n (§ III-2.1.). The relevant cross-sections for secondary formation could then be largely those below $\sim$ 100 MeV/n, which are often unmeasured, but known to be far from constant ; for nearby secondaries, they tend to sharply peak at low energy before decreasing towards threshold. I think the low energy B-^{15}N contradiction may be a good case for distributed reacceleration, and justifies a serious effort to investigate the point (see next § IV-2. for recommendations).

Anyway, as long as the low energy B-^{15}N contradiction is not understood, I think the determination of source abundances of ^{14}N and other largely secondary nuclei (Na, ^{25,26}Mg, Al, ^{29,30}Si, P, Ar, Ca) from low energy data ($E \lesssim 600$ MeV/n) cannot give reliable results. At higher energies, the cross-sections are much more constant, at least for comparatively light nuclei, so that distributed reacceleration, if present, has much less effect on the interpretation of the data.

As regards specifically the ^{14}N source abundance (§ III-2.2.), we are left with the high energy studies based on elemental data, which lead to $(N/O)_{source} \approx 6\%$, and with the high energy isotopic values, which, though scattered, are all consistent with that same value (fig. 25). The ratio $(N/O)_{source} \approx 6\%$ implies no deficiency of N relative to other high-FIP elements (at least those not affected by the Wolf-Rayet nucleosynthesis ; § III-4.) (figs. 14, 15, 17).

The B-^{15}N contradiction also precludes any conclusion on a truncation of the exponential pathlength distribution (PLD) at low energy (§ III-2.3.3. ; figs. 23, 24 and 26). At higher energies, the situation is open : studies of elements up to Fe do not request a truncation, but could allow a limited one (fig. 26) ; properly taking into account spallation on interstellar He could possibly increase the need for truncation (§ III-2.3.1.). Interpretation of the data on UH nuclei, which are most sensitive to truncation, is complicated due to an energy dependence of the cross-sections that extends up to very high energies [where distributed reacceleration, if present, would further change the picture] (§ III-2.3.2. ; fig. 27).

After these remarks on CR propagation, we can get back to the source composition. Let me first discuss the elemental GCRS composition up to Z = 30 as derived, for safety's sake, mainly from observations in the GeV/n range (§ II-1. ; figs. 14, 15). Up to Z = 30, there is no great novelty : the GCRS/LG (LG : "Local Galactic" abundance standard) ratios follow the well known correlation with First Ionization Potential

(FIP) ; it is clear that this correlation does not follow an exponential law (fig. 18), but has rather a two-plateau structure (fig. 15) ; it is very similar to that found in Solar Energetic Particles (SEP) and, more important, in coronal composition [except for a distinct excess of C and a probable one of O in GCRS] (fig. 17). This structure is not too consistent with an ionized fraction in a gas at any simple temperature or with a monotonic distribution of temperatures. It rather suggests a picking out, with different efficiencies, of both ions and neutrals out of a gas at $\sim$ 6000 K, such as the gas in the chromospheres underlying the coronae of the Sun and of most main sequence F to M stars (§ II-1.3. and 1.4.).

It should be stressed that H and He, which have a unique, odd temporal behaviour in SEP's, have a GCR source spectrum that is distinctly flatter than the common source spectrum of heavier species (between 3 and 60 GeV/n) (§ II-1.2.3. and III-1.1. ; e.g. fig. 15). H and He are both deficient relative to heavier nuclei, but the He/H ratio itself is remarkably normal and energy-independent. The attempts to explain the H, He deficiency by a rigidity-dependent injection of GCR's directly out of the hot ISM gas face very serious difficulties : they do not account for the normal He/H ratio, nor for the discontinuities of the heavy element GCRS/LG ratios versus Z (§ III-1.2. ; figs. 21, 22).

Back to the C and O excesses in GCRS as compared to SEP, they are probably related to the ^{22}Ne and associated isotopic anomalies. Where do we stand as regards our knowledge of the ^{22}Ne, $^{25,26}Mg$, $^{29,30}Si$ excesses at GCR sources (§ III-4.1.) ?

The ^{22}Ne excess is, of course, confirmed. As regards the heavy Mg and Si isotopes, observed mainly at low energy, new data do not find any more evidence at all for a $^{29,30}Si$ excess (§ I-2. and III-4.1. ; figs. 2 and 29). In addition, new cross-section measurements (§ I-3.1. ; fig. 5) suggest a larger than expected secondary contribution to the observed $^{25,26}Mg$ and $^{29,30}Si$. This, together with the unknown effects of a possible distributed reacceleration, leads me to very prudent about the magnitude of the $^{25,26}Mg$ excess itself, which has, however, still a good chance to be real (§ III-4.1. ; fig. 29).

A lack of $^{29,30}Si$ excess, if confirmed, could fit well into the helium-burning (Wolf-Rayet) scenario for the excess ^{12}C, ^{16}O, ^{22}Ne, $^{25,26}Mg$, in which heavy Si isotopes are not produced.

But atomic selection effects interfere with this interpretation of ^{12}C, ^{16}O, ^{22}Ne, $^{25,26}Mg$ and correlated weak s-process excesses in terms of a small fraction of CR's originating in He-burning material, plausibly at the surface of WC-WO Wolf-Rayet stars (§ III-4.2.). A question should indeed be posed : did the processed component go through the same FIP-filtering as the main CR component ? As regards the main component, we now have good reasons to believe that the cause for its bias with FIP lies in the composition of the cool star coronal medium they have been extracted from, rather than in the injection or acceleration process (§ II-1.3. , III-4.3.). There is no reason whatsoever for the source material of the ^{22}Ne rich component to have been affected by the same FIP-filtering, especially if it originates in hot WC-WO stars. So,

the processed component, in all likelihood not FIP-biased, is diluted in a main CR component in which low-FIP elements are comparatively $\sim$ 6 times as abundant as high-FIP elements. Therefore the processed low-FIP $^{25,26}Mg$ and weak s-process species are $\sim$ 6 times as diluted as the high-FIP ^{12}C, ^{16}O and ^{22}Ne. Their predicted excesses at GCRS thus become minute, essentially impossible to evidence (§ III-4.3. and 4.4. ; fig.30, bottom). The large uncertainty on the presently determined $^{25,26}Mg$ source abundance does not conflict with these views (fig. 30, bottom).

Conversely, if the GCRS $^{25,26}Mg$ and/or $^{29,30}Si$ excesses eventually turned out to be significant (say, a factor of $\sim$ 1.5), it would probably imply roughly equal excesses of ^{22}Ne, $^{25,26}Mg$ and/or $^{29,30}Si$ in the source material of the processed component (fig. 31, bottom), which could no longer be explained in terms of He-burning in WC-WO stars. Other hypothesis, such as supermetallicity, should then be considered.

Now, let us turn to "Ultra-Heavy" (UH) elements, beyond Z = 30. There, we have real new stuff ! The most important point brought up at this conference is serious evidence for excesses of all elements for which we have source abundance determinations between Z = 40 and 58, relative to the FIP pattern f(FIP) describing the composition for elements with $Z \leqslant 30$ [excesses of $_{40}Zr$, $_{42}Mo$ and of the r-s-peaks elements $_{52}Te$, $_{54}Xe$, $_{56}Ba$, $_{58}Ce$; the excesses of $_{42}Mo$ and $_{58}Ce$ are certain, the others are probable] (§ II-2. ; figs. 10, 19, 20). Once again, I tend to interpret these excesses in terms of a specific processed component, highly diluted in the main, solar coronal-like, CR component. In deriving the excesses in the processed component material itself from the "observed" GCRS excesses, we again have to take into account the fact that, in all likelihood, the processed component itself is not FIP-biased (§ III-5.1. ; fig. 32, bottom).

A key point here is that elements in the range Z = 30 to 38, and in particular definitely $_{38}Sr$, are not enhanced : they just nicely follow the correlation f(FIP) (figs. 19, 20, 32 bottom). So, the enhancements seem to start abruptly at Z = 40. Actually, the enhancement of $_{42}Mo$ is established beyond any doubt, while that of $_{40}Zr$ is probable, but not yet certain (fig. 10). This $_{40}Zr$ excess (or lack of excess) is the cornerstone of the interpretation of all these UH excesses, and is worth any effort to be confirmed (or not).

If $_{40}Zr$ is indeed in excess, the sharp onset of the excesses between $_{38}Sr$ and $_{40}Zr$, right after the neutron magic number N = 50 (fig. 33) is almost a signature of a s-process contribution, implying that a specific component having undergone strong neutron irradiation (average number of neutrons captured per seed Fe nucleus $n_c \geqslant 54$, see Clayton 1968) is present in the cosmic radiation. It is then very tempting to interpret the excesses of predominantly s $_{42}Mo$, $_{56}Ba$ and $_{58}Ce$ in terms of this same intense neutron irradiation. There seems to be also an r-process excess, as judged from $_{52}Te$ and $_{54}Xe$. But the excesses for these two elements are not very strongly established from the data (fig. 19 ; § III-5.2.2.).

If, by contrast, the $_{40}Zr$ excess is not confirmed, the interpretation of the various excesses in terms of s and/or r-process excesses is

much more confused, since the elements for which we have best evidence for an excess, $_{42}$Mo and $_{58}$Ce, (figs. 19, 20, 32 bottom) have both significant s and r components in "solar mix" material. If r-process excesses are present, the may be related to a possible excess of Pt-group elements (see below).

Finally, we have still the old puzzles of the low Ge and low Pb/Pt ratio, unusually interpreted in terms of an underabundance of Pb. Contrary to excesses, deficiencies cannot be explained by admixture of a specific extra-component ! Thus explaining a low Pb in terms of a special nucleosynthesis requires the bulk of the cosmic radiation to originate in a spot of active nucleosynthesis, while we have so much evidence that most CR's are made of nucleosynthetically "solar mix" material, just fractionated like solar coronal gas. An excess of r-process Pt would be more plausible (§ III-3.3. and 5.3.). On the other hand, a coupled deficiency of Ge and Pb could indicate a fractionation of "solar mix" material according, not to FIP, but to volatility ; this would indicate that CR's are interstellar grain destruction products, another hypothesis not easy to live with [similarity with solar corona and SEP's ; noble gas abundances] (§ III-3.4.). Finally, the standard abundances to which we refer the CR abundances of Ge and Pb may be inadequate, in which case they could be not deficient at all ! For these two elements, the photospheric value indeed seems to differ significantly from the usually adopted C1 meteoritic value (§ III-3.5. ; figs. 19, 20, 28). This would be the easiest explanation. But the question is open.

IV-2. RECOMMENDATIONS FOR FUTURE WORK

(i) Distributed reacceleration

The hypothesis of distributed reacceleration should be throroughly investigated (§ III-2.1.). Only its modelling (in the presence of solar modulation) will allow to tell whether it can, not only solve the low energy B-^{15}N contradiction, but consistently account for the fluxes of D, ^{3}He, ^{6,7}Li, ^{7,9}Be, ^{10,11}B, ^{15}N, ^{17}O, F and sub-Fe nuclei observed at low energy. Also, will it yield low energy source abundances for ^{14}N,Na,Al,P,Ar, Ca consistent with the higher energy determinations ? Will it have an effect on the ^{22}Ne, ^{25,26}Mg and ^{29,30}Si source abundances, which are mainly determined from low energy data ? One must also investigate the problem posed by the differences in energy loss rates between nuclei, if they are kept a long time at low energy, say below 100 MeV/n. Last but not least, such a study requires a program of very low energy cross-section measurements (all the way down to thresholds) which I shall evoke below.

(ii) Fluorine

I insist on the possibility to get independent information on propagation from F, a purely secondary element, close to B and ^{15}N, but not made from C and O [in recent CR experiments, F is well resolved from O]. It might help to understand what is going on in the Li, Be, B, ^{15}N region (§ III-2.1.). But, first, we need cross-sections.

(iii) Energy range for source abundance determinations

In order to get safest source abundances of comparatively light nuclei, CR observations and propagation studies should concentrate in the range $\sim$ 1 to 2 GeV/n. At higher energies, we cannot get any more cross-section measurements at the Bevalac, and have to use extrapolated cross-sections (which, however, usually remain quite constant with energy for lighter nuclei). At lower energies, the combined effect of the strong cross-section variations below $\sim$ 100 MeV/n and of possible distributed reacceleration (plus modulation !) casts doubt on any results one may obtain [for heavier nuclei, such as Fe or UH nuclei, the cross-sections become energy-independent only at significantly higher energies ; e.g. Webber 1984 ; Kaufman and Steinberg 1980].

(iv) Zr abundance and s-process

In the UH range, make all efforts to confirm (or not) the high abundance of $_{40}Zr$, which is essential in the interpretation of the UH element excesses in terms of a CR component having undergone a specific s-process (fig. 10 ; § III-5.2.1. and 5.3.). If feasible at all, an estimate of the abundance of the neighbouring odd-Z single isotope element $^{89}_{39}Y$ (N=50) would also be valuable.

(v) Cross-sections

Although much effort has been invested in recent years on cross-section measurements and semi-empirical estimates (§ I-3.), insufficient knowledge of spallation cross-sections is still the weak point of many a CR problem :

- A major specific effort must be undertaken to measure all relevant cross-sections at lowest energies, down to thresholds (below the $\sim$ 300 MeV/n lower bound of the Bevalac range). Such a program is essential to investigate the reality of distributed reacceleration and to assess its consequences (§ III-2.1.).

- Measurements of cross-sections on a He target are necessary to progress on the question of the truncation of the PLD (§ III-2.3.1.).

- Measurement of cross-sections for the formation of F can give an essential new tool to untangle the low energy propagation puzzle (isotopic cross-sections ; undecayed elemental cross-sections are always much less useful) (§ III-2.1.).

- Be conscious that, once the cross-sections for the major contributors to the formation of a daughter product have been accurately measured, the much larger errors on the unmeasured cross-sections for the numerous minor contributors can become dominant (see, e.g., Table 2 and figs. 23 to 26). Therefore, measurements on a large number of parent nuclei are useful and, for lack of it, a significant improvement of the semi-empirical estimates is essential. This remark applies in particular to crucial nuclei whose formation cross-sections from dominant parents have been intensively measured recently :

  - B, $^{14,15}N$: (Table 2). Note the importance of $^{14,15}N$ parents in the formation of B and even ^{14}N !

- Se-Cr : (Table 2). Note the importance of parents other than ^{56}Fe (mainly Mn, $^{54,55}Fe$, Ni).
- $^{25,26}Mg$, $^{29,30}Si$: to the secondary production of $^{25,26}Mg$, while Si contributes $\sim$ 63 %, Al makes $\sim$19 %, S $\sim$ 9 % and heavier nuclei $\sim$ 9 % ; to that of $^{29,30}Si$, while S contributes $\sim$ 52 %, Ar makes $\sim$ 12 %, Ca $\sim$13 %, Sc-Mn $\sim$15 % and Fe $\sim$8 %.

- As regards UH nuclei, where cross-sections remain energy dependent up to very high energies, try to semi-empirically combine the recent Bevalac data on $\sigma = f(Z_{parent})$ at $\sim$ 1 GeV/n (§ I-3.1. ; fig. 7) with the comprehensive data on $\sigma = f(E)$ for a Au target over the wide range of energies from 0.2 to 6 GeV/n by Kaufman and Steinberg (1980). [If possible, of course, complement the Bevalac measurements at $\sim$ 1 GeV/n by other ones at other (including lower) energies within the $\sim$ 0.3 to 2 GeV/n Bevalac range]. To master the energy-dependence of the cross-sections is obviously essential to interpret the UH data in terms of propagation (truncation problem ; § III-2.3.2. ; fig.27).
- Try to diversify the groups performing cross-section measurements, to permit inter-laboratory check of the results. In particular check thick target against thin target data.
- With the large body of recent and forthcoming measurements of spallation cross-sections for ^{12}C, ^{16}O, ^{20}Ne, ^{24}Mg, ^{28}Si, ^{32}S, ^{40}Ar, ^{40}Ca, ^{56}Fe, ^{58}Ni and of the low energy dependence of the cross-section for ^{56}Fe, time should be ripe for real improvement of the parametrization of the (still essential) semi-empirical formulae. These should be based, as much as possible, on a better physical understanding of what is going on (see detailed discussion in § I-3.2.).

Acknowledgements

I am first of all highly indebted to Aimé Soutoul for a number of essential discussions we have had before and after the Conference, and for introducing me to the delights of the Saclay HEAO-C2 team propagation code. Many of the ideas put forward in this report, especially on CR propagation, originated in these exchanges with him. I also profited from discussions with Philippe Ferrando and Philippe Goret. From Jean-Jacques Engelmann and Michel Cassé, I got wise criticism of the manuscript. I also wish to thank a large number of colleagues for the patience with which they endured my endless inquisitorial questioning under the ever present beautiful sun (or moon) of La Jolla. I am highly indebted to the HEAO-C3 team, and particularly to Ed Stone, for their permission to print the results of the preliminary, but capital new analysis of their data, which have been given only orally at the Conference and are thus not present in the printed "Conference Papers". I apologize for not having discussed the important field of the shape of the CR spectra (see footnote # 5), nor other interesting papers dealing with the properties of the interstellar medium in which CR's propagate. Finally, last but not least, I wish to thank Franck Jones and the Publications Committee for they patience in waiting for the arrival of this never-ending manuscript.

APPENDIX

FORMALISM FOR THE DILUTION OF THE ^{22}Ne-RICH OR OTHER PROCESSED COMPONENTS

With X_i being the mass fraction of the nuclear species i, let me define various excesses E_{ik} of species i relative to species k : [37]

(i) As regards elemental composition, I define the GCRS "main component", biased according to FIP, as following strictly the correlation f(FIP) defined in fig. 15. As regards isotopic ratios, they are assumed to have standard LG values. Thus, the excesses relative to LG for the main component are :

$$E_{ik,main} \equiv \frac{X_{i,main}}{X_{i,LG}} \Big/ \frac{X_{k,main}}{X_{k,LG}} = \frac{f_i(FIP)}{f_k(FIP)} \equiv f_{ik}(FIP)$$

where $f_i(FIP)$ and $f_k(FIP)$ are the values of f(FIP) for species i and k, and $f_{ik}(FIP)$ is its value for species i normalized to its value for species k. An uncertainty should be associated with f(FIP) ; for simplicity, I shall ignore it here.

(ii) In the "processed component", we have :

$$E_{ik,proc} \equiv \frac{X_{i,proc}}{X_{i,LG}} \Big/ \frac{X_{k,proc}}{X_{k,LG}}$$

$E_{ik,proc}$ describes abundance anomalies of any origin in the processed component : local nucleosynthesis and, if any, atomic selection effects on this component. To separate the two possible effects, atomic and nuclear, let me define :

$$E_{ik,proc} \equiv f_{ik,proc}(atom) \cdot E_{ik,proc,nucl} \cdot$$

I choose as a reference species k a species whose mass fraction is not affected by the nuclear processing (e.g. ^{20}Ne, ^{28}Si). Since in addition, $f_{ik,proc}(atom)$ is normalized to species k, we have $X_{k,proc}/X_{k,LG} = 1$.

(iii) In the GCRS composition, obtained after mixing of the two components (for brevity, I use the symbol CR), we have :

$$E_{ik,CR} \equiv \frac{X_{i,CR}}{X_{i,LG}} \Big/ \frac{X_{k,CR}}{X_{k,LG}}$$

$E_{ik,CR}$ is essentially a "measured" quantity, which will later have to be confronted with the model-related excesses $E_{ik,main}$ and $E_{ik,proc}$.

---

[37] Working directly on the excess of mass fraction of a single species (without reference to a comparison species, e.g. $E_{i,CR} \equiv X_{i,CR}/X_{i,LG}$ is very inconvenient because $X_{i,CR}$ depends on the behaviour of H and He in GCR's, which is irrelevant here (cosmic rays are not a closed system with fixed mass).

It will often be more significant to consider the GCRS excess relative to the FIP pattern f(FIP) describing the main component (i.e. the quantity plotted in fig. 20) ; let :

$$E^{*}_{ik,CR} \equiv \frac{E_{ik,CR}}{E_{ik,main}} = \frac{E_{ik,CR}}{f(FIP)} = \frac{X_{i,CR}}{X_{i,main}} \Big/ \frac{X_{k,CR}}{X_{k,main}}$$

Now let p_k be the fraction of the species k (unaffected by the nuclear processing) in GCRS that originates from the processed component. So $1/p_k$ is the dilution factor for species k. I shall work in the approximation $p_k << 1$, implying that the processed component is a minor one, highly diluted in the main component (for a more general treatment - though not entirely adequate, as we shall see below - see Maeder 1983).

When $p_k << 1$, it is readily shown that :

$$E_{ik,CR} = E_{ik,main} + p_k \cdot E_{ik,proc} \qquad (A1)^{38}$$

$$E_{ik,CR} = f_{ik}(FIP) + p_k \cdot f_{ik,proc}(atom) \cdot E_{ik,proc,nucl}$$

Or, dividing by $f_{ik}(FIP)$:

$$E^{*}_{ik,CR} = 1 + p_k \cdot \frac{f_{ik,proc}(atom)}{f_{ik}(FIP)} \cdot E_{ik,proc,nucl} \qquad (A2)$$

This is the general expression (for $p << 1$) we need. It relates the observed excess at GCRS $E^{*}_{ik,CR}$ (corrected for the bias with FIP), the excess in the processed component material $E_{ik,proc,nucl}$, and the dilution factor $1/p_k$; and it includes possible atomic selection effects in the processed component. It can be used either way to derive one of three quantities from the other two.

The traditional treatment (Meyer 1981c, 1985b ; Cassé and Paul 1981, 1982 ; Maeder 1983 ; Blake and Dearborn 1984 ; Arnould 1984 ; Prantzos 1984a,b ; Prantzos et al. 1983 ; 3, 167) assumes $f_{ik,proc}(atom) = f_{ik}(FIP)$ and gets hence :

$$E^{*}_{ik,CR} = 1 + p_k \cdot E_{ik,proc,nucl} \qquad (A3)^{39}$$

As discussed in the text (§ III-4.3. ; Meyer 1985b), I think this assumption is not a plausible one.

---

38 In eq.(A1) the reference to LG composition has merely introduced a constant factor $X_{i,LG}/X_{k,LG}$ on both sides of the equation, which is superfluous. So, the relationship between $E_{ik,CR}$, $E_{ik,main}$, $E_{ik,proc}$ and p_k is unaffected by changes of, and hence uncertainties on the LG standard. Uncertainties on the LG composition of a large number of elements (not specifically species i and k) intervene when $E_{ik,main} = f_{ik}(FIP)$ is being defined ; I ignore this uncertainty here. On the other hand, $E_{ik,CR}$ is an observational quantity, and, when this excess has to be determined, uncertainties on the LG abundances of species i and k fully play their role.

39 It is also equivalent to forget about any atomic selection effect whatsoever in both the main and the processed component, as Maeder (1983) did.

In our ignorance of possible other atomic selection effects in the processed component, we can also simply not consider any, and set $f_{ik,proc}(atom) = 1$. Then we get the more plausible, though possibly oversimplified expression :

$$E^*_{ik,CR} = 1 + \frac{p_k}{f_{ik}(FIP)} E_{ik,proc,nucl} \qquad (A4)$$

which expresses simply the effect of the higher degree of dilution of the "processed" species belonging to elements more abundant in the main component (low-FIP elements).

Of course, expressions (A3) and (A4) do not differ when dealing with elements in the same FIP-plateau as the reference element k, since then $f_{ik}(FIP) = 1$. With $k = {}^{20}Ne$, the two formulae yield identical results for ^{22}Ne, C, O (see footnote 29).

As regards the ^{22}Ne excess (§ III-4.), $p_k = p_{^{20}Ne}$ is determined from (A3) or (A4), from the "observed" $E^*_{ik,CR}$ and the reliable theoretical estimates of $E_{ik,proc,nucl}$ for $^{22}Ne = i$ (Meyer 1981c, 1985b ; Cassé and Paul 1981, 1982 ; Maeder 1983 ; Blake and Dearborn 1984 ; Arnould 1984 ; Prantzos 1984a,b ; Prantzos et al. 1983 ; 3, 167).

To build up fig. 30, eqs. (A3) and (A4) have been used, while these same formulae, explicited for $E_{ik,proc,nucl}$ have been used for fig. 31. In both figures, the top plot results from eq.(A3) and the bottom one from (A4).[40]

As regards the excesses of UH nuclei (§ III-5.), we do not have any theoretical estimate of $E_{ik,proc,nucl}$, so that p_k cannot be derived from eq. (A3) or (A4). $E_{ik,proc,nucl}$ can only be related to the "observed" $E^*_{ik,CR}$ to within an unknown factor p_k, corresponding to the unknown degree of dilution (of whatever species k). Fig. 32, otherwise similar to fig. 31, has been built up in this way, and gives only relative enhancements $E_{ik,proc,nucl}$. [Since there is no calculation to compare the data with, there is no point in drawing an analog to fig. 30].

[40] On the r.h.s. of eq. (A2) through (A4), should strictly appear the term $[E_{ik,proc,nucl} - 1]$. Since it is assumed that $E_{ik,proc,nucl} >> 1$, the 1 has been neglected. In figs. 31 and 32, where the equations are explicited for $E_{ik,proc,nucl}$, it must be clear that, in case of a small excess, $E_{ik,proc,nucl} \to 1$, and not $\to 0$.

References

Anders, E. 1971, GCA 35, 516.
Anders, E., and Ebihara, M. 1982, GCA 46, 2363.
Arnaud, M., and Cassé, M. 1985, Astr. Ap. 144, 64.
Arnaud, M., and Rothenflug, R. 1985, Astr. Ap. Suppl. 60, 425.
Arnould, M. 1984, Adv. Space Res. 4, N°2-3, 45.
Arnould, M., and Norgaard, H. 1978, Astr. Ap. 64, 195.
Arnould, M., and Norgaard, H. 1981, Comments Ap. 9, 145.
Arnould, M., Norgaard, H., Thielemann, F.K., and Hillebrandt, W. 1980, Ap. J. 237, 931.
Axford, W.I. 1981, 17th ICRC, Paris, 12, 155.
Axford, W.I., Leer, E., and Skadron, G., 1977, 15th ICRC, Plovdiv, 11, 132.
Badhwar, G.D., et al. 1979, 16th ICRC, Kyoto, 1, 345.
Beer, H., and Macklin, R.L. 1985, Phys. Rev. C 32, 738.
Bell, A.R. 1978a, MNRAS 182, 147.
Bell, A.R. 1978b, MNRAS 182, 443.
Bibring, J.P., and Cesarsky, C.J. 1981, 17th ICRC, Paris, 2, 289.
Binns, W.R., et al. 1983, 18th ICRC, Bangalore, 9, 106.
Binns, W.R., et al. 1984, Adv. Space Res. 4, N°2-3, 25.
Binns, W.R., et al. 1985, Ap. J. 297, 111.
Blake, J.B., and Dearborn, D.S.P. 1984, Adv. Space Res. 4, N°2-3, 89.
Blanford, R.D., and Ostriker, J.P. 1978, Ap. J. Letters 221, L29.
Brewster, N.R., et al. 1983, 18th ICRC, Bangalore, 9,259.
Brewster, N.R., Freier, P.S., and Waddington, C.J. 1983, Ap. J. 264, 324.
Byrnak, B., et al. 1983a, 18th ICRC, Bangalore, 9, 135.
Byrnak, B., et al. 1983b, 18th ICRC, Bangalore, 2, 29.
Cassé, M. 1981, 17th ICRC, Paris, 13, 111.
Cassé, M. 1983, in "Composition and Origin of Cosmic Rays", M.M. Shapiro ed.,(Reidel), p.193.
Cassé, M., and Paul, J.A. 1981, 17th ICRC, Paris, 2, 293.
Cassé, M., and Paul, J.A. 1982, Ap. J. 258, 860.
Cesarsky, C.J., and Bibring, J.P. 1980, IAU Symp. N°94, Origin of Cosmic Rays, G. Setti, G. Spada, A.W. Wolfendale ed., p. 361.
Cesarsky, C.J., and Montmerle, T. 1981,17th ICRC, Paris, 9, 207.
Cesarsky, C.J., Rothenflug, R., and Cassé, M. 1981, 17th ICRC, Paris, 2, 269.
Cesarsky, C.J., Rothenflug, R., and Cassé, M. 1985, in preparation.
Clayton, D.D. 1968, Principles of stellar evolution and nucleosynthesis, Mc Graw Hill.
Clayton, D.D., and Rassbach, M.E. 1967, Ap. J. 148, 69.
Cook, W.R., Stone, E.C., and Vogt, R.E. 1980, Ap. J. Letters 238, L 97.
Cook, W.R., Stone, E.C., and Vogt, R.E. 1984, Ap. J. 279, 827.
Cook, W.R., et al. 1979, 16th ICRC, Kyoto, 12, 265.
Cowsik, R., and Gaisser, T.K. 1981, 17th ICRC, Paris, 2, 218.
Cowsik, R., and Wilson, L.W. 1973, 13th ICRC, Denver, 1, 500.
Dearborn, D.S.P., and Blake, J.B. 1985, Ap. J. Letters 288, L 21.
Dwyer, R., and Meyer, P. 1985, Ap. J. 294, 441.
Ebihara, M., Wolf, F.R., and Anders, E., 1982, GCA 46, 1849.
Eichler, D. 1979, Ap. J. 229, 419.
Eichler, D. 1980, Ap. J. 237, 809.
Eichler, D., and Hainbach, K. 1981, Phys. Rev. Letters 47, 1560.
Ellison, D.C. 1981, Ph. D Thesis.
Ellison, D.C. 1985, J. Geophys. Res. 90, 29.
Ellison, D.C., Jones, F.C., and Eichler, D. 1981, J. Geophys. 50, 110.
Engelmann, J.J. 1984, 9th European Cosmic Ray Symp., Kosice, K. Kudela and S. Pinter ed., (Slovak Acad. Sci.), p. 141.
Engelmann, J.J. et al. 1983, 18th ICRC, Bangalore, 2, 17.
Engelmann, J.J. et al. 1985, Astr. Ap. 148, 12.
Epstein, R.I. 1980a, IAU Symp. N°94, Origin of Cosmic Rays, G. Setti, G. Spada, A.W. Wolfendale ed., p.109.
Epstein, R.I. 1980b, MNRAS 193, 723.
Fixsen, D.J. 1985, U. of Minn. C.R. Rep. CR-195.
Fixsen, D.J. et al. 1983, 18th ICRC, Bangalore, 9, 119.
Fontes, P. 1977, Phys. Rev. C 15, 2159.
Garcia-Munoz, M., Guzik, T.G., Simpson, J.A., and Wefel, J.P. 1984, Ap. J. Letters 280, L13.
Garcia-Munoz, M., Margolis, S.A., Simpson, J.A., and Wefel, J.P. 1979, 16th ICRC, Kyoto, 1, 310.
Garcia-Munoz, M., and Simpson, J.A. 1979, 16th ICRC, Kyoto, 1, 270.
Geiss, J. 1985, ESA Workshop on Future Missions in Solar, Heliosphere and Space Plasma Physics, Garmisch-Partenkirchen, May 1985, ESA SP-235, p. 37.
Geiss, J., and Bochsler, P. 1984, in Isotopic Ratios in the Solar System, Paris (CNES), in press.
Goret, P. et al. 1981, 17th ICRC, Paris, 9, 122.
Goret, P. et al. 1983, 18th ICRC, Bangalore, 9, 139.
Grevesse, N. 1984a, Phys. Scripta, T8, 49.
Grevesse, N. 1984b, in Frontiers of Astronomy and Astrophysics, ed. R. Pallavicini (Florence : Italian Astron. Soc.), p. 71.
Guzik, T.G. 1981, Ap. J. 244, 695.
Hillebrandt, W., and Thielemann, F.K. 1982, Ap. J. 255, 617.
Hsieh, K.C., Mason, G.M., and Simpson, J.A. 1971, Ap. J. 166, 221.
Israel, M.H. et al. 1983, 18th ICRC, Bangalore, 9, 305.
Jordan, S.P. 1985, Ap. J. 291, 207.
Jordan, S.P., and Meyer, P. 1984, Phys. Rev. Letters 53, 505.
Juliusson, E. 1974, Ap. J. 191, 331.
Juliusson, E. et al. 1983, 18th ICRC, Bangalore, 2, 21.
Käppeler, F. et al. 1982, Ap. J. 257, 821.
Kaufman, S.B., and Steinberg, E.P. 1980, Phys. Rev. C 22, 167.
Krimsky, G.F. 1977, Dokl. Akad. Nauk. SSSR 234, 1306.
Lagage, P.O., and Cesarsky, C.J. 1985, Astr. Ap. 147,127.
Lau, K.H., Mewaldt, R.A., and Wiedenbeck, M.E. 1983, 18th ICRC, Bangalore, 9, 255.
Letaw, J.P., Silberberg, R., and Tsao, C.H. 1984, Ap. J. 279, 144.
Lindstrom, P.J. et al. 1975, Lawrence Berkeley Laboratory Report LBL-3650.
Lockwood, J.A., and Webber, W.R. 1984, J. Geophys. Res. 89, 17.
Lund, N. 1984, Adv. Space Res. 4, N°2-3, 5.
Maeder, A. 1983, Astr. Ap. 120, 130.
Mason, G.M., Gloeckler, G., and Hovestadt, D. 1983, Ap. J. 267, 844.
Mauger, B.G., and Ormes, J.F. 1983, 18th ICRC, Bangalore, 2, 65.
McGuire, R.E., Von Rosenvinge, T.T., and McDonald, F.B. 1979, 16th ICRC, Kyoto, 5, 61.
McGuire, R.E., Von Rosenvinge, T.T., and McDonald, F.B. 1986, Ap. J., in press.
Mewaldt, R.A. 1980, in Proc. Conf. Ancient Sun (Boulder 1979), R.O. Pepin, J.A. Eddy and R.B. Merrill eds., p. 81.
Mewaldt, R.A. 1981, 17th ICRC, Paris, 13, 49.
Mewaldt, R.A., Spalding, J.D., Stone, E.C., and Vogt, R.E., 1981, Ap. J. Letters 251, L 27.
Meyer, J.P. 1974, Ph. D. Thesis, Universitè de Paris, Orsay.
Meyer, J.P. 1975, 14th ICRC, Munich, 11, 3698.
Meyer, J.P. 1979a, in "Les Elements et leurs Isotopes dans l'Univers", 22nd Liège Internat. Astrophys. Symp. (U. of Liège Press), p. 153, 465, 477, 489.
Meyer, J.P. 1979b, 16th ICRC, Kyoto, 2, 115.
Meyer, J.P. 1981a, 17th ICRC, Paris, 3, 145.
Meyer, J.P. 1981b, 17th ICRC, Paris, 3, 149.
Meyer, J.P. 1981c, 17th ICRC, Paris, 2, 265.
Meyer, J.P. 1981d, 17th ICRC, Paris, 2, 281.
Meyer, J.P. 1985a, Ap. J. Suppl. 57, 151.
Meyer, J.P. 1985b, Ap. J. Suppl. 57, 173.
Montmerle, T. 1984, Adv. Space Res. 4, N°2-3, 357.
Müller, D., and Tang, J. 1983, 18th ICRC, Bangalore, 2,60.
Nishimura, J. et al. 1981, 17th ICRC, Paris, 2, 94.
Norgaard, H. 1980, Ap. J. 236, 895.
Olson, D.L. et al. 1983, Phys. Rev. C 28, 1602.

Orth, C.J. et al. 1976, J. Inorg. Nucl. Chem. 38, 13.
Perron, C. 1976, Phys. Rev. C 14, 1108.
Prantzos, N. 1984a, Adv. Space Res. 4, N°2-3, 109.
Prantzos, N. 1984b, in High Energy Astrophysics, 19th Moriond Ap. Meeting, J. Audouze and J. Tran Thanh Van ed. (Ed. Frontières), p. 341.
Prantzos, N., Arnould, M., and Cassé, M. 1983, 18th ICRC, Bangalore, 9, 155.
Prantzos, N., and Cassé, M. 1985, Ap. J., in press.
Preszler, A.M. et al. 1975, 14th ICCR, Munich, 12, 4096.
Raisbeck, R.G., and Yiou, F. 1976, in Spallation Nuclear Reactions and Their Applications, B.S.P. Shen and M. Merker ed. (Reidel), p. 83.
Read, S.M., and Viola, V.E. 1984, Atom. Nucl. Data Tables 31, 359.
Silberberg, R., and Tsao, C.H. 1973a, Ap.J.Suppl. 25,315.
Silberberg, R., and Tsao, C.H. 1973b, Ap.J.Suppl. 25,335.
Silberberg, R., Tsao, C.H., and Letaw, J.R. 1985, Ap. J. Suppl. 58, 873.
Silberberg, R., Tsao, C.H., Letaw, J.R., and Shapiro, M.H. 1983, Phys. Rev. Letters 51, 1217.
Smith, L.H. et al. 1973, Ap. J. 180, 987.
Stone, E.C. et al. 1983, 18th ICRC, Bangalore, 9, 115.
Tan, L.C., and Ng, L.K. 1983, Ap. J. 269, 751.
Tang, J., and Müller, D. 1983, 18th ICRC, Bangalore, 9, 251.
Tang, K.K. 1984, Ap. J. 278, 881.
Tarlé, G., Ahlen, S.P., Cartwright, B.G., and Solarz, M. 1979, Ap. J. Letters, 232, L161.
Tsao, C.H., and Silberberg, R. 1979, 16th ICRC, Kyoto, 2, 202.
Van der Hucht, K.A., and Olnon, F.M. 1985, Astr. Ap. 149, L17.
Ward, R.A., and Newman 1978, Ap. J. 219, 195.
Webber, W.R. 1975, 14th ICRC, Munich, 5, 1597.
Webber, W.R. 1981, 17th ICRC, Paris, 2, 80.
Webber, W.R. 1982a, Ap. J. 252, 386.
Webber, W.R. 1982b, Ap. J. 255, 329.
Webber, W.R. 1983a, in "Composition and Origin of Cosmic Rays", M.M. Shapiro ed., (Reidel), p. 25.
Webber, W.R. 1983b, 18th ICRC, Bangalore, 9, 151.
Webber, W.R. 1984, Workshop on Cosmic Ray and High Energy Gamma-Ray Experiments for the Space Station Era, Baton Rouge (Louisiana State U.), p. 283.
Webber, W.R., and Brautigam, D.A. 1982, Ap. J. 260, 894.
Webber, W.R., Brautigam, D.A., Kish, J.C., and Schrier, D.A. 1983a, 18th ICRC, Bangalore, 2, 198.
Webber, W.R., Brautigam, D.A., Kish, J.C., and Schrier, D.A. 1983b, 18th ICRC, Bangalore, 2, 202.
Webber, W.R., Damle, S.V., and Kish, J.M. 1972, Ap. Space Sci. 15, 245.
Webber, W.R., and Lezniak, J.A. 1974, Ap. Space Sci. 30, 361.
Webber, W.R., and Yushak, S.M. 1983, Ap. J. 275, 391.
Westfall, G.D., et al. 1979, Phys. Rev. C 19, 1309.
Wiedenbeck, M.E. 1974, Adv. Space Res. 4, N° 2-3, 15.
Wiedenbeck, M.E., et al. 1979, 16th ICRC, Kyoto, 1, 412.
Woosley, S.E., and Weaver, T.A. 1981, Ap. J. 243, 651.
Young, J.S. et al. 1981, Ap. J. 246, 1014.